To the Graduate Council:

I am submitting herewith a thesis written by Devdutt Dash entitled "Heat Transfer in a Double-Pipe Bayonet Heat Exchanger." I have examined the final copy of this thesis for form and content and recommend that it be accepted in partial fulfillment of the requirements for the degree of Master of Science, with a major in Mechanical Engineering.

Roy J. Schulz

Roy J. Schulz, Major Professor

We have read this thesis and recommend its acceptance:

John P [illegible]

[illegible]

Accepted for the Council:

[illegible]

Associate Vice Chancellor and Dean of the Graduate School

Heat Transfer in a Double-Pipe Bayonet Heat Exchanger

A Thesis

Presented for the

Master of Science

Degree

The University of Tennessee, Knoxville

Devdutt Dash

May 1994

DEDICATION

This thesis is dedicated to

"THE VOLUNTEER STATE" - TENNESSEE

who "volunteered" to give me a financial assistantship, and hence make it possible to come and study in the United States of America,

and to

INDIA

my country,

which made me capable enough in the first place.

ACKNOWLEDGMENTS

This research experience has been rewarding both in terms of academic achievement and in learning about life. Working with the Energy Conversion Program at UTSI gave me the unique opportunity to work independently, and also as a part of a very big family, solving problems of the real engineering world.

I would like to acknowledge the advice, help and support of all the people who have contributed both directly and indirectly in making this thesis possible. I would like to thank my major professor and advisor, Dr. Roy J. Schulz, and committee members Dr. John P. Foote and Dr. K. C. Reddy for their advice and assistance in writing this thesis. They gave a lot of their time and patience at every stage of this research. I am grateful to my research supervisors Mr. William H. Boss and Mr. Douglas M. Jackson for their advice, support and understanding during the course of my study and research here. I owe a lot to people at the facility (both CFFF and ECF), especially Bill Millard, Ricky Meekes and Harold Sartain, for all their help in getting my apparatus together. The support services of the library and computer center were commendable. I would like to thank Dr. Brad Winkleman and Mr. Charles Wagoner for providing me their computing resources. Dr. Ed Gleason and Callie Taylor have been especially kind and helpful during my stay here. I will fondly remember "The Indian Contingent" who were always there in the times of crisis.

At a personal level my family and friends, both here and in India, have provided me with the moral encouragement, emotional support and all the opportunities to get me this far in life.

ABSTRACT

Modern energy conversion and power systems require compact and highly effective heat exchanger systems that are economical and achieve process requirements. Indirectly fired combustion systems for power plants must use heat exchangers operating with hot products of combustion at atmospheric pressure on one side, and clean pressurized air on the other. The air is indirectly heated before being expanded through a power turbine. Studies at UTSI and elsewhere show that the heat transfer coefficient on the hot gas side limits the efficiency of the heat exchanger and determines its size. Therefore to make the heat exchanger compact and efficient, convective heat transfer augmentation is required.

Convective heat transfer augmentation incurs an increase in the pressure drop associated with the gas flow. This increases the pumping power required by the system. It thus becomes essential to balance the trade off between an increase in the amount of heat transferred and the increase in pump work required to move the fluids through the heat exchanger. This research is an experimental study of convective heat transfer and its enhancements in a bayonet tube heat exchanger. The bayonet style heat exchanger holds promise in high temperature (1650 °K and greater) heat exchangers, which will probably be made, at least partially, of ceramics. The

enhancement technique investigated in the present study is based on swirl flow. Swirl flow has been found to be effective in increasing heat transfer in tubes. However, its effect in annulus flows and bayonet tubes has not been extensively studied. In addition, the complex nature of the flow phenomenon in bayonet tubes makes it difficult to directly apply standard heat transfer and pressure drop correlations.

Inlet swirl was generated in a standard double-pipe bayonet heat exchanger using a four vane swirler with a 70° vane angle. The swirler was positioned in the entrance of the annular section of the exchanger. The heat transfer characteristics of the bayonet tube with a non uniform temperature boundary condition was studied for annular flow in the Reynolds number regime of 8900 to 17870. The bayonet tube was fully instrumented with thermocouples for wall and gas temperature measurements. The resulting temperature distributions were analyzed to determine heat flux and surface heat transfer coefficient distributions in the system. The analysis accounted for both radiation heat transfer, and non-developed flow conditions, for various Reynolds numbers, in computing the heat transfer coefficients. Experimentation and subsequent analysis has shown that swirl flow indeed enhances the heat transfer performance of bayonet tubes by approximately two to three times over the (actual) heat transfer coefficient for non-swirl, straight-flow conditions, for the Reynolds numbers investigated.

TABLE OF CONTENTS

LIST OF TABLES

LIST OF FIGURES

LIST OF SYMBOLS

A	surface area, m^2
D	hydraulic diameter, 4A/P, m
E_i	Emissive power of surface i, W/m^2
F_{ij}	radiation view factor from surface i to surface j
L	length of cylinder/inner tube, m
MWth	thermal energy expressed in 10^6 watts
NTU	Number of transfer units (of a heat exchanger)
Nu	Nusselt number
R	radius of cylinder, m
Re_D	Reynolds number based on hydraulic diameter D
P	perimeter of the heat transfer surface, m
Pr	Prandtl number
Q	net flux interchange, W
S	swirl number
T	temperature, C or K
U	overall heat conductance, $W/m^2\,K$
c_p	specific heat, J/kg °C
d	diameter, m
h	convective heat transfer coefficient, $W/m^2\,K$
h_{cL}	heat transfer coefficient associated with entry lengths, $W/m^2\,K$

h_c heat transfer coefficient for fully developed flow, $W/m^2 K$

k thermal conductivity of material, W/m K

m mass flow rate, kg/s

q_i heat into surface i, W

r radius, m

$s_i s_j$ total exchange area from surface i to j

u velocity of air flow, m/s

x distance along flow in bayonet tube, Figure A1.10

(x=L - y, where L=length of tube)

y distance along flow in bayonet tube, Figure A1.10

σ Stefan-Boltzmann constant, 5.67×10^{-8}, $W/m^2 K^4$

ρ density, kg/m^3

ε emissivity of surface, effectiveness of heat exchanger

δ_{ij} Kroneker delta

μ dynamic viscosity, kg/m s

$\varnothing$ angle, radians

χ dimensionless ratio of the overall heat transfer coefficient times the area of heat transfer, of the two streams in the heat exchanger

ζ normalized axial length

ϑ normalized temperature variable

Subscripts

s	surface
1	tube inner surface, figure A1.10
2	tube outer surface, figure A1.10
3	shell inner surface, figure A1.10
4	shell outer surface, figure A1.10
ai	air flowing in (inside tube), figure A1.10
ann	annulus
ao	air flowing out (inside annulus), figure A1.10
b	constant boundary condition
bead	thermocouple tip/bead
db	refers to the Dittus-Boelter heat transfer correlations for fully developed flow conditions
fd	refers to fully developed flow conditions
h	hydraulic diameter
i	inner annulus diameter
o	outer annulus diameter
shell	shell of the bayonet tube assembly
tube	central tube
∞	value at free stream conditions

Chapter 1

INTRODUCTION

High temperature thermal power cycles promise higher energy conversion process efficiencies. This has prompted research and development of systems capable of operating at higher temperatures, of materials capable of being used at the specified temperatures, and of heat exchangers for process air heating and heat recovery from waste gases in these systems, [1]. Many industrial processes like steel soaking pits, specialty glass manufacturing, textile and insulation fiberglass production, aluminum melting furnaces, etc., use combustion heating to achieve temperatures in the region of 800 K to 1600 K. Such systems typically lose 30% - 65% of the fuel energy content when the exhaust gases leave the stack. Recuperators can and should be installed in the exhaust stack to recover some of this waste heat energy. If air used in the combustion process is preheated in such a recuperator, fuel savings of the order of 20% - 30% could be realized, [2].

In high temperature recuperators, the heat exchange process combines convection and radiation heat transfer from the hot combustion, or waste gases, to the furnace walls and to the heat exchanger/recuperator tubes or surface area. In fact, radiation plays so important a role in the high temperature regime of the heat exchange process, that these heat exchangers are also called radiation recuperators. Heat is transferred through the recuperator walls to the cold stream by a combination of radiation and convection, depending on the nature of the cold stream medium. In cases where air for combustion is preheated in such recuperators, the heat exchange is almost exclusively through convection as air is transparent to radiation, but, any interior walls will be heated by radiation, and they will transfer this heat to the air by convective contact. Performance of these recuperators is important, not only for the energy recovery, but also because of the direct relationship of combustion temperature to fuel savings, [3].

The operating environment for most high temperature recuperators is one of high oxidation corrosion, and erosion if the high temperature flue gases are also particle-laden. This requires that recuperators be manufactured from high performance super alloys or ceramics (conventional metallic recuperators can be used up to a temperature of approximately 1140 K), both of which are extremely expensive. Thus it is desirable that recuperators be as small as possible, using the bare minimum of construction material. Since the heat transfer rate is proportional to the product of the heat transfer coefficient and the heat transfer surface area (for the same temperature difference), a reduction of materials (surface area) requires a proportionate increase in the heat transfer coefficient. Convective heat transfer augmentation is the technical process of determining the technological methods and procedures for increasing the rate of convective heat transfer over that obtained in steady flows at equivalent Reynolds numbers.

1.1 HEAT TRANSFER RESEARCH AT U.T.S.I.

Magnetohydrodynamics

UTSI has been conducting extensive research on proof-of-concept (POC) testing of a coal based magnetohydrodynamic (MHD) power generation cycle, as part of its Energy Conversion Research and Development Programs. UTSI operates and maintains the United States Department of Energy (US DOE) Coal Fired Flow Facility (CFFF) which is a pilot scale facility capable of operating on either pulverized coal, fuel oil, natural gas, or all of these in combination. Figure A1.1 is a schematic of the flow train. A description of this facility is provided elsewhere. The MHD power cycle is a very high temperature topping cycle for fossil-fueled electric power plants. This cycle operates by firing coal and/or oil mixtures to ultra-high (3000 K) combustion temperatures, together with a "seed" material such as potassium carbonate, to generate a combustion gas plasma. Specifically, prior to combustion, the coal is pulverized and fed to the primary combustor together with a potassium salt in either crystalline or aqueous solution. At very high combustion temperatures (approximately 2200 K- 3100 K) the salt dissociates releasing potassium ions in the gas, forming a plasma. The electrically conducting plasma is accelerated to a slightly supersonic velocity through a duct/channel, which is enclosed in a strong magnetic field in the core of a large magnet. An electric current flows across the channel and is tapped off the conducting channel walls, which act as electrodes. The hot combustion gases are then fed into a conventional steam power generation flow train, where the heat is extracted to generate steam. In the CFFF, the steam generated is dumped to the atmosphere; however, in an operational MHD plant, the steam would be used to power a steam turbine to generate additional electricity. When the MHD system and steam turbine cycles are combined, a net plant efficiency of approximately 50% can be achieved. This is at least a 15% increase over a conventional thermal power plant. In addition, the unique high-temperature, two stage combustion process and the presence of potassium seed drastically reduce the plant NO_x, SO_x, and particulate emissions, making the system environmentally sound.

The efficiency of a MHD system is directly related to the primary coal and/or oil combustion temperatures. These temperatures can be achieved by either using pure oxygen for combustion, or by sufficiently preheating the air used in combustion, or a combination of the two. Use of pure oxygen requires a nearby oxygen gas plant, and combustion gas preheating requires a high temperature air heater using the exhaust gases for this energy.

The MHD power generation cycle can be divided into two systems, a topping cycle (upstream) and a bottoming cycle (downstream). The bottoming cycle is the conventional steam power plant, the rest forms the topping cycle. Intermediate to these two cycles is a secondary combustion and NO_x reduction zone, where the topping cycle exhaust is completely burned and allowed to cool to manageable temperature before being fed to the bottoming cycle. This zone, called the radiant furnace, is where the thermal relaxation of nitrogen oxides to nitrogen and oxygen occurs, [4]. Theoretically, this would be an ideal location to use a high temperature air heater to preheat the combustion air. The use of a heat exchanger here in the flow train is made difficult by the particle laden exhaust gas that is still at very high temperatures (1500 K- 2200 K). Among the research interests at UTSI are the identification of suitable materials for heat exchanger applications in this type of environment, and the design and testing of suitable configurations of heat exchangers that could be employed.

Material testing

Boss and others at UTSI, [5] have conducted extensive material surveys and tested samples in the radiant furnace. In addition to general survivability (i.e. resistance to cracking, spalling and erosion), these materials must have adequate strength at elevated temperatures, have known and desirable failure modes and possess low thermal expansion and creep characteristics. They must also be easily manufactured, fabricated, assembled and maintained, that is, cost effective to use. One of the most promising materials tested so far is Dupont Lanxide Corporation's DIMOX® ceramic composite. It is a 45% - 45% combination of silicon carbide particulate in an aluminum oxide matrix with 10% reinforcing free aluminum. The material is manufactured by a proprietary process called "direct metal oxidation" (DIMOX), and is available in the form of tubes. Hollow tubes are manufactured with a hemispherical capped or closed end. The end can be machined or cut off to form a tube or pipe.

Heat exchanger design

Various designs have been proposed for a high temperature air heater, a heat exchanger, for a MHD system. They can be categorized into the regenerative and the recuperative kinds. Regenerative heat exchangers operate in a cycle, starting with the heating of a thermal mass by the hot exhaust gases in one part of the cycle, which then transfers the stored heat to the cold stream in the other part of the cycle, before being heated up again. Cold and hot gases have to be periodically shunted through the system for the heating and cooling processes. Recuperators on the other hand do not experience such a cycling. Heat is continuously transferred from the hot stream to the cold stream through the recuperator walls. There are several advantages of a recuperator over a regenerator, chief being life, fouling characteristics, space and the absence of extensive ducting, flow diverting and flow regulation requirements.

Studies and design calculations for recuperator application show the following:

In the case of a 500 MWt MHD power plant, the typical recuperator would heat combustion air to a temperature of 1300 K (1875°F), so as to sustain combustion at 2700 K (4400°F). The approximate mass flow rate in the recuperator would be 165 lbs/sec, that is, a flow rate of 2.17×10^6 scfm at an air pressure of 50-75 psig. The combined MHD and steam bottoming system would then deliver an overall theoretical efficiency of 45%, much higher than conventional coal fired, steam driven power plants, [6].

Design calculations by personnel at UTSI have shown that it would be relatively extremely expensive to build a high temperature, ceramic heat exchanger at the desired size because of material costs. Thus, for a ceramic recuperator to be commercially feasible, it is necessary to significantly reduce the amount of material used in the design. One way to accomplish this is to augment the heat transfer rate, which would in turn decrease the surface area required for the same heat exchange. This directly translates into a savings in material costs.

DeBellis and Kneidel, [7] report that the relative ratios between heat transfer coefficients involved in the heat transfer process are:

flue side convection / air side convection / flue side radiation = 2 / 9 / 16 - 40

(The range of values for the radiation heat transfer coefficient arises due temperature variation in the heat exchanger system). This clearly shows that the heat exchange process is limited by the air side convection coefficient, and stresses the need for convection enhancement.

Choice of a bayonet tube heat exchanger design

A conventional heat exchanger design consists of metal tubes separating the fluids involved in heat transfer. One fluid usually flows inside the tubes, and the other flows over the outside of the tubes. The tube walls then represent the heat transfer surface area, [8]. Construction methods for these heat exchangers usually involve welding the tubes to the manifolds and body elements for sealing and required structure. In high temperature recuperators, two major design problems are encountered: large thermal expansion of tubes, and joining and sealing problems, especially for ceramic material. Babcock & Wilcox Co., [9] introduced the bayonet tube heat exchanger, which consisted of an outer tube closed at one end with a coaxial inner tube (Figure A1.2). A fluid introduced at one end would then flow the length of the assembly, turn at the closed end of the outer tube and return to the initial position. Thus the fluid being heated, would have a tube-annulus flow or an annulus-tube flow path.

The advantages of the bayonet tube heat exchanger are, [10]:

1. Since the tube assemblies are fastened at only one end (the other end freely suspended) the entire tube assembly is free to expand or contract under the influence of temperature variation. This reduces stresses from deformation, misalignment of the tube components or assemblies, and thermal expansion.
2. The tubes are not fixed between two tube sheets and there is no need of any expansion device commonly found in most metallic recuperators.
3. The tubes tend to be self-cleaning because the normal expansions and contractions would shake off any foreign material, like slag, which gets attached to the surface.
4. Maintenance is easy since a single tube can be changed without a major shutdown.
5. The tubes exposed to impinging inlet gases can be turned through 180 degrees, so as to double the life of the tube exposed to erosion.
6. In ceramic recuperators, it is a less formidable task to seal one end rather than two ends.
7. In high temperature applications where radiation heat transfer becomes predominant, the inner bayonet tube provides extra surface

area for heat transfer. Thus, in addition to the inner surface of the outer shell, the inner and outer surfaces of the inner tube are also available for convective heat transfer.

A bayonet tube heat exchanger system was used by Babcock & Wilcox Co. in the U. S. Department of Energy, Office of Industrial Technologies sponsored program in High Temperature Burner-Duct-Recuperator System. The concept used ceramic bayonet tubes. A tube-annulus air flow pattern was adopted as it gave better performance, [2].

1.2 HEAT TRANSFER AUGMENTATION

Heat transfer augmentation or enhancement has been achieved by various methods. Pertinent for application in high temperature recuperators are those techniques that can withstand the operating temperatures, are manufacturable, and which have allowable increases in pressure drop involved with their implementation. Listed below are some feasible techniques:

1 Use of extended surfaces, such as fins. The problems arising with fin applications are availability of suitable fin materials and their manufacturability.

2 Use of radiation walls: A radiation wall is a passive surface that participates in radiation exchange, heats up, and in turn dissipates heat to the surrounding environment by radiation and convection. Radiation accounts for a large portion of heat transfer at high temperatures. If the gas participating in heat transfer is an absorbing medium, the effect of radiation is even more pronounced. In the case of non-absorbing gases, extra surface area from a radiation wall allows for increase in convective heat transfer, [11].

3 Improvements in flow pattern: changing the flow pattern by the use of special devices, surface improvements or inserts can influence the heat transfer coefficient. For example, inlet devices which cause one or more of the heat transfer fluids to swirl, have been found effective in some designs.

4 Combined augmentation, which incorporates two or more regular augmentation techniques.

Choice of an augmentation technique

Each kind of an augmentation technique causes an increase in pressure drop. However, some methods produce a smaller pressure drop than others. Hence attention must be paid to the choice of the augmentation system. In addition, the geometry (relative physical dimensions) of the augmentation system used plays an important role in the efficiency of the system under consideration. To quantify effectiveness, a criteria called efficiency index η_{index} may be defined as

$$\eta_{index} = \frac{\text{heat transferred per unit of temperature difference}}{\text{pressure drop per unit length}}$$

with conditions of same flow rate, passage cross section area, length and temperature level. It may also be defined as the ratio of two ratios: (heat transfer coefficient of enhanced system/heat transfer coefficient plain tube) to (friction factor enhanced system/friction factor plain tube.)

The mechanisms of enhancement can be grouped as:

1 boundary layer thinning with 3D roughness;

2 surface area addition as with fins;

3 swirl and recirculation;

4 swirl;

5 flow separation and recirculation;

6 flow separation and reattachment.

Experiments, [12] have shown that swirl flow heat transfer has a very high effectiveness. The least effectiveness is gotten from extended surfaces. Rabas notes that at the same time there exist other considerations for the choice of an augmentation system based on operational characteristics and cost. The above criteria do not include the economic aspects of enhancement. In fact, most reported literature do not take such a view point in their recommendation. The trade-off between increase in pumping power and increase in heat transfer depends on the specific application.

Chapter 2

PROBLEM STATEMENT AND RESEARCH OBJECTIVES

The objective of this research is to study heat transfer enhancements in a bayonet tube heat exchanger. It is proposed to first characterize the heat transfer process in a standard bayonet tube heat exchanger, and then study the enhancements caused by an augmentation scheme. The augmentation scheme chosen is inlet swirl flow generated by a short four-vane swirler.

The flow phenomenon in a bayonet tube heat exchanger is not well documented. Research and experiments have shown that, depending on the length of the tube, the system does not always behave thermally as a simple combination of a tube and an annulus flow, because of complex flow phenomenon. Nevertheless, this model of a bayonet tube heat transfer process as a pipe flow and an annulus flow in series does provide a starting point for the analysis. For bayonet tubes of relatively short length, the flow is not well developed along most of the flow path inside the bayonet tube. Hence, fully developed flow correlations may not predict heat transfer performance well, nor are effects of swirl well correlated. The overall heat transfer coefficient in such flow conditions is the average of the sum of the heat transfer coefficients along the entire flow path, and can only be accurately determined if the heat transfer coefficient values are known along the entire flow path.

The present research is unique in the sense that it seeks to determine the variation in the heat transfer coefficient along the flow path in a bayonet tube heat exchanger based on well-documented temperature distributions. The study accounts for radiative heat transfer between outer and inner walls of the annulus, and seeks to determine the effectiveness of the inner tube in the heat exchange process. On the other hand, it must be recognized that the system performance is affected by the specific details of the selected bayonet design, and its fabrication. The design utilized in the present study was an actual hardware prototype of a full-scale bayonet heater for application in the US DOE CFFF. Therefore it presents some design features that are not optimal for an experimental heat transfer study. These features, and their effects on heat transfer data, will be pointed out and discussed later in this thesis.

Chapter 3

BACKGROUND

A wide variety of generalized correlations are available for heat transfer Nusselt numbers for both developing and fully developed straight flow conditions in pipes and annuli, and also for some methods of heat transfer augmentation. For example, a considerable amount of research has been done on convection enhancements in tubes using methods of swirl, extended surfaces, surface enhancements, turbulators, etc., as this has wide application in heat exchangers.

Heat Transfer in Annular Channels

The return flow of the fluid in a bayonet tube is along an annulus. Hence, an understanding of the annular heat transfer with and without convection enhancement becomes important.

Annular heat transfer is usually associated with nuclear fuel rod cooling and to a lesser extent with double pipe heat exchangers. Thus, in the case of annuli, studies have usually been limited to conditions with heating from a single surface. Convection enhancement techniques usually involve surface roughness and ribs, which are schemes that can be implemented in most lower temperature operating conditions. Studies involving heating from both surfaces of annuli have been primarily to confirm theoretical predictions. Hence, there are available a large number of studies based on simulating these operational conditions. Petukhov and Roizen [14,15], and Kays and Leung [16], have studied the flow in an annulus, and have developed extensive correlations of Nusselt numbers along the flow path. The heat transfer characteristics are seen to differ at the inner and outer surfaces of the annulus because of the flow velocity distribution. Equations have been developed to calculate the Nusselt numbers at both surfaces, under different dimensional and heating conditions. These results may be combined to calculate the Nusselt numbers in special cases using superposition [16].

3.1 RESEARCH CONDUCTED IN HEAT TRANSFER AUGMENTATION

Swirl Flow Heat Transfer

Swirling flows have been widely used in industrial heat transfer applications and in combustion systems. Swirl flow is classified as either continuous swirl, achieved by inserting coiled wires, full length twisted tape, or spiral fins along the length of a pipe, or decaying swirl flow, achieved by tangential inlet slots, tangential vanes, short helical inserts, or jets. In a decaying swirl, the swirl is generated at the inlet and decays along the flow path. Swirl flow is characterized by a swirl number S, which is defined as the ratio of angular momentum to the product of the axial momentum and radius, and may be expressed as:

$$S = \frac{\int_0^R \rho\, \omega\, u\, r\, dr}{\int_0^R \rho\, u^2 r\, dr}$$

where ω is the angular velocity, u is the axial velocity, r is the radius and ρ is the density. The swirl number generally decreases along a decaying swirl flow, because ω decreases due to dissipation of angular momentum, whereas u is maintained by the axial pressure gradient.

Presented below are some of the conclusion drawn by researchers investigating the fluid flow in pipes and annuli and the different mechanisms for convection enhancement by application of swirl flows.

Swirling Flow in Pipes

Hong and Bergles [17], experimentally observed an increase in heat transfer due to continuous swirl generated by full length twisted tape inserts in circular pipes. The Nusselt number in swirl flow was found to be a function of flow rate, tape twist ratio and Prandtl number. Huang and Tsou [18], calculated the increase in heat transfer in free laminar swirling flow in pipes. They found that naturally decaying swirl is better than a continuous forced swirl, based on heat transfer, for the same pressure drop. The enhancement in heat transfer, measured as a ratio of the Nusselt numbers of flow with swirl to flow without swirl (i.e. fully developed pipe or annular flow) varies from 3 at the inlet to 1.15 at 100 diameters. There is also an associated increase in pressure drop. However the incremental increase in heat transfer with swirl is greater than the corresponding increase in pressure drop, thereby producing a net enhancement in heat transfer. Thus, based on individual trade-off allowances, application of swirl along the length could be economically justified to increase the amount of heat transfer and perhaps minimize the amount of heat transfer materials. Studies have shown that the pressure drop increases with higher swirl angles. Also swirl decays much faster at lower swirl angles, and heat transfer enhancement is higher with high swirl angles. However, regularly boosted swirl, with smaller swirl angles, could be optimized to provide better effectiveness in heat transfer augmentation, possibly with acceptable pressure drops.

The research of Hays and West, [19] in free turbulent swirling flow in pipes estimates the ratio of experimental heat transfer coefficients, for the case with swirl to that without swirl, varying from 10 at the inlet and dropping to 3 at 17.5 diameters. This ratio is based on the heat transfer coefficient for fully developed pipe flow conditions, for example, the Dittus-Boelter Nusselt number. However, based on the corresponding heat transfer coefficient at the inlet of a pipe, without swirl, the ratio drops to 2.5. This latter comparison shows the true effect of swirl on convection enhancements in an annulus. Algifri et al., [20] also studied heat transfer for turbulent air flow in a pipe with inlet swirl generated by a radial blade cascade and reported a 90% increase in heat transfer at the inlet over fully developed pipe flow without swirl. This enhancement decreased from 90% to 40% at an axial position of 50 pipe diameters. They attributed the decrease in heat transfer to the decrease in swirl intensity. It was reported that entrance effects like those in pipe flow did not occur in swirl flow, because of turbulent mixing. They reported that the results of Hays and West, [19] were on the higher side because of experimental error introduced by the measurement of tube wall temperatures.

Analytical predictions and experimental results of Kreith and Sonju, [21] show that freely decaying turbulent swirl flow decreases to approximately 10 - 20% of its swirl number at distances of 50 pipe diameters. Swirl decay is more rapid at lower Reynolds numbers. They also found that the profile of the tangential velocity component changed drastically during the flow. Thorsen and Landis, [22] studied swirl flow heat transfer subject to large transverse temperature gradients, with the swirl being generated by a continuous twisted tape. Their conditions of large transverse gradients were achieved with wall to bulk fluid temperature ratios around 1 - 1.9 and outlet to inlet bulk fluid temperature ratios around 1 - 1.9. They also reported the effect of buoyancy forces acting during swirl flow, which aided in heat transfer during heating of the fluid. They used nichrome wire coils to heat the tube to a temperature of 923 K (1200°F) and achieved constant heat flux boundary conditions. The resulting tube wall temperature distribution was linear in the fully developed region of the fluid flow, where the convective coefficient is constant. This was a refinement to the earlier work done by Smithberg and Landis, [23] on twisted-tape generated swirl flow in tubes. Smithberg and Landis reported a study of the flow field inside tape generated swirl flow and reported that the increased heat transfer and pressure drop was a result of continuous mixing of the boundary layer and the core flow, which was labelled vortex mixing. It was expected that the boundary layer in swirl flow would be much thinner than in purely axial flows. The heat transfer was expected to result from: (1) the boundary layer flow at the tube wall; (2) the energy interchange due to vortex mixing; and (3) the fin effect of the twisted tape in contact with the wall. The authors reported a clear effect of fin effectiveness and contact resistance of the twisted-tape in the tube on tube heat transfer. With 100% fin effectiveness, there was almost a 67% increase in Nusselt number.

Gambill and Bundy, [24] conducted an evaluation of all swirl flow data available to them (in 1962) and compared them with studies conducted at Oak Ridge National Laboratories. They presented plots of Nusselt numbers versus pumping power for swirl flow and plain flow that show that swirl does increase heat transfer at the same pumping power. But this is true only below a certain threshold flow rate, above which axial flow has better heat transfer characteristics.

Lopina and Bergles, [25] represent the heat transfer phenomenon in swirl flow in the form of the following equation:

$$q_{total} = q_{spiral\ channel} + q_{centrifugal\ convection} + q_{fin}$$

which implies that, in the case of turbulent swirl flow in pipes, the increase in heat transfer is attributed to:

1 the increase in velocity of the flow along the walls of the spiral channel and the increase in contact length over axial flow, (which can also be thought of as increased residence time for fluid to be in the heat transfer tube)

2 the centrifugal convection effect experienced by the fluid during the swirl flow, which forces colder air outward against the heating concave surface, and

3 the fin effect of the twisted tape which produces the swirl.

It is conjectured that the tape may account for up to 25% of the increase in heat transfer. (It is interesting to note that this study did not attempt to include a conscious estimation of the fin effect as the authors had isolated it from heating.) Sud, et al.; [26] found a smaller fin effect of about 20% in similar conditions.

Turbulators in Heat Pipes

Inserts, also called turbulators, have been used to augment heat transfer. Three commercial turbulators were studied by Junkhan, et al., [27] and correlations were developed for heat transfer predictions. Heat transfer enhancements of the order of 65% - 175% were achieved with corresponding friction factor increases of 160% - 1110%. Their study divided the pipe length into four sections. They did observe an entrance effect, in which the entrance region had higher heat transfer coefficients than the fully developed regions.

Swirl Enhancement of Annular Heat Transfer

Computational and experimental studies by Kim, [29] in annular heat transfer arrangements reported a 1 to 1.5 time increase in heat transfer from the outer annular surface, and a 0.5 to 1 time increase in heat transfer from the inner surface with swirl over non-swirling flow. Kim's studies were in annular passage of an air blast fuel injector of a jet engine.

Convection Enhancements in a Bayonet Tube with Naturally Decaying Swirl

Experiments have been conducted at UTSI, by Knollenberg, [28] to investigate the effect of naturally decaying swirl, at Reynolds numbers of 6900 to 55400 in bayonet tubes. Convection enhancements of 40% over fully developed pipe flow were consistently reported in the swirl flow case for the entire range of flow conditions. The Nusselt number was found to depend on flow rates and the distance from the swirl generator, decreasing as the swirl decayed. The dependence of heat transfer on relative dimensions of the annular gap were also studied and an optimum diameter ratio, d_i/d_o, of 0.774 was recommended. This study was conducted at relatively cold temperatures, at which radiation heat transfer had no significant effect on transferring heat between the outer and inner surfaces of the annulus, and thus did not simulate the effects of the inner tube acting as a radiation wall on the overall system heat transfer.

Extended Surface Enhancement Techniques

Rabas, [12] noted that extended surfaces have the lowest effectiveness in the enhancement techniques because of high pressure drops. However it must be noted that in conventional extended systems, where heat is put into the fluid, the fin surface has a lower temperature than the base (primary surface) and hence the increase in heat transfer is not directly proportional to the increase in area (but depends on fin effectiveness). At the same time, the pressure drop is still proportional to the increase in surface area. In high temperature applications, the fin is expected to be heated by radiation as well as by conduction from the base, and hence will have a much higher effectiveness. In addition, use of helical fins promoting a swirl flow might be quite effective. Research in the heat transfer characteristics of silicon carbide (SiC) tubes, [30] has provided many interesting results. Because the thermal conductivity of SiC is much higher than steels and with radiation effects and the inherent geometry of the fins that are feasible to be manufactured in SiC tubes, the effectiveness of these extended surfaces was very high. Usually these fins had an effectiveness of about 95%. Heat transfer coefficients were approximately 30%-100% greater than those in plain tubes. In the case of twisted tape inserted inside a SiC tube, the heat transfer coefficient varied with the tightness of the helix. Resulting heat transfer coefficients were 30%-70% greater than those of corresponding plain tubes due to the swirl flow alone. If, in addition, radiation heating of the tape insert was considered, a 30% increase in heat transfer coefficient would be possible. This study, however, did not include the effect of helical fins in tubes, which would provide for both swirl flow and extended surfaces.

Patankar, et al., [31] have reported studies on the analysis of turbulent flow and heat transfer in tubes and annuli with longitudinal internal finning. They found the fins to be generally as effective in heat transfer as the walls. Their analysis of flow in annuli, heated from the inside with fins on the inner tube, showed that the heat transfer characteristics was similar to finned tube flow. They also reported an increase in the effectiveness of fins over the base surface with an increase in the number of fins. The analysis also throws some light on the change in convective coefficient along fin height.

Carnavos, [32] studied the heat transfer performance of internally finned tubes with turbulent air flow. The fins were integral internal fins, both longitudinal and spiral in nature. His experiments showed an increase in heat transfer with increase in spiral angle of the fins.

Jet Impingement and Swirl Flow

Tauscher, et al., [33] have shown that heat transfer can be augmented by the injection of fluid into a turbulent tube flow. They experimented with injecting water radially into a pipe having axial water flow at various ratios of mass flow rates. The heat transfer coefficient in the downstream region showed an increase in value, 2 to 8 times that of fully developed pipe flow condition at similar Reynolds numbers. The degree of increase depended on the mass flow rates, with higher heat transfer for greater amounts of radially injected fluid. The augmentation was significant in the region 0-10 diameters downstream from the point of injection, and was sensitive to the Reynolds number, decreasing in effect with increasing axial flow. It was also found that the thermal development region was lengthened and there was strong mixing in the downstream region. This study and others suggests a potential design modification for the bayonet tube heat exchanger. If holes were drilled in the bayonet tube, and air were allowed to flow into the annular passage, it would result in enhancing heat transfer at the outer shell wall due to mixing and jet impingement at the shell surface. If the air injection were tangential to the annulus, a swirl flow would also be created which would further enhance heat transfer. While this design modification merits, perhaps, some future study, in the present investigation it was not pursued.

Chapter 4

APPARATUS AND EXPERIMENTATION

4.1 APPARATUS

The heat transfer experiments were conducted using a bayonet style heat exchanger element modeled after an actual proposed ceramic bayonet tube design for applications to the US DOE CFFF test program. The test system consisted of a fluid (air) source, and an electric tube furnace. Data was collected using an automatic data acquisition system. Figure A1.3 shows a schematic of the flow circuit. The dimensions and specifications of the equipment used is as given below.

Bayonet Tube Heat Exchanger Element

Table 1 lists the main elements in the construction of the bayonet tube heat exchanger element used in the experimentation.

Table 1 Specifications of Bayonet tube heat exchanger element

Element	Material	Inner Dia.	Outer Dia.	Length
Outer Shell	S.S. 304	3.095 inches	3.5 inches	50 inches
Inner Tube	Inconel® 601	1.58 inches	1.9 inches	48 inches

Construction: The outer shell was manufactured from a regular 3 inch, schedule 40 stainless steel pipe with a hemispherical end cap welded at one end and having threads at the other. A small flange screws on at the free end. This flange is then placed in a tube sheet with glass wool and ceramic fiber board packing which acts as a seal. The tube sheet is in the form of a circular flange which can be bolted on the heat exchanger body. The shell was modeled after a closed-end Dupont Lanxide® Ceramic tube [34], and is representative of the heat exchanger element type proposed for use in an advanced air heater. The ceramic tube itself was not used because it would be difficult to instrument. The stainless steel has approximately the same thermal conductivity as the ceramic material at the temperature of the experiment, so it was a logical choice for use. The inner tube was manufactured from a regular schedule 40 Inconel® tube. One end of the Inconel® tube was welded to a stainless steel reducer which connected to the air inlet. This end is integral to the exhaust manifold, and consists of a flange welded to a dome shaped cap sealed at the bottom with a flat retainer plate. The central Inconel® tube passes through this flat plate. The flange, when bolted to the tube sheet, interspaced with necessary gaskets, seals the bayonet tube heat exchanger element. A (single) hole cut in the retainer plate, provides the exhaust passage for the gas flowing out of the annulus, through a standard one inch elbow placed in the dome shaped cap. The hole is an inch in diameter, and corresponds to the standard elbow used. It is placed at radius of 1.875 inches (3.75 BC) from the central axis of the assembly. The dome shaped cap houses the exhaust manifold for the heated gases coming out of the annulus. Alumina-silicate fiber insulation is provided inside the dome cavity to insulate the hot exhaust gas from the cold inlet gas. At a later stage of the research, a spacer ring was provided between the tube sheet and the exhaust manifold flange to provide clearance for the flow straighteners at the free end of the inner tube. These construction details can be seen in Figure A1.2.

The entire heat exchanger element was placed horizontally in a tube furnace. The bayonet tube assembly was supported at three locations. First, the shell was simply supported on the refractory lining of the oven at both ends. Next, the bayonet assembly was bolted to a support at one end of the oven, with the inner tube sticking into the shell as a cantilever. This support system was similar to a proposed installation scheme of a bayonet-style recuperator in a high temperature furnace.

Heat exchanger element instrumentation: The external surface of the shell and the tube were instrumented with thermocouples by directly welding the beads to the metal surface using a spot welder. The thermocouples in the annulus and inside the tube had exposed ends standing up straight in the air flow. A thermocouple rake was devised for measurements inside the tube, and consisted of a tube enclosing thermocouple lead wires, with the thermocouple bead sticking out perpendicularly into the air stream through holes in the tube surface. The lead wires for thermocouples measuring tube surface and the annulus air temperatures were strapped on the tube surface (thus covering some amount of the tube surface and increasing roughness). At a later stage, they were coated with a thin layer of alumina or zirconia refractory to protect the insulation from the high temperature effects. The wires exited through ducts provided near the exhaust manifold. Figure A1.4 provides a sketch of the instrumentation described above. Static pressure probes were provided at the inlet and exhaust locations of the assembly.

<u>Swirler</u>

The swirler was a manufactured by welding four helical stainless steel vanes in a short cylinder. The helix angle was 20° relative to the base, and extended for an entire pitch length. There was a slight clearance between the inner tube and the vanes (approximately 2 mm). The swirler assembly was attached to the bayonet tube by set screws and slid into the shell. Care was taken to ensure concentricity of the swirler with the shell and tube. Figures A1.5 and A1.6 provide details on swirler design and construction.

Flow Straightener

At the end of the inner tube the air changes directions to reverse flow back out through the annulus. Experiments showed that there is a marked recirculation zone at the tip of bayonet tube and in the annulus flow entrance region. To straighten the air flow in the annulus, a flow straightener, consisting of two stainless steel perforated plates and a wire mesh screen were placed at the entrance to the annulus inside the shell as shown in Figure A1.7. The purpose of the flow straighteners was to determine whether their use would significantly increase the heat transfer effectiveness of the bayonet design by reducing non-uniformity caused by the reversed flow at the tip of the central tube. The flow straighteners may or may not increase pressure drop for the bayonet design, relative to the case without flow straighteners; however data on the pressure losses was not obtained in the study. Heat transfer data was available for flow conditions with and without end-cap flow straighteners.

Electric Furnace

The furnace used was a Lindberg type 58475-3 81 8P-HL, 3 zone electric furnace with Eurotherm model 818 digital programmable controllers for each zone. The controllers had digital temperature readouts, and indicated the duty cycle and percentage power consumption continuously.

A maximum temperature ramp of approximately 10°C/minute could be achieved under no load conditions. Other oven data are:

Length: 46.5 inches overall Heated length: 39.5 inches

Voltage: 240 V AC Power: 15650 Watts

Rated temperature: 1773 K (2731°F)

Though the furnace was divided into three zones, the refractory lining separating them had broken. The end walls of the refractory were machined to allow insertion of the bayonet tube. All holes were then plugged with ceramic wool for insulation.

Air Preheater

A Lindberg type 54571 Tube Furnace with a single tube and twisted tape heat exchanger element was used as an air preheater. The furnace had a rated capacity of 6.75 KW (30 Amp, 225 V AC), and a maximum temperature of 1283 K (1849°F). The furnace was controlled by a Honeywell Dialatron 217816 controller.

Process Air

Three 25 hp Pennsylvania Compressor Co. compressors supplied standard shop air, without moisture/oil removal, at a maximum flow rate of 2.7 Kg/minute, each at a maximum air pressure of 830 KPa. The flow rate was metered with an Omega model FL-7922 in-line flow meter with a Safecase Master Test type 210 pressure gauge.

Instrumentation

Thermocouples used were all K type, though different gauge wires were used as per requirement. Rosemount® pressure transducers with ranges 0-100 psi (to measure inlet pressure) and 0-7 psi (to measure pressure drop during flow) were used for pressure measurements. Power input to the oven was measured by a regular cyclotron type GE watt-hour meter, with a minimum scale deflection of 250 W-hours.

Data Acquisition

The data was recorded using a Fluke 8842A multimeter, a Fluke 2205A switch controller and an Apple Macintosh II® running Labview® software. The computer was connected to the multimeter by a standard card and interface. The data acquisition system performed a scan of all data channels, both pressure and temperature, about every 35 seconds. It had a graphing facility that plotted out current and previous temperature profiles of the shell and tube surface, and air temperatures inside the tube and annulus versus flow path. The air flow rate, power consumption by the oven and oven temperatures were manually recorded.

4.2 EXPERIMENTATION

Experiment Methodology

The ovens were set at required temperatures and allowed to heat up until the required temperature was reached. Temperature profiles in the heat exchanger tube were monitored to ensure that steady state conditions had been reached. Steady state conditions were determined when there was no change in the temperature profiles in approximately a five minute period. Air was allowed to flow through the system and the flow rates adjusted. The entire system was allowed to reach steady state. Periodic adjustment had to be made to ensure air flow rates were constant, and the ovens maintained a steady temperature. At steady state, the data acquisition system was triggered to save temperature and pressure data. The data sampled was at least over 15 time intervals, each corresponding to a 7.5 minute period. Power consumption to the oven was recorded in this same period. The controllers on the oven indicated a periodic cycling and a variation in the power consumed over time. However the length of the time interval during data acquisition ensured the averaging of all such fluctuations. After required readings were taken, power and air flow were shut off. Three general sets of experiments were conducted.

Experiment Set One

Studies had been conducted by Knollenberg [27],on heat transfer enhancements using naturally decaying swirl. As a continuation of Knollenberg's experiments and to validate some of his results, tests were repeated using the same apparatus. The data obtained from these preliminary tests showed the following:

The inner tube did not get hot by radiation from the outer shell but by convection from the annular air. The way the heated air is removed from the annulus is a critical design problem for the bayonet-type heat exchanger, because a significant heat loss occurred from the heated gas as it flowed out of the system.

Also because the heated air is forced to exit the annulus through the single circular hole in the flange, Figure A1.2, there occurs a non-uniform flow pattern at the exit. Experimental temperature distributions show that the effects of this exit condition are felt upstream of the hole at about 30 inches from the free end of the tube, which is about 18 inches from the flange. The apparent effects of this asymmetric exit flow on heat transfer, temperature distributions, and heat transfer surface coefficient distributions will be discussed in the experimental results section.

With the availability of a new furnace with higher power and temperature rated than that used by Knollenberg, it was decided to repeat experimentation using the new furnace and higher shell temperatures.

This would attempt to introduce radiant heat transfer between the shell and the inner tube. It was expected that the shell and tube surface temperature would both be higher than the air temperature in the annulus. If this were the case, the effect of heat transfer from both surfaces to the air could be studied.

Experiment Set Two

Experiments were conducted with the new furnace and a new bayonet tube heat exchanger element (whose dimensions have been given earlier). No heat transfer enhancement techniques were used. Air was pumped through the inner tube, allowed to turn around at the capped end (no flow straighteners), then flow through the annulus and out through the flange into an exhaust manifold.

It was again observed that the exhaust manifold had a strong effect on cooling the exiting hot gases. At the same time it was observed that a characteristic temperature profile developed along the inner tube with relation to shell temperatures at steady state conditions. The end of the tube facing the shell cap end had a flat temperature profile and was much cooler than the middle half of the tube. It was observed that the air gained heat until it reached a maximum temperature as it flowed through the annulus, but lost heat when it contacted the cooler shell and tube surfaces near the exhaust. Observation of oxidation effects on the tube surface at its free end, and the characteristic central tube temperature profile at the tube free end, indicate that the air turning at the capped end of the bayonet tube sticks to the shell walls and forms a recirculation zone near the tube surface as seen in Figure A1.8. This view is corroborated by the study of Yang and Hsieh [35], on laminar flow patterns in bayonet tubes. The authors also report a drop in heat transfer coefficient (due to such a recirculation zone), until fully developed conditions are reached farther along the flow path. In the present experiment, the inner tube showed heavy oxidation in its middle section, which is probably where the air flow reattaches to the inner tube.

The capped end of the shell had been placed on refractory tube supports of the furnace, and as a result, did not receive direct heating from the heating elements. However in actual operating conditions the capped end would be in a gas stream and would receive direct heating. To simulate actual conditions it was decided to move the end cap where it would receive direct heating.

Because a base condition was required to study the effects of heat transfer augmentation techniques in bayonet tubes, it was decided to conduct a further set of experiments with flow straighteners placed at the start of the annular section of the bayonet tube, that is, at the end cap location. It was hoped that by using the flow straightener, uniform flow conditions would be created at the start of the annular flow path. This would be taken as the base condition. The subsequent presence of the swirler would produce a hopefully substantial enhancement in heat transfer from this base case. Figure A1.9 provides a pictorial view of the expected modifications in the flow due to the use of the swirler. Thus the effect of the heat transfer augmentation system would be available compared to the base case.

Experiment Set Three

This set of experiments incorporated the above mentioned design modifications, that is, using flow straighteners, placement of the shell end cap inside the furnace heating zone and an augmentation scheme. The augmentation scheme used was swirl flow generated by a four vane swirler, with 70° vane angle. The experiment matrix is as shown in Table 2 for the non-swirl flow condition and Table 3 for the enhanced (swirl) flow condition.

Table 2 Experimental test-matrix for non-swirl flow condition

Test Name	Flow Rate SCFM	Oven Temp. °C	Re_D Tube	Re_D Annulus	Expt. Set
R1	40	300	36158.4	11435.7	Set 2
R2	40	500	35468.9	11219.4	Set 2
R3	40	500	32541.5	10293.4	Set 3
R4	40	600	31978.7	10115.4	Set 3
R5	40	800	30008.3	9492.1	Set 3
R6	60	500	51903.7	16418.0	Set 3
R7	60	600	50684.1	16032.2	Set 3
R8	60	800	48579.2	15366.4	Set 3
R9	80	300	72423.1	22908.6	Set 2
R10	80	600	69866.5	22099.9	Set 3
R11	80	800	68381.5	21630.2	Set 3

Table 3 Experimental test-matrix for swirl flow condition

Test Name	Flow Rate SCFM	Oven Temp. °C	Re_D Tube	Re_D Annulus	Expt. Set
S1	30	600	25313.23	8006.99	Set 2
S2	30	900	22476.45	7109.67	Set 2
S3	30	500	23231.3	7348.44	Set 3
S4	30	900	21122.97	6681.54	Set 3
S5	40	500	35100.14	11102.75	Set 2
S6	40	700	33791.61	10688.84	Set 2
S7	40	500	32472.39	10271.55	Set 3
S8	40	900	29630.11	9372.49	Set 3
S9	60	500	54443.53	17221.38	Set 2
S10	60	700	52632.84	16648.63	Set 2
S11	60	500	51596.79	16320.91	Set 3
S12	60	900	48995.12	15497.96	Set 3

Chapter 5

ANALYTICAL MODELS OF THE BAYONET TUBE HEAT TRANSFER PROCESS

5.1 UTSI MODEL

The Heat Transfer Phenomenon

Air entered the bayonet tube heat exchanger element through the inner tube and flowed towards the free end where it turned around and flowed out through the annulus. The outer shell of the bayonet tube was heated by the furnace. Depending on the temperature regime and heat input to the shell, heat is transferred to the air flowing in the annulus by convection and to the inner tube by radiation. Depending on the temperatures of the annular air and the inner tube, the inner tube experiences an energy exchange by convection and radiation. The inner tube, thus heated, transfers a portion of its heat to the cold air flowing inside it.

Model Assumptions

In the UTSI model of the bayonet tube heat transfer process, which was developed by Dr. John P. Foote of UTSI and the author, the following conditions are assumed:

1 The flow of air in the annulus is assumed to be slug flow.

2 The thermo-physical properties used are assigned constant values appropriate to the temperature regime being analyzed.

3 The bayonet tube is sub-divided into small elements or segments, each of which has a constant, but possibly different temperature.

Consider one of the segments of the system Figure A1.10. A heat balance is conducted at each surface to account for the heat inputs and outputs. (The nomenclature is explained in figure A1.10.) Figures A1.11 and A1.12 explain the heat flow convention for the control volumes at the tube and shell surfaces. The convention adopted in the subsequent analysis is: flux is considered positive in the radially inward direction.

Basic Definitions

The parameters used in the analysis are defined as:

$T_{ao} = [T_{ao}(y) + T_{ao}(y+dy)] / 2$

$\Delta T_{ao} = T_{ao}(y+dy) - T_{ao}(y)$

$T_{ai} = [T_{ai}(x) + T_{ai}(x+dx)] / 2$

$\Delta T_{ai} = T_{ai}(x+dx) - T_{ai}(x)$

Keep in mind that y is not a radial co-ordinate in this study, but is defined as L-x.

Equations for Energy Transfer

Surface 3 energy balance:

$$q_3 = 2\pi\, \delta x\, k_2 (T_{s4} - T_{s3}) / \ln(r_4/r_3) \qquad (1)$$

however, the energy flow through surface 3 is also given by

$$q_3 = h_{s3} A_3 (T_{s3} - T_{ao}) + F_{32} A_3 E_3 - F_{23} A_2 E_2 \qquad (2)$$

using reciprocity, i.e. $F_{32} A_3 = F_{23} A_2$

$$q_3 = h_{s3} A_3 (T_{s3} - T_{ao}) + F_{32} A_3 (E_3 - E_2) \qquad (3)$$

The energy rise of the annulus air stream is given by

$$m_a\ c_{pa}\ \Delta T_{ao} = h_{s3}\ A_3\ (T_{s3} - T_{ao}) - h_{s2}\ A_2\ (T_{ao} - T_{s2}) \qquad (4)$$

where radiant heating of air has been neglected.

The heat flow to surface 2 is given by:

$$q_2 = h_{s2} A_2 (T_{ao} - T_{s2}) + F_{32} A_3 E_3 - F_{23} A_2 E_2 \qquad (5)$$

using reciprocity this becomes

$$q_2 = h_{s2} A_2 (T_{ao} - T_{s2}) + F_{32} A_3 (E_3 - E_2) \qquad (6)$$

It is obvious that :

$$m_a\ c_{pa}\ \Delta T_{ao} = q_3 - q_2 \qquad (7)$$

because the right hand side represents the energy that went into the gas by definition.

Also q_2, the heat flow into surface 2 is given by:

$$q_2 = 2\pi\, \delta x\, k_1 (T_{s2} - T_{s1}) / \ln(r_2/r_1) \qquad (8)$$

also, by energy conservation

$$q_2 = h_{s1} A_1 \, (T_{s1} - T_{ai}) \qquad (9)$$

and,

$$q_2 = m_a \, c_{pa} \, \Delta T_{ai} \qquad (10)$$

Note that also by definition, the overall heat balance must be given by:

$$q_3 = m_a \, c_{pa} \, \Delta T_{ao} + m_a \, c_{pa} \, \Delta T_{ai} \qquad (11)$$

since, axial conduction and radiation are neglected.

Application of the Model for Data Reduction

Note that the equations for the elemental or segmental heat balances can be integrated analytically, if radiation is neglected, and the heat transfer coefficients or thermal resistances are treated as constants [36]. If radiation is included, the system can be integrated numerically [10]. Also, however, if certain of the quantities in the equations are given experimental values, then the remaining quantities can be determined algebraically. Thus, the analytical bayonet heat transfer model also becomes a data reduction procedure, that is used to determine the surface heat transfer coefficients, h_{s1}, h_{s2} and h_{s3}, after experimental values for the relevant temperatures of the surface and the bulk flow are input. Note also, that the model can be exercised with and without the radiation heat transfer terms, to gauge the effects of system radiation heat transfer on the magnitudes and distribution of the heat transfer coefficients.

Equations (9) and (10) are used in the data reduction process, based on measured temperatures. To account for the effects of radiative heating on the thermocouple beads measuring air temperatures, a heat balance on the beads needs to be conducted. Since the aspect ratio of the annulus compared to bead diameter is large, each zone is modelled as an infinitely long cylinder radiating to a infinitesimal element of area. The view factor for this system may be calculated as [37],

$$F=\frac{(\sin\varphi_1-\sin\varphi_2)}{2} \tag{12}$$

where $ø_1$ and $ø_2$ are as shown in the figure A1.13

This formula assumes radiation only in one hemispherical direction. For the present case we require spherical radiation and hence incorporate a factor of 0.5.

The heat balance equation for a spherical thermocouple bead is then given by:

Net radiation from shell to thermocouple bead + Net radiation from bayonet tube to thermocouple bead = Heat convection from air to the thermocouple bead

or, mathematically

$$AF_3(\varepsilon_3\sigma T_3^4-\varepsilon_{bead}\sigma T_{bead}^4)+AF_2(\varepsilon_2\sigma T_2^4-\varepsilon_{bead}\sigma T_{bead}^4)=A\,h\,(T_{air}-T_{bead}) \tag{13}$$

where A is the surface area of the spherical bead (= πD^2), and

F_1 is the view factor to the shell = 0.6, and

F_2 is the view factor to the bayonet tube = 0.4

ε_{bead} is the emissivity of the bead and is taken as 0.5

The thermocouple bead may be modelled as a sphere in cross flow. The bead diameter is 6.35×10^{-4} m.The heat transfer coefficient from the bead to the annular air can be calculated from the equation, [38]:

$$\frac{hD}{k} = 2 + (0.4\,Re_D^{0.5} + 0.06\,Re_D^{0.67})\,Pr^{0.4}\left(\frac{\mu_s}{\mu_\infty}\right)^{0.25} \tag{14}$$

where h is the average heat transfer coefficient, D is the sphere diameter, Re_D is the Reynolds number for the flow, and Pr is Prandtl number for air and is taken as 0.707.

Hence, since the thermocouple bead temperature is a measured quantity, the corrected temperature of the air stream is given by:

$$T_{air} = T_{bead} - \frac{F_3(\varepsilon_3\sigma T_3^4 - \varepsilon_{bead}\sigma T_{bead}^4) + F_2(\varepsilon_2\sigma T_2^4 - \varepsilon_{bead}\sigma T_{bead}^4)}{h} \tag{15}$$

The temperature correction calculated depended on the surrounding surface temperatures, and could range from 2.8 °C upto 10.2 °C in an experiment.

<u>Radiation Interchange Between Surfaces</u>

In the UTSI model for the bayonet tube heat transfer process, whether used for data reduction or for theoretical performance prediction, the radiation heat transfer for the elements (or segments) of the heat exchanger model is based on a zonal method. The zonal method consists of subdividing the enclosure into a number of surface and volume zones. Each zone is small enough to be assumed to be isothermal with uniform properties. Thus surfaces and gas volumes are represented in the model by discrete elements or segments.

The geometry of the enclosure of the bayonet tube heat exchanger is approximated as a combination of (i) an annular channel closed at both ends by flat end caps, and (ii) a tube closed at both ends by flat discs. The end caps in both cases are hypothetical surfaces, which are needed to complete the enclosure while calculating exchange areas. These end surfaces represent the energy interchange between the surfaces of the tube and annulus with the inlet and outlet surfaces at one end and the end cap of the shell at the other. Assumptions regarding the temperature and emission characteristics of these surfaces need to be made so that they represent the actual conditions. They have been modelled in other literature [39], as black, porous (zero pressure drop) and isothermal surfaces. For the current case it would be more appropriate to model them as metal surfaces because of the view factors involved. The choice of the temperature would be based on air/metal temperatures in that region.

Because air is essentially a non absorbing medium, its effect is not considered in the radiation analysis. However, if the concentrations of carbon dioxide and water vapor were increased it would behave as an absorbing medium and the gas interaction in the radiation process would have to be modelled.

The view factor between elements of two concentric cylinders of equal length L with inner and outer radii r and R is given by [40],:

$$F_{33} = 1 + \frac{L}{4R} - \frac{r}{R} + \frac{2r}{\pi R}\tan^{-1}\left\{2\left[\left((R/L)^2 - (r/L)^2\right)\right]^{0.5}\right\} + \frac{L}{2\pi R}\sin^{-1}\left[1 - 2(r/R)^2\right]$$

$$- \frac{\left[4 + (L/R)^2\right]^{0.5}}{2\pi}\left\{\frac{\pi}{2} + \sin^{-1}\left[1 - \frac{2\,(r/R)^2}{4(R/L)^2 - 4(r/L)^2 + 1}\right]\right\} \qquad (16)$$

where subscript 3 denotes the inner surface of the outer cylinder, and

$$F_{32} = \frac{r}{R} - \frac{r}{\pi R}\cos^{-1}\left[\frac{(L/R)^2 + (r/R)^2 - 1}{(L/R)^2 - (r/R)^2 + 1}\right]$$

$$+ \frac{1}{2\pi}\left[\left(\frac{L}{R} + \frac{R}{L} + \frac{r^2}{RL}\right)^2 - \left(\frac{2r}{L}\right)^2\right]^{0.5}\cos^{-1}\left[\frac{(L/R)^2 + (r/R)^2 - 1}{(L/R)^2 - (r/R)^2 + 1}\,\frac{r}{R}\right]$$

$$+ \frac{1}{2\pi}\left[\left(\frac{L}{R} - \frac{R}{L} + \frac{r^2}{RL}\right)\right]\sin^{-1}\frac{r}{R} - \frac{1}{4}\left(\frac{L}{R} + \frac{R}{L} - \frac{r^2}{RL}\right) \qquad (17)$$

where subscript 2 denotes the outer surface of the inner cylinder.

In the case of a tube of radius r and length L , the view factor from one end to the other is given by:

$$F_{ee} = \frac{1}{2\,r^2}\left\{2\,r^2 + L^2 - \left[\left(2\,r^2 + L^2\right)^2 - 4\,r^4\right]^{0.5}\right\} \qquad (18)$$

The view factors from the surface of the tube and the annulus to the end plates can then be found by view factor algebra (summation and reciprocity rules.)

Based on the zone method of radiation analysis, both the enclosures, namely the annulus with end caps and the tube with end caps, are divided into isothermal segments, each segment having uniform emissivity ε. A heat balance is conducted on each zone to evaluate the radiant flux interchanges (both direct and indirect) based on the temperature at each zone at steady state. The system of equations to be solved is [41],

$$\sum \left(s_i s_j - \delta_{ij} \frac{A_j}{\rho_j} \right) W_i = - \frac{A_j \varepsilon_j E_j}{\rho_j} \tag{19}$$

where:

δ_{ij} is the Kroneker delta, $\delta_{ij} = 1$ when i=j, else $\delta_{ij} = 0$;

ρ_j is the reflectivity at the zone,

W_i is the response vector , and

ε_j is the emissivity of the surface.

E_j is the emissive power of the j surface = σT_j^4

$s_i s_j$ is the total exchange area between surface i and surface j

Instead of using view factors, total interchange areas are used to account for the energy reaching a surface both by direct interaction and indirect interaction from all other surfaces, and are evaluated from the view factors.

The above expression may be written in vector notation as

[Transfer Matrix] x [Response Vector] = [Excitation Vector]

or, mathematically as,

$$\vec{A} \times \vec{R} = \vec{E} \tag{20}$$

The net flux interchange between two surfaces $Q_{j\leftrightarrow i}$, is then given by:

$$Q_{j\leftrightarrow i} = \frac{A_i\, \varepsilon_i}{\rho_i} \left(\frac{{}_jW_i}{E_i} - \delta_{ij}\, \varepsilon_j \right) \left(E_j - E_i \right) \tag{21}$$

where ${}_jW_i$ is evaluated by solving the above equation with all $E_j = 0$, $j \neq i$. Again, this heat interchange is only due to radiation and is independent of all other modes of heat transfer.

An iterative technique based on a combination of Gauss-Seidel and Newton-Raphson techniques is used to iteratively evaluate the temperature at each zone of the bayonet tube surface and all the air temperatures inside the system. The technique accepts variable shell temperature boundary (user input) condition and uses estimates of heat transfer coefficients, based on known correlations, for convection from the three surfaces: annulus-outer, annulus-inner and tube-inner. An initial temperature distribution is assumed in the system (all temperatures may be set equal to T_{inlet}.) The temperature at each zone on the bayonet tube are next solved for, based on the latest temperature profile, so as to satisfy the heat balance.

For heat balance at each zone, the temperature T_x at that zone satisfies a non-linear equation of the form:

$$a \left(T_x\right)^4 + b\ T_x = c \tag{22}$$

where a, b and c are independent of T_x.

After obtaining T_x , the temperature at another zone is evaluated. The entire process is repeated until the entire system converges.

5.2 ALTERNATE MODELS OF THE BAYONET TUBE HEAT TRANSFER PROCESS

To better evaluate the performance of bayonet tube heat exchanger under consideration, it would be helpful to compare its performance with some standard case. Holger Martin [38], analyzed the heat transfer phenomenon in a bayonet tube based on an analytical solution to the differential equations of heat transfer in the system, neglecting radiation. He analyzed the two cases where, fluid enters the heat exchanger through the inner tube, turns around at the closed end and flows out through the annulus; and, also, the case where the fluid travels in the opposite sense. For the first case, the fluid receives heat inside the central tube from the hotter annular fluid. The annular fluid in turn receives heat from shell side convection and looses a portion of the heat at inner tube side convection, just as previously discussed for the UTSI model. Thus the inner tube temperature always lies between the temperatures of the annular fluid and fluid inside the tube. The analytical solution assumes constant boundary conditions, constant properties, and known uniform heat transfer coefficients at all heat transfer surfaces.

The temperature profile of the fluid inside the annulus and inside the tube was expressed by Martin in the normalized form as:

$$\vartheta_i(\zeta) = A\ e^{m_1\zeta} + B\ e^{m_2\zeta} \tag{23}$$

$$\vartheta_a(\zeta) = C\ e^{m_1\zeta} + D\ e^{m_2\zeta} \tag{24}$$

where, ϑ_a and ϑ_i are normalized temperature variables for the inner tube flow and outer annulus flow respectively, ζ is the normalized axial length (given below), and A, B, C, and D are constants.

The normalized temperature is given as

$$\vartheta = \frac{T - T_b}{T_{in} - T_b} \tag{25}$$

where, T is the temperature (as a function of x or y), T_{in} is the inlet temperature of the fluid into the bayonet tube and T_b is the constant shell boundary condition. The independent variable is

$$\zeta = \frac{N\ x}{L} \tag{26}$$

where x is the axial distance, l is the length of the tube and N is given by

$$N = \frac{U_i A_i}{M\ c_p} \tag{27}$$

and is the ratio of overall heat transfer coefficient times area of heat transfer at the annular inner surface, over the stream (heat) capacity of the fluid in the system.

The terms m_1 and m_2 in the above equations are given by

$$m_{1,2} = \left[1 \pm \left(1 + \frac{4}{\chi} \right)^{0.5} \right] \frac{\chi}{2} \tag{28}$$

where, χ is the ratio of overall heat transfer coefficient times area of heat transfer at the annulus outer wall to that at the inner wall, and is given as

$$\chi = \frac{U_o\ A_o}{U_i\ A_i} \tag{29}$$

The values of the constant coefficients A, B, C and D are evaluated from the boundary conditions. Martin's analysis assumes continuity in the fluid temperatures exiting the tube and entering the annulus, thus neglecting heating in the capped end of the tube. These constants are evaluated as:

$$A = -\frac{m_2\, e^{m_2 N}}{m_1\, e^{m_1 N} - m_2\, e^{m_2 N}} \tag{30}$$

$$B = +\frac{m_1\, e^{m_1 N}}{m_1\, e^{m_1 N} - m_2\, e^{m_2 N}} \tag{31}$$

$$C = + \frac{m_1 e^{m_2 N}}{m_1 e^{m_1 N} - m_2 e^{m_2 N}} \tag{32}$$

$$D = - \frac{m_2 e^{m_1 N}}{m_1 e^{m_1 N} - m_2 e^{m_2 N}} \tag{33}$$

Incorporating radiative heat transfer into this analysis does not provide for an analytical solution. If radiation is included, it is necessary to solve for the temperature distribution in the system based by a numerical technique that solves the same set of equations, but which allows for the effects of radiation. A method along these lines has been provided by Li [10], and also, of course, by the UTSI model.

5.3 ε-NTU METHOD OF HEAT EXCHANGER ANALYSIS

A common method of analyzing heat exchangers from a practical viewpoint is the ε-NTU method, ε where is the effectiveness of the heat exchanger. The effectiveness of a heat exchanger is defined as,

$$\varepsilon = \frac{\text{actual heat transfer rate}}{\text{max. possible heat transfer rate}}$$

If we assume a constant boundary condition T_b, then ε for a bayonet tube heat exchanger can be written as,

$$\varepsilon = \frac{T_{out} - T_{in}}{T_b - T_{in}} \tag{34}$$

where $0 \leq \varepsilon \leq 1$.

Thus given the effectiveness of a heat exchanger, the heat transfer rate for the bayonet tube heat exchanger can be obtained from the equation

$$q = \varepsilon \dot{m} c_p (T_b - T_{in}) \tag{35}$$

The NTU (number of transfer units) of a heat exchanger is a dimensionless parameter and is defined as

$$NTU = \frac{UA}{C_{min}} \tag{36}$$

where U is the overall heat transfer coefficient, A is the surface area of heat transfer, and C_{min} is the lower of the stream capacities of the heat exchanging streams. In the present case, the stream capacity is for a single stream, the air flow, given by

$$C_{min} = \dot{m}\, \overline{c_p} \tag{37}$$

where m is the mass flow rate of air, and c_p is its mean specific heat.

In the case of a heat exchanger with a constant temperature boundary condition the effectiveness is given as [8],

$$\varepsilon = 1 - \exp^{(-NTU)} \tag{38}$$

Thus by evaluating ε and NTU for the various experimental conditions, the performance of the bayonet tube under consideration can be compared with other standard heat exchangers, such as that given above by equation (38).

Chapter 6

RESULTS OF THE STUDY

Discussions of the General Features of the Experimental Data

Experimental data consisting of the measured temperatures were obtained and are presented in Appendix A2 and A3. Figures A2.1 through A2.8 present the axial profiles of the air temperature in the central tube and the annulus, as well as the tube surface temperature and the shell outer temperature for cases without swirl. Figures A3.1 through A3.6 provide the same data for experiments with swirl. In all of these figures, it is apparent that the air temperature increases as the air flows through the tube (right to left on the figure), experiences a temperature jump at the end cap location (x=48 or y=0), then further increases as the flow passes down the annulus towards the exit manifold (left to right on the figures). Note that the data plots show that the air temperatures do not always reach a maximum at the exit, as would be expected. In some cases, the maximum is reached upstream of the exit. This effect is believed to be due to the way the air is forced to flow out of the annulus in a single circular hole in the flange at the base of the bayonet tube. Obviously, the flow must converge to pass through the circular hole, which thus affects the flow pattern, and hence, the air heating pattern at the exit.

In the reduced data which shows the distributions of annulus surface convective heat transfer coefficient, h, provided in appendix A4, (Figures A4.1, A4.3, A4.5, A4.7, A4.9 and A4.11), the behavior of the h-distributions is one of uniformly decreasing h, until about 30 inches from the free end. At this point in the annulus flow in some tests, variations in h became quite non-uniform, oscillating up and down, and suddenly increasing at the end of the annulus flow. These non-uniform h-distributions at the end of the annulus flow are thought to be caused by the end condition caused by the exiting flow leaving through the single hole exit in the flange.

The experimental values of the convective heat transfer coefficient inside the inner tube vary from the fully developed flow heat transfer coefficients for tube flow based on the Dittus-Boelter correlation. Figures for the heat transfer coefficient distribution inside the central tube, in appendix A4 (figures A4.2 through A4.12, even numbers only), show a marked increase in heat transfer at the free end (i.e. towards x=48), as if there exists an "exit length" at that end. This may be due to the local pressure in a recirculation zone in the end cap caused by the fluid exiting into the capped end, and turning into the annulus. It is suspected that this might cause a flow constriction resulting in a decreased local static pressure, thus a higher flow velocity near the central tube inner wall and hence, a higher heat transfer coefficient.

In the data in figures A2.1 - A2.8, and A3.1 - A3.6, it is seen that the inner tube temperature is greater at the middle of the tube, that is, higher than at the base at where it passes through the base flange. The tube temperature is generally lower than the temperature of the air in the annulus as expected. On the other hand, the temperatures generally follow the trends predicted by simple analytic models, so that the experiments confirm the theoretical models. This means that the numerical models, which include radiation and can include variable heat transfer surface coefficients, should be capable of predicting the performance of this class of heat exchangers.

Radial Non-uniformity in Air Annulus Temperatures

While analyzing the temperature profiles it was observed that two different, though similar, curves enclosed the spread in the data points of the annular gas. The inner and the outer curves were determined by the height of the thermocouple beads in the annular air stream. This indicates a radial temperature gradient in the annulus flow, deviating from our assumption of slug flow. It was beyond the scope of this research to determine the radial temperature distribution due to the nature of the equipment design. The temperatures were simply averaged to provide the bulk temperature of the air. It should be recognized that the actual bulk temperature is the integrated average temperature across the velocity profile. In spite of such a cognizance, the slug flow assumption and the arithmetically averaged radial temperatures were used in the study.

Effect of Radiation on a Bayonet Tube Heat Exchanger

In his analysis of bayonet tube heat exchangers Li, [10] states that, if radiation is neglected in a bayonet tube heat exchanger wherein fluid is being heated in an annulus-tube flow path, the maximum temperature reached by the fluid is at the capped end of the shell. However, if radiation is included the maximum temperature reached is at about 76 percent of its flow length inside the central tube. Li shows that radiation has its greatest effect in the heating of the central fluid. His calculations also predict that for high shell temperatures, the inner central tube can be at a higher temperature than the annular air. It was observed in the present experiments, that the inner tube temperature was indeed higher than the annular gas for a small portion of its length, at about 62 percent of its length from the end cap, or free end, especially at high oven temperature conditions. The inner tube temperature axial distribution generally followed the shell axial temperature profile. At lower temperatures, the inner tube was heated more by convection from the annular gas, when the gas was at a higher temperature than the central tube. However, the inner tube did not contribute the most to heating the air at either lower or higher shell temperatures. The rise in air temperature was always greatest in the annular part of the bayonet tube heat exchanger. The greatest temperature rise in the air occurred in the annular flow at the greatest shell temperatures, and at the lowest flow rate. However, the greatest energy transfer rate occurred at the highest flow rates, for each shell temperature.

Effect of Swirl Flow

Swirl was seen to have a significant effect on both the temperature distributions as well as on the heat transfer. Heat transfer coefficients with swirl flow conditions were about 2-3 times the non-swirl flow condition values. By comparing the experimental temperature profiles of the system for non-swirl and swirl flow, figures of appendix A2 and A3 respectively, the initial 25 inches of the shell has a gradually increasing temperature for swirl flow. In the case of non-swirl flow the increase is much more rapid. This implies that the heat transfer coefficient at the shell outer surface is much greater for the swirl case than the non-swirl case, because the heat flux distribution on the shell outer surface remains the same for both cases. The heat transfer coefficients for swirl flow cases were seen to increase drastically, over the fully developed tube flow value and also over the inlet heat transfer coefficient for the non-swirl cases, immediately downstream of the swirler. As figures A4.1 - A4.12 show, the heat transfer coefficients in the annulus decreased along the flow path. However, this decrease was much slower than with the non-swirl cases.

Results of the Theoretical Predictions made with the UTSI Model

The UTSI numerical model was set up to predict the surface and air temperatures for cases without swirl, but with and without radiation effects. In order to account for radiation heat transfer, the emmissivities of all surfaces, real and fictitious, must be a priori defined or specified. The thermo-physical constants used were determined at average (air and surface) temperature conditions for each experiment. The values used are listed in Table A6.1.

Emissivity is a surface phenomenon and depends on surface conditions, surface temperature and on wavelength. The UTSI theoretical model was exercised with reasonable estimates of overall hemispherical emissivity for the shell and tube surfaces. Emissivity values selected for the shell and bayonet tube for each experiment are also listed in Table A6.1. These values are constant over an experiment set (i.e. set 2 and set 3). The use of different values of emissivity over time (i.e. for the different experiment sets) was attributed to surface effects for oxidation and foreign particle deposition on the inner tube surface.

Required Modifications to the Theoretical Models

In Martin's simple analytical (convection-only) model [36], and in Li's iterative technique [10], it was assumed that the air temperatures at exit of the inner tube and entry to the annulus are equal. However the experiments showed that this is not the case if there is heat transfer at the capped end of the shell. There can be a sharp jump between the temperature of air at the exit of the inner tube and entry into the annulus if the end cap is exposed to high temperatures. Rather than model the heat transfer mechanism at the capped end, which was unknown, a jump discontinuity in air temperatures was applied based on actual experimental values. Corresponding equations thus had to be modified suitably. Table A6.2 gives the jump discontinuity for each experiment condition.

As previously mentioned, correlations do not exist for heat transfer coefficients at either surface of the annulus in a bayonet tube heat exchanger. As a first approximation, fully developed tube flow coefficients based on the Dittus-Boelter correlation for Nusselt numbers, given as

$$Nu = \frac{h\,D}{k} = 0.023\,Re^{0.8}Pr^{0.4} \tag{39}$$

was used, where D was the corresponding annulus hydraulic diameter, to predict heat transfer in the model. The corresponding values of the heat transfer coefficients at both the annular surfaces (which have equal values of h), and the tube inner surface, for fully developed non-swirl flow conditions are listed in Table A6.2. It was found that the air temperature rise was consistently over-predicted by these values. But as these coefficients have an uncertainty of up to ±30%, [38] calculations were repeated with lower estimates of the convective heat transfer coefficient, specifically at 80% of the values predicted by the correlation equation, and these calculations resulted in much closer comparisons of theory to experiment.

Finally, for a closer fit of data with the theoretical model, an entry length correction was also incorporated. The entry length heat transfer coefficient was based on the correlations for short circular tubes. Kreith, [38] provides the following correlations for short tube ($2<x/D_h<60$) flow heat transfer coefficient:

$$\frac{h_{cL}}{h_c} = 1+\left(\frac{D_h}{x}\right)^{0.7} \qquad 2<\frac{x}{D_h}<20 \tag{40}$$

$$\frac{h_{cL}}{h_c} = 1+6\left(\frac{D_h}{x}\right) \qquad 20<\frac{x}{D_h}<60 \tag{41}$$

where x is the axial position along the flow length, D_h is the hydraulic diameter, h_{cL} is the heat transfer coefficient corresponding to the entry length, and h_c is the fully developed value predicted by the Dittus-Boelter correlation. The utilization of these corrections helped predict the air and inner tube temperature more accurately.

Figures A5.1 through A5.4 show comparison between predicted air and surface temperatures with corresponding experimentally measured temperatures. To demonstrate the capability of the analytical model of Martin [36], that does not incorporate radiative heat transfer, an experiment with a relatively low shell temperature was selected as the experiment for comparison. This is experiment R1 from experiment set 2, Table 2. In order to apply the analytical model to this experiment, the shell temperature which varied over the length of the shell, was averaged to give a single constant boundary temperature of 93.62 °C, as Figure A5.1 indicates.

Figure A5.1 shows that, using constant values for the convective heat transfer coefficients that were based on fully developed (pipe and annulus) flow at equivalent Reynold's numbers resulted in a good prediction for the air temperature in the tube, but rather poor prediction for the air temperature in the annulus flow. Of course, better predictions could be obtained by reducing the value of the annulus heat transfer coefficient. However, this was not of interest in the present study, because the UTSI numerical model is more general, and includes the effects of radiation heat transfer.

Figures A5.2 through A5.4 show the results of applying the UTSI numerical model to predict the temperatures of the air and the various surfaces of the bayonet heat exchanger. Figure A5.2 shows the same experimental case as that of Figure A5.1, test R1, so that the analytical model can also be compared to the numerical model. Figure A5.2 shows that all of the temperatures predicted compare very well to the corresponding experimentally measured temperatures, except, again, the air annulus temperature. This is also, as in the case of the analytical model, attributed to using too high a value for the annulus surface heat transfer coefficient. Nevertheless, the overall results are very favorable, at this low shell temperature. Note that the actual shell temperature distribution was incorporated in the numerical solution, rather than an averaged value that the analytical model requires.

To continue the evaluation of the UTSI numerical model, a different experiment was selected for comparison, experiment R5, Table 2. This experiment has the same flow rate as that used for figures A5.1 and A5.2, but the shell temperature is significantly greater. Again, agreement between the numerical solution and the experimental data is very good. The annular air temperature is also reasonably well predicted.

To investigate the effects of varying the surface heat transfer coefficients on the predicted temperatures , a calculation of the same experiment, R5, was made with the surface heat transfer coefficients in both the tube flow and the annulus flow reduced to 80 percent of the fully developed flow values at the same Reynolds numbers with a superimposed inlet effect. The fully developed flow heat transfer correlations used are based on the Dittus-Boelter equation, and the inlet effects are derived from equation (2) and (3), above for short tubes. The results of the calculation are shown compared to the experimental data in Figure A5.4. The results show a slightly better prediction of the inner tube temperature, but overall, not a great deal of change in the theoretical predictions has been achieved by lowering the surface heat transfer coefficients to 80 percent of the fully developed values.

The best calculated results should come from predictions made using the surface coefficient distributions that were experimentally obtained in the present study. Figure 5.5 shows one such effort. The heat transfer coefficients used in the analysis were based on the family of heat transfer coefficient distributions of the outer-annulus and central tube corresponding to a flow rate of 40 scfm. These distributions can be found in Figure A4.1 and A4.2 respectively. A curve-fit of the h-distribution yielded the following equations:

$$\frac{Nu_{\text{ann actual}}}{Nu_{\text{ann fd}}} = 2.4462\, x^{-0.54971} \quad \text{with } R = 79.35\%,$$

and

$$\frac{Nu_{\text{tube actual}}}{Nu_{\text{tube fd}}} = 3.8853\, x^{-0.57255} \quad \text{with } R = 87.61\%,$$

where R is the coefficient of correlation. The heat transfer coefficient at the annulus inner wall was based on the Dittus-Boelter correlation.

Based on these modifications the model under-predicted the annular air temperature. The predicted bayonet temperature however, matched up in segments with the experimental temperature. This is a further validation of the UTSI model. No other test cases were attempted as this was beyond the scope of the present study and is left for future work.

ε-NTU Relationship for the Bayonet Tube Heat Exchanger

It has been seen that swirl flow increases the heat transfer coefficient over non-swirl flow for the conditions studied. Everything else remaining constant, the NTU of a swirl enhanced heat exchanger is greater than a non-swirl flow enhanced heat exchanger, because of the increase in the overall heat transfer coefficient. Recall that NTU means "number of transfer units" and is defined as

$$\mathrm{NTU} = \frac{U_o A}{\dot{m} c_p} \tag{42}$$

where U_o is the overall heat transfer coefficient, A is the heat transfer surface area and mc_p is the stream capacity. The experimental data for the bayonet tube heating process was used, together with equation (34), to calculate the heat transfer effectiveness of non-swirl and swirl flow experiments. The resulting effectiveness is plotted in figure A5.6, versus NTU. Also plotted on this figure is the ε-NTU relationship for any heat exchanger under the conditions of constant surrounding temperature. As the data in this figure shows, there is close agreement between the measured bayonet tube heat transfer effectiveness and the general equation for any heat exchanger (for the mentioned boundary condition). The value of NTU used to reduce the data was calculated from the definition of NTU, where for a single stream, double-pipe, bayonet heat exchanger U_o was given by,

$$U_o = \frac{\dot{m}\, c_p \left(T_{out} - T_{in}\right)}{A\left(T_b - \dfrac{T_{out} + T_{in}}{2}\right)} \tag{43}$$

and, A is the heat transfer area at the annulus outer surface given by,

$$A = \pi\, D\, z \tag{44}$$

where D is the shell diameter and z is the length of the heat exchange surface under consideration and is listed in Table A6.3 for each case.

To the authors knowledge, this data represents the only reported experimental data on double-pipe, bayonet tube heat exchanger effectiveness for both swirl flow and non-swirl flow conditions in the annulus flow.

Chapter 7

SUMMARY AND CONCLUSIONS

7.1 SUMMARY

Annular Heat Transfer

In the double-pipe, bayonet-type heat exchanger, there is a significant increase in the convective heat transfer coefficient in the annulus flow due to swirl flow. Heat transfer coefficients 3-7 times the fully developed flow value, at corresponding Reynolds numbers, were observed. Compared to the heat transfer coefficients at the inlet for non-swirled flow conditions, the enhancement was approximately 2-3 times. This enhancement is predominantly at the annulus outer surface. The local heat transfer coefficient decreases almost linearly along the flow path from the annulus inlet to a length of about 20-30 inches from the inlet (corresponding to about 18-27 hydraulic diameters,) where it approaches (with some observed oscillations) a constant value for the rest of the flow inside the annulus. A similar phenomenon was observed with non-swirled flow inside the annulus, however in the non-swirled flow case, the annulus-outer heat transfer coefficient decreased much faster to a constant value. These terminal heat transfer coefficients were different in both the swirl flow and non-swirled flow cases. For non-swirled flow, the terminal heat transfer coefficient was smaller than that predicted by the Dittus-Boelter correlation for tubes with the same hydraulic diameter. In the case of swirl flow, the corresponding heat transfer coefficient was more comparable with the Dittus-Boelter value. It is inappropriate to call these terminal convection coefficients fully developed flow heat transfer coefficients because the actual flow conditions are unknown, and they are affected by the exit flow conditions of the annulus fluid.

Performance Predictions using Models

The numerical model used to predict heat transfer in the bayonet tube system performed quite satisfactorily in matching the experimental data, even though the convective coefficient at the outside of the (central) tube could not be accurately evaluated nor were the emissivity values used exact. The model was, however, flexible enough to incorporate axial distributions of heat transfer coefficients and surface emissivities. The model provided an estimate of the relative magnitudes of heat transfer from the various surfaces. It was observed that the heat convected from the inner tube outer surface to the annular air was quite negligible compared to that from the shell. This is because the thermal potential, that is, the heat transfer coefficient times temperature difference of the shell is much higher than that at the inner tube. The inner tube does provide some small amount of heating of the air inside the tube, but not the major part.

It was found that the performance of the bayonet tube heat exchanger (with an assumed constant temperature boundary condition) matched well with general ε-NTU correlations for any heat exchangers with a constant surrounding temperature. Swirl helped boost the exchanger effectiveness. The use of swirl promises a reduction in size of the exchanger for the same performance. This was, in fact, one of the premises of this research.

Radiation Heat Transfer

Radiation plays an important role in transferring heat from the shell to the inner tube. This is evident from the temperature profile of the inner tube, which quite closely follows that of the shell. The radiant energy exchange between the two surfaces is dependent on the emissivities, increasing as emissivity and the temperature difference between the two surfaces.

Flow Patterns inside the Bayonet Tube Heat Exchanger System

The design features of the particular bayonet tube assembly under study further confounded the already complex nature of the fluid flow inside the bayonet tube element. As a result, there were believed to be significant recirculation zones near the exhaust manifold and near the capped end of the shell, inside the annulus. Inside the central tube, recirculation zones existed near the free end. Due to these flow phenomena, there are significant heat losses and drops in effectiveness. At the same time, it was noted that there is significant amount of heat transfer at the capped end of the bayonet tube where the flow reverses direction. Due to the impingement flow there is a jump in air temperature between the exit of the tube and entry to the annulus.

It is observed that inlet and exit manifolds are critical in the successful design of a bayonet heat exchanger because of the cooling effects associated with the unheated portion at these manifolds. The exit gas temperature fell considerably as it contacted these cooler ends.

Thus, the performance of bayonet tube heat exchangers can be improved by:

- the use of swirl at strategic locations along the length of the tube, taking advantage of both natural increase in convection due to inlet conditions and swirl flow enhancement,
- the use of convection enhancement devices inside the inner tube,
- the use of radiation enhancing coatings on the exchanger surfaces to increase preheating of the fluid before it enters the annular path, and
- the proper manifolding of inlet and exit air flow paths.

7.2 CONCLUSIONS

This research has successfully demonstrated the use of swirl as a convection enhancement technique that can be efficiently used in bayonet tube heat exchanger technology. As these experiments have been conducted on a full scale industrial (although prototype) design, they served as proof of concept testing, as well as a source of engineering data. Previous experiments conducted in industrial applications of bayonet tube heat exchangers [2], did not consider convection enhancement as an integral element of their technology. Practical applications however, will mandate the use of enhancement techniques, especially because of economic considerations.

Engineering data on heat transfer in annuli, with or without swirl is quite limited, especially for flows in industrial equipments. The analysis has shown that for steady state conditions, the use of fully developed flow correlations to predict heat exchanger performance can be quite erroneous. These experiments provide much needed information to reliably predict equipment performance. Distributions of heat transfer coefficients in an annulus with and without swirl flow show the deviation from fully developed flow values.

The model developed to predict bayonet tube heat exchanger performance was verified with actual experimental data and was proven to be an invaluable design tool. The model incorporated radiative heat transfer between surfaces of the heat exchanger and convective heat exchange with air. It had the capability to accept (variable) true outer shell temperature boundary conditions and distributions of heat transfer coefficients along the flow path. Using such a technique, the design of a bayonet tube heat exchanger can be optimized and its performance accurately predicted.

ε-NTU curves developed during this analysis from the experimental data, provide a handy method to compare and evaluate bayonet tube heat exchangers.

Chapter 8

RECOMMENDATIONS

This chapter seeks to examine some of the problems faced during this research and provide a critique on the analysis technique. Recommendations based on the experience of this experimentation, analysis and associated literature survey can be categorized as:

- Requirement of a modular approach to experimentation
- Flow visualization requirements
- Modifications in equipment and apparatus
- Analytical techniques

This experiment tried to analyze the effects of and the inter-relationship between the many variables associated with flow and heat transfer in a bayonet tube heat exchanger element. The following variables could not be exactly determined prior to analysis:

1. power input and distribution, and power losses,
2 ε_{shell}, $\varepsilon_{bayonet\ tube}$, $\varepsilon_{thermocouple\ tip}$ were all assumed values,
3 $h_{annulus}$, h_{tube} were based on correlations,
4 the flow phenomena involved (which was quite complicated)

5 there is no cross-check available for calculated values of radiative heat transfer.

It is extremely advisable to divide the current problem into simpler ones that can be more deterministically solved. The complete solution comprises characterizing:

the flow and heat transfer in the annulus,

the radiative heat transfer between the surfaces,

the flow and heat transfer in the tube, and

the flow and heat transfer in the capped end of the shell.

It is obvious such an approach would require a different experimental setup. The following paragraphs describe some of the problems encountered with the current apparatus and could serve as a list of caveats in subsequent design processes.

The instrumentation of the tube was very cumbersome. The operational conditions (high temperatures) had destructive effects on the thermocouples used, which had to be changed every test. The thermocouple leads were also on the tube surface thus creating some amount of flow obstruction. Because the furnace was heated from the top and bottom there were definitely temperature gradients along the circumference of the shell. An axial temperature gradient developed due to the higher cooling rate at the shell cap and the connection to a heat sink at the flange end of the shell and tube. This also caused some cooling of the air as it exited the annulus. Researchers of similar problems have not used tube furnaces for heating. Their heating methodologies have been heating-coils wrapped around the tubes or direct electrical resistance heating of the tubes. As a result the heat transferred to the internally flowing air can be directly measured from the power input to the tube. Hence temperature was functionally dependent on power and not an independent variable as in the case with the current experiments. In addition the axial variation of heat input could be more easily controlled.

In the present study heat flux was not a measured quantity. It was calculated based on the temperature profile in the metal and the convective heating of the air. Due to experimental limitations, calculated quantities could not be checked for accuracy. Heat flux gauges are necessary to determine convective coefficients from the inner and outer surfaces of the annulus. However, such devices were not available for the temperature regime investigated. The radiative fluxes calculated were based on tabulated values of emissivity for the various surfaces obtained from literature. Variation in the values of emissivity due to surface finish and condition have not been verified. Most reported experiments do not allow a large temperature differential between inner and outer annulus surfaces, which contribute to uncertainties in calculating the radiant flux contribution. Large temperature gradients in the air flows at some positions also imply that a radial temperature profile does exist in the annulus air. However, the data reduction analysis and the numerical model are based on slug flow conditions, and arithmetically averaged air temperatures at a given axial station may not represent true bulk conditions fluid conditions.

Temperature corrections have been incorporated to account for radiative heating of the thermocouples. However exact values for emissivity of the thermocouple beads could not be obtained.

Heat transfer correlation studies often report correlations for fully developed flow heat transfer . The bayonet tubes of the dimensions investigated in the present study did not exhibit well developed flow heat transfer conditions over any portion of their length. This makes it difficult to correlate the experimental result with correlations for fully developed flows.

The current research effort needs refinement in terms of actual flux measurements and using different enhancement geometries. Most heat transfer experiments reported in journals strive to achieve a very close balance between heat input to the system and heat gain by the exiting fluid. All of the heat exchanges should be very deterministic in nature, i.e. should balance as closely as possible. In the present study, there is significant amount of uncertainty involved in calculating heat exchanges. Close control of the heating mechanism could not be maintained in the present apparatus.

Further Research

The UTSI model for analysis of the bayonet tube heat exchanger provides an useful tool for bayonet tube heat exchanger performance anaysis and design. It can be further developed to provide more accurate performance modelling using better estimates of heat transfer coefficient distributions and surface emissivities. The model is only based on heat transfer, but might also be extended to incorporate the fluid physics into it. Such a tool would be invaluable while designing heat exchanger systems at the cutting edge of technology.

A significant portion of the current research is in convection enhancement. There exist other methods and options to augment convection. The following methods for heat transfer augmentation have been suggested by Bergles, [39]: repeated rib roughness inside tube with a helical character, integral inner tube finning, external surfaces with augmentation, displaced promoters - for very large scale augmentation over small distances with less severe pressure drop penalty, full length and interrupted twisted tape inserts, compound techniques involving two or more augmentation techniques. It would be interesting to study the heat transfer effectiveness of external spiral finned inner tubes at high temperatures (assuming that manufacturing an integrally finned ceramic shell is not possible and hence extended surface can only be provided on the inner tube). It is felt that the fins would provide extra surface area for heat transfer while being at a temperature closer to the outer shell temperature. The inner tube would receive radiation from the outer tube and transfer some amount of it to the air flowing inside it. Because the amount of air over the inner tube would be reduced, due to surface crowding by the presence of fins and swirling flow, its cooling effect on the hotter annulus air would decrease.

LIST OF REFERENCES

LIST OF REFERENCES

[1] Thompson, T. R., Chapman, J. N., and Boss, W. H., "Application of High Temperature Air Heaters to Advanced Power Generation Cycles," Proceedings of the American Power Conference

[2] U.S., D.O.E., Office of Industrial Programs, "Evaluation of a High-Temperature-Burner-Duct-Recuperator System."

[3] Jobst W. Seehausen, "Radiation Recuperators - High Temperature Heat Recovery Systems that advance thermal processes," Industrial Heating, Jan. 1984

[4] Crawford, L. W., et al, "Nitrogen Oxide Control in a Coal Fired MHD System," DOE Contract Number DE-AC02-79ET10815

[5] Boss, W. H. and Babu, S., "An investigation into the feasibility of a Radiant Recuperator Air-heater for a MHD/Steam Power Plant," UTSI Oct 1989, DOE-ET-10815-139

[6] Stewart Way, "Application of Radiative Recuperators in MHD Power Plants," Eighth International MHD Symposium, Moscow, 1983

[7] DeBellis, C. L. and Kneidel, K. E., "Thermal and Fluid Design of a High Temperature Ceramic Fiber Composite Heat Exchanger.", AIChE Heat Transfer Symposium, Pittsburgh 1987

[8] Kays, W. M. and London, A. L, "Compact Heat Exchangers," McGraw Hill Book Company, 1964

[9] Bliem, C., et al, "Ceramic Heat Exchanger Concepts and Materials Technology," Noyes Publication, 1985, pp 14

[10] Li, C. H., "Analytical Solution of the Heat Transfer Equation for a Bayonet Tube Heat Exchanger.", ASME paper 81-WA/NE-3

[11] Yamada, Y., Akai, M., Mori, Y., "Shell and tube side heat transfer augmentation by the use of wall radiation in a cross flow shell and tube heat exchanger," Journal of Heat Transfer November 1984

[12] Rabas, T. J., "Selection of Energy efficient enhancement geometry for single phase turbulent flow inside tubes.", National Heat transfer Conference 1989, HTD Vol. 108

[13] Bergles, A. E., "Enhanced Forced Convection," Section 503.10, General Electric Company Heat Transfer Data Book, January 1978, pp 1-30

[14] Petukhov, B. S., and Roizen, L. I., "An Experimental Investigation of Heat Transfer in a Turbulent Flow of Gas in Tubes of Annular Section." Translated from Teplofizika Vysokikh Temperatur (High Temperature Institute, Academy of Sciences of the USSR),Vol. 1, No. 3, pp 416 - 424

[15] Petukhov, B. S., and Roizen, L. I., "Generalized Dependencies for Heat Transfer in Tubes of Annular Cross Section." Translated from Teplofizika Vysokikh Temperatur, (High Temperature Institute, Academy of Sciences of the USSR), Vol. 12, No. 3, pp 565 - 569

[16] Kays, W. M, and Leung, E. M., "Heat Transfer in Annular Passages: Hydrodynamically Developed Turbulent Flow with Prescribed Heat Flux," Intl. Journal of Heat Mass Transfer, Vol. 6, pp 537-557, 1963

[17] Hong, S. W., and Bergles, A. E., "Augmentation of Laminar Flow Heat Transfer in Tubes by means of Twisted Tape Inserts," Journal of Heat Transfer, May 1976

[18] Frank Huang and Tsou,F. K., "Friction and Heat Transfer in Free Laminar Flow in Pipes." Dept. of Mechanical Engr. and Mechanics, Drexel University, Philadelphia, PA, 1978

[19] Hays, N., and West, P. D., "Heat transfer in free swirling flow in a pipe.", Journal of Heat Transfer, Aug. 1979

[20] Algifri, A. H., et al, "Heat Transfer in the Turbulent Decaying swirl flow in a circular pipe," Int. Journal of Heat Mass Transfer, Vol. 31, No. 8, pp 1563-1568

[21] Frank Kreith and Sonju, O. K., "The Decay of a Turbulent Swirl in a Pipe," Journal of Fluid Mechanics 1965, Vol. 22, part 2

[22] Thorsen, R., and Landis, F., "Friction and Heat Transfer Characteristics in Turbulent Swirl Flow Subjected to Large Transverse Temperature Gradients.", Journal of Heat Transfer, February 1968

[23] Smithberg, E., and Landis, F., "Friction and Forced Convection Heat Transfer Characterization in Tubes with Twisted Tape Swirl Generators," Journal of Heat Transfer, February 1964

[24] Gambill, W. R., and Bundy, R. D., "An Evaluation of the Present Status of Swirl Flow Heat Transfer.", ASME paper number 62-HT-42

[25] Bergles, A. E., and Lopina, R. F., "Heat transfer and pressure drop in tape generated swirl flow of single phase water.", Transactions of ASME, August 1969

[26] Sud, Y. C., et al, "Contribution to Swirl Flow Heat Transfer and Friction Factor Calculations," Institute of Engineers (India) Journal, Mechanical Engineering Division, Vol. 48, pp 34-43, September 1967

[27] Junkhan, G. H., Bergles, A. E., Nirmalan, V., Ravigururajan, T. "Investigation of Turbulators for Fire Tube Boilers.", Journal of Heat Transfer Vol. 107, May 1985

[28] Knollenberg, P. J., "An Experimental Investigation into Convection Enhancements by means of naturally decaying swirl.", M. S. Thesis, The University of Tennessee, Knoxville, May 1992

[29] Kim, J. C., "Computational and Experimental Investigation of Annular Heat Transfer with Swirl.", Ph.D Dissertation, The University of Connecticut 1992

[30] Armstrong, R. D., and Bergles, A. E., "A study of enhanced ceramic tubes for high pressure waste heat recovery," Renssalear Polytechnic Institute, Troy, NY, USA 10-EH-04

[31] Patankar, S. V., Ivanovic, M, and Sparrow, E. M., "Analysis of Turbulent Flow Heat Transfer in Internally Finned Tubes and Annuli.", Journal of Heat Transfer Feb. 1979, Vol 101

[32] Carnavos, T. C., "Heat Transfer Performance of Internally Finned Tubes, Advances in Enhanced Heat Transfer.", The 18th National Heat Transfer Conference 1979

[33] Tauscher, W. A., Sparrow, E. M., and Lloyd,J. R., "Amplification of Heat Transfer by Local Injection of Fluid into a Turbulent Pipe Flow.", Int. Journal of Heat Mass Transfer, Vol. 13, pp 681-688

[34] UTSI Drawing Number SK 0479, "HTAH Bayonet Tube Installation CFFF/LMF5 Test Series," DOE Contract Number DE-AC02-79ET10815

[35] Yang, S. L., and Hsieh, C. K., "Fluid flow and Heat Transfer in a single pass return flow Bayonet heat exchanger.", ASME Proceedings of 1988 National Heat Transfer Conference.

[36] Holger Martin, "Chapter One: Analysis of some standard types of heat exchangers on an elementary basis," Heat Exchangers, Hemisphere Publishing, 1992

[37] Robert Siegel and John R. Howell, "Appendix C Equation 2, Catalog of Selected Configuration Factors.", Thermal Radiation Heat Transfer, Third Edition, Hemisphere Publishing Corporation, 1992.

[38] Frank Kreith, "Equation 9-4c.", Principle of Heat Transfer, Third Edition, Harper & Row Publishers, 1973.

[39] D. Voelkel and Frank P. Incropera, "Performance model of a Radiation Recuperator.", Heat Transfer Engineering Vol. 5, Nos. 1-2 1984.

[40] Bergles, A. E., "Suggestions for Further Research.", Turbulent Forced Convection in Channels and Bundles, Vol. 2, editors Kakaç, S., and Spalding, D. B., Hemisphere Publishing Corporation, 1979

BIBLIOGRAPHY

BIBLIOGRAPHY

Hottel, H. C., and Sarofim, A. F., Radiative Transfer, McGraw-Hill Book Company 1967

Boss, W. H., and Schulz, R. J., "The Development of Convection Enhancing Techniques for a High Temperature High Pressure Air Heater.", Unsolicited proposal to D. O. E. , UTSI 1991.

Puchkov, P. I., and Vinogradov, O. S., "Heat transfer and Hydraulic Resistance in Annular Channels with Smooth and Rough Heat Transfer Surfaces.", The Central Boiler and Turbines Institute im I. I. Polzunov

Marner, W. J., and Bergles, A. E., "Augmentation of Tube-side Laminar Flow Heat Transfer by Means of Twisted Tape Inserts, Static Mixer Inserts, and Internally Finned Tubes."

Shevchenko, S. N., and Bryukhanov, O. N., "Heat Transfer in Radiative Recuperators with Perforated Cylindrical Inserts.", Heat Transfer Soviet Research, Vol. 20, No. 2, March - April 1988

Incropera, F. P., and DeWitt, D. P., Fundamentals of Heat and Mass Transfer, John Wiley and Sons, Third Edition

Bergles, A. E., "Techniques to Augment Heat Transfer.", Handbook of Heat Transfer Fundamentals - edited by M. R. Warren, McGraw-Hill, 1985

Bergles, A. E., "Heat Transfer Enhancement - Applications to High Temperature Heat Exchangers.", Heat Transfer in High Technology and Power Engineering, edited by Yang, W. J., and Mori, Y., Hemisphere Publishers, 1987.

"Forced Convection", General Electric Company - Heat Transfer Data Book, Section 503, Jan. 1978.

Kakac, S., Shah, R. K., and Win Aung, Handbook of Single-Phase Convective Heat Transfer, Wiley Interscience 1987

Nakra, N. K., and Smith, T. F., "Combined Radiation - Convection from a Real Gas.", Transactions of the ASME, February 1977

Smith, T. F., and Clausen, C. W., "Radiative and Convective Transfer for Tube flow of a Real Gas."

APPENDICES

APPENDIX A1

FIGURES

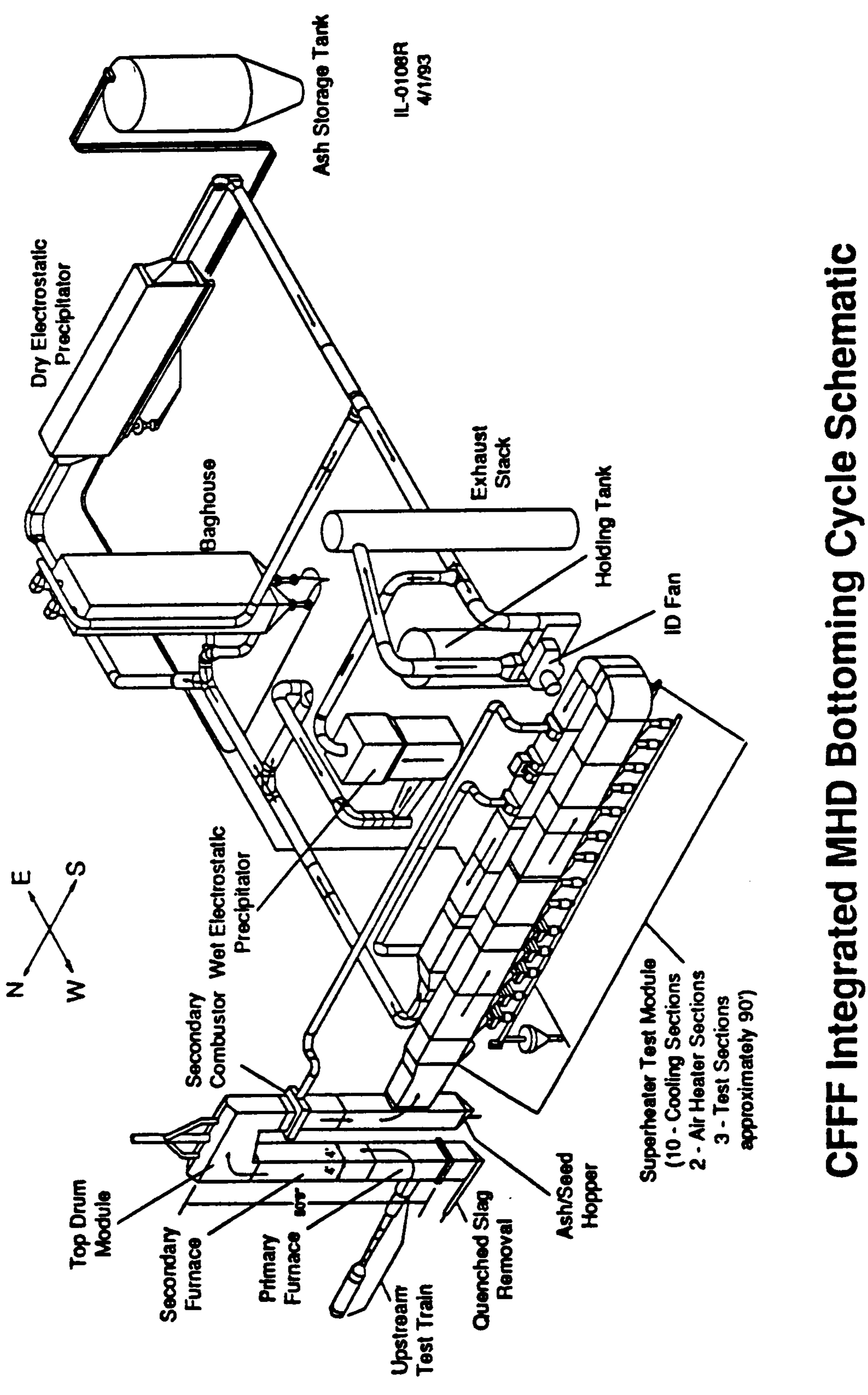

Figure A1.1 Coal Fired Flow Facility Schematic

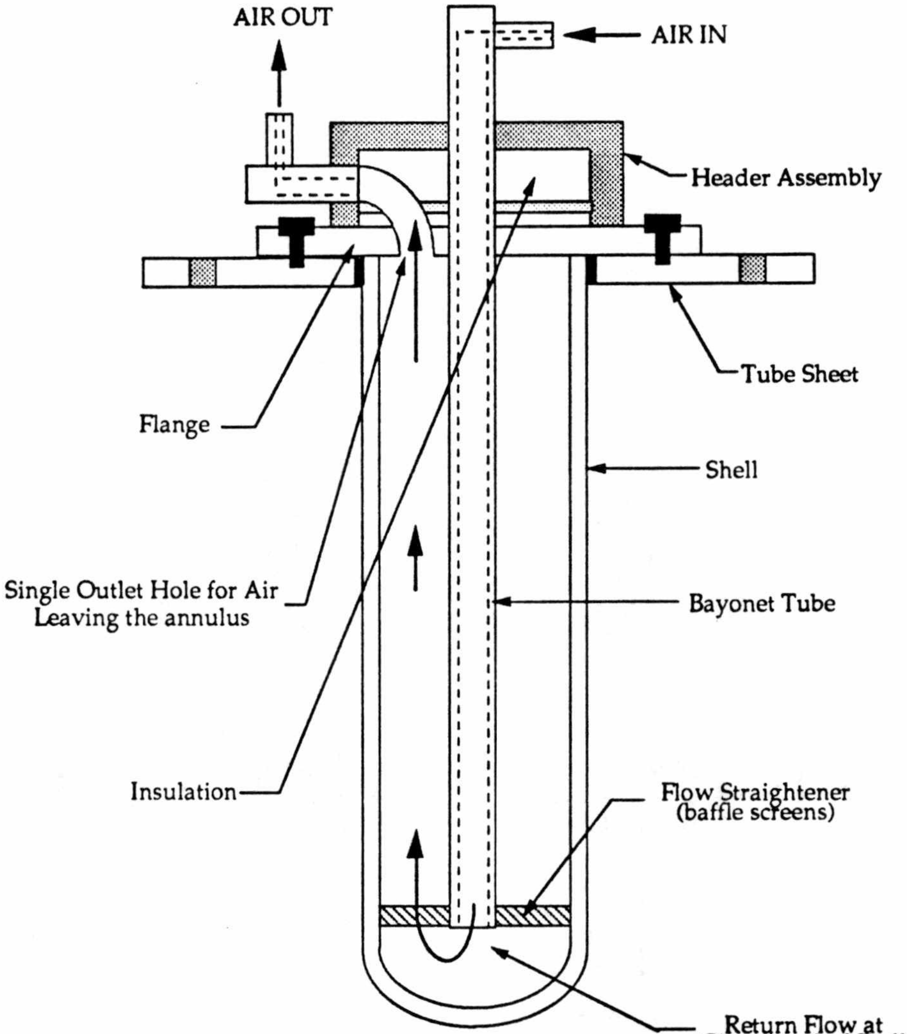

Figure A1.2 Single Element Bayonet Tube Assembly

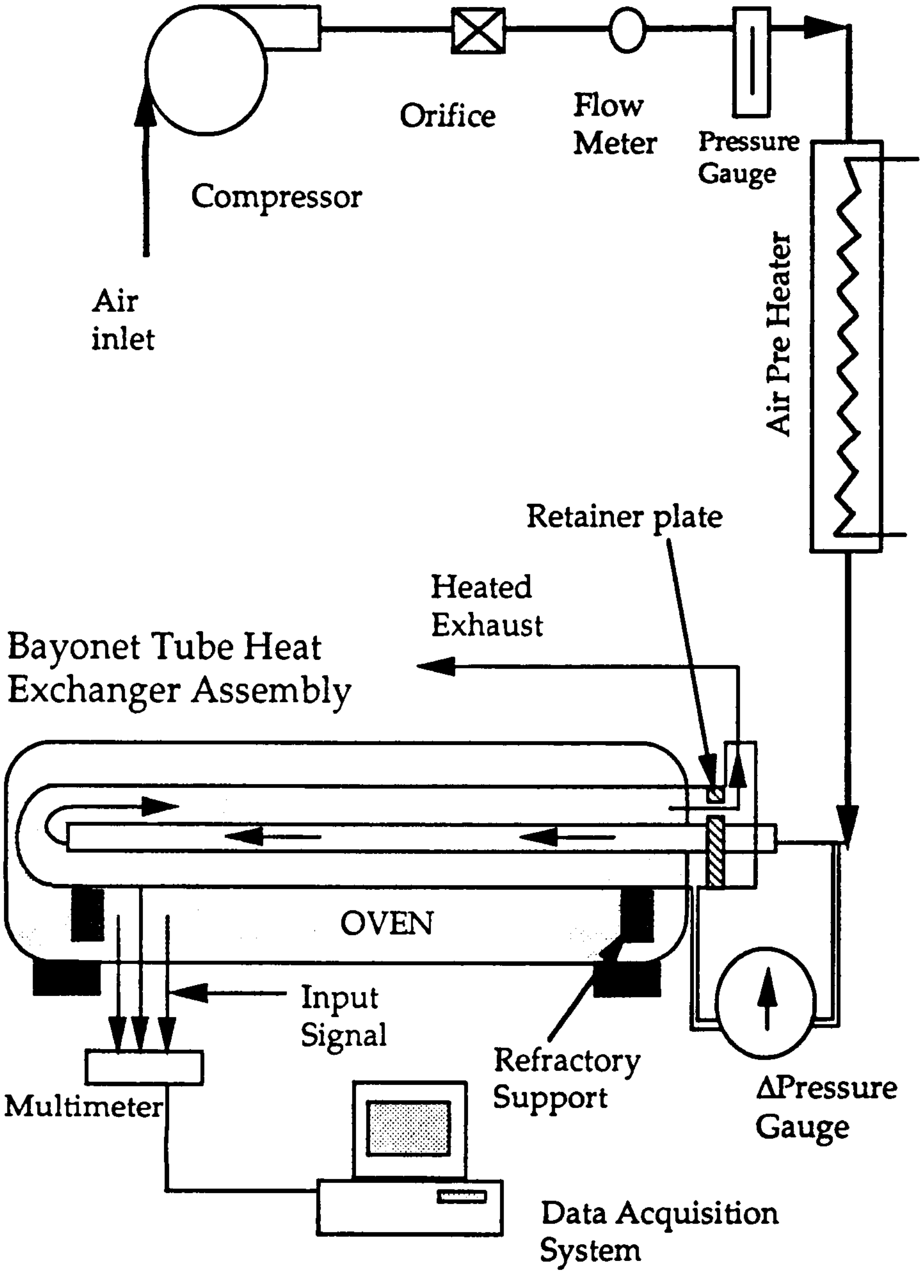

Figure A1.3 Experimental Flow Circuit

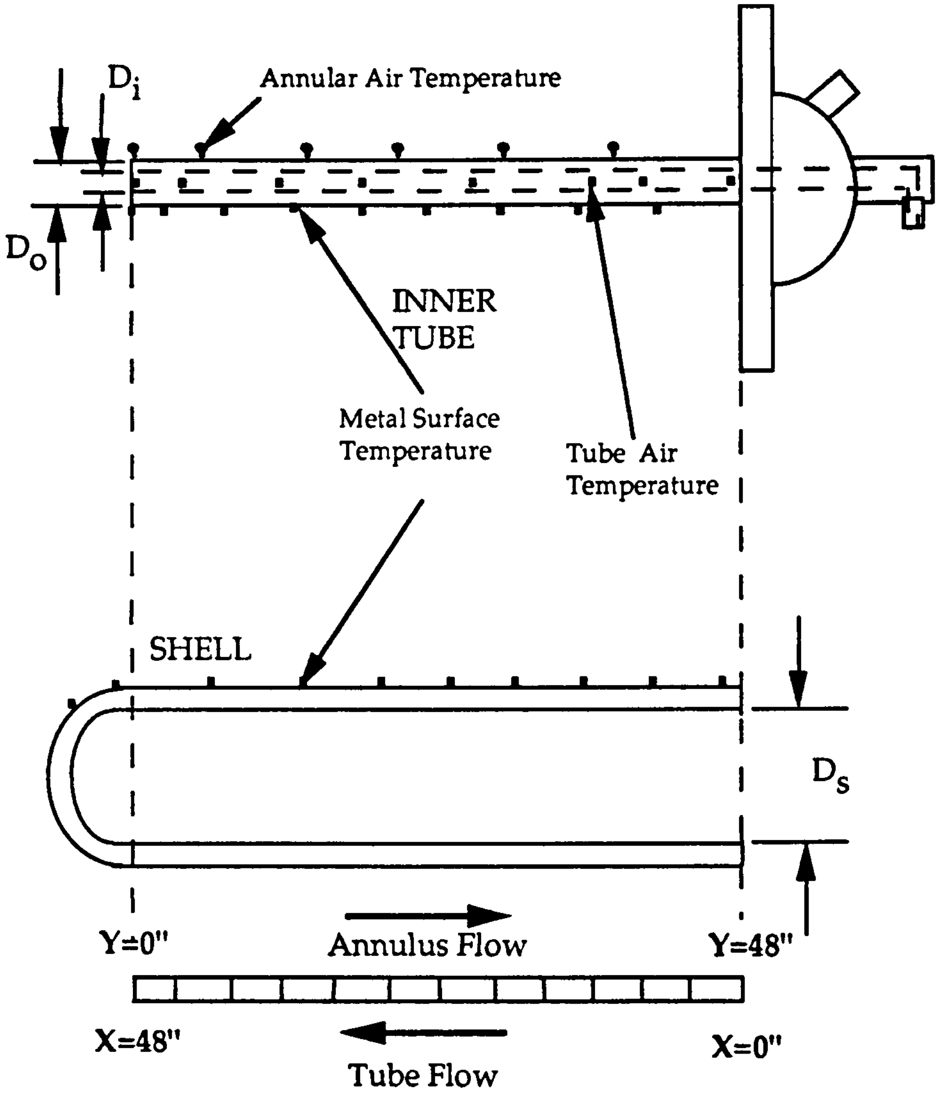

Figure A1.4 Bayonet Tube Instrumentation

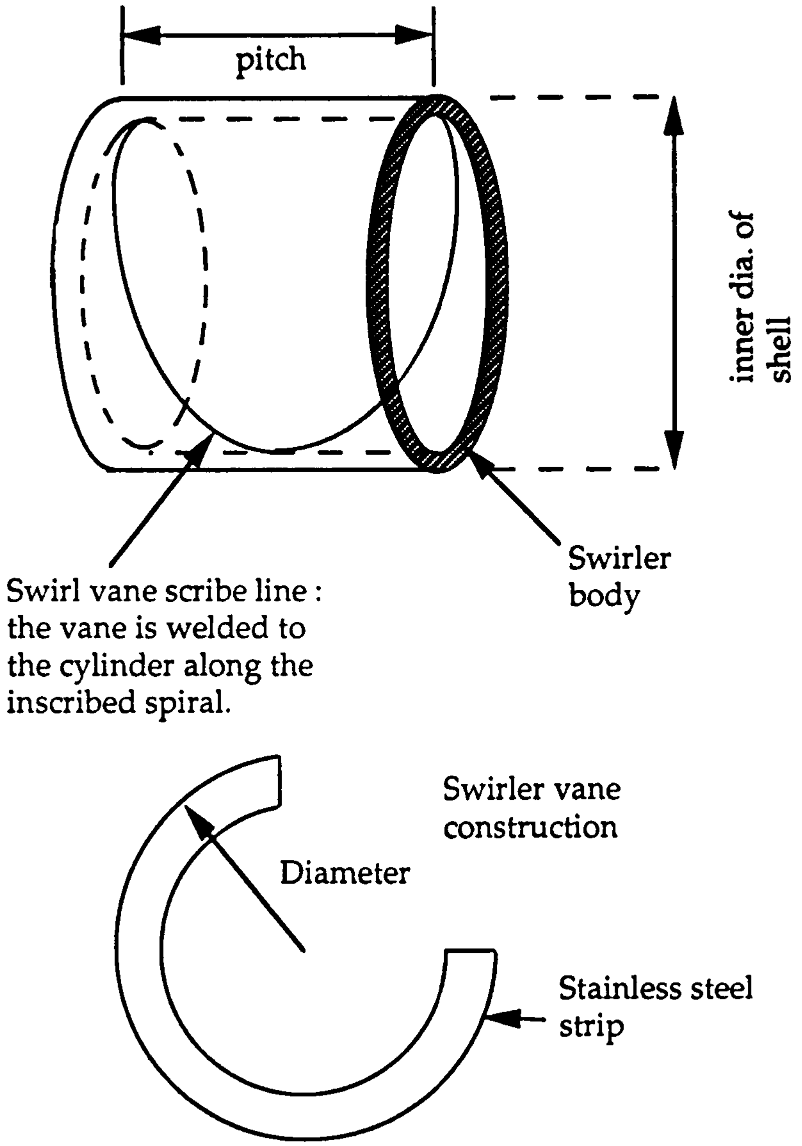

Figure A1.5 Swirler Design and Construction

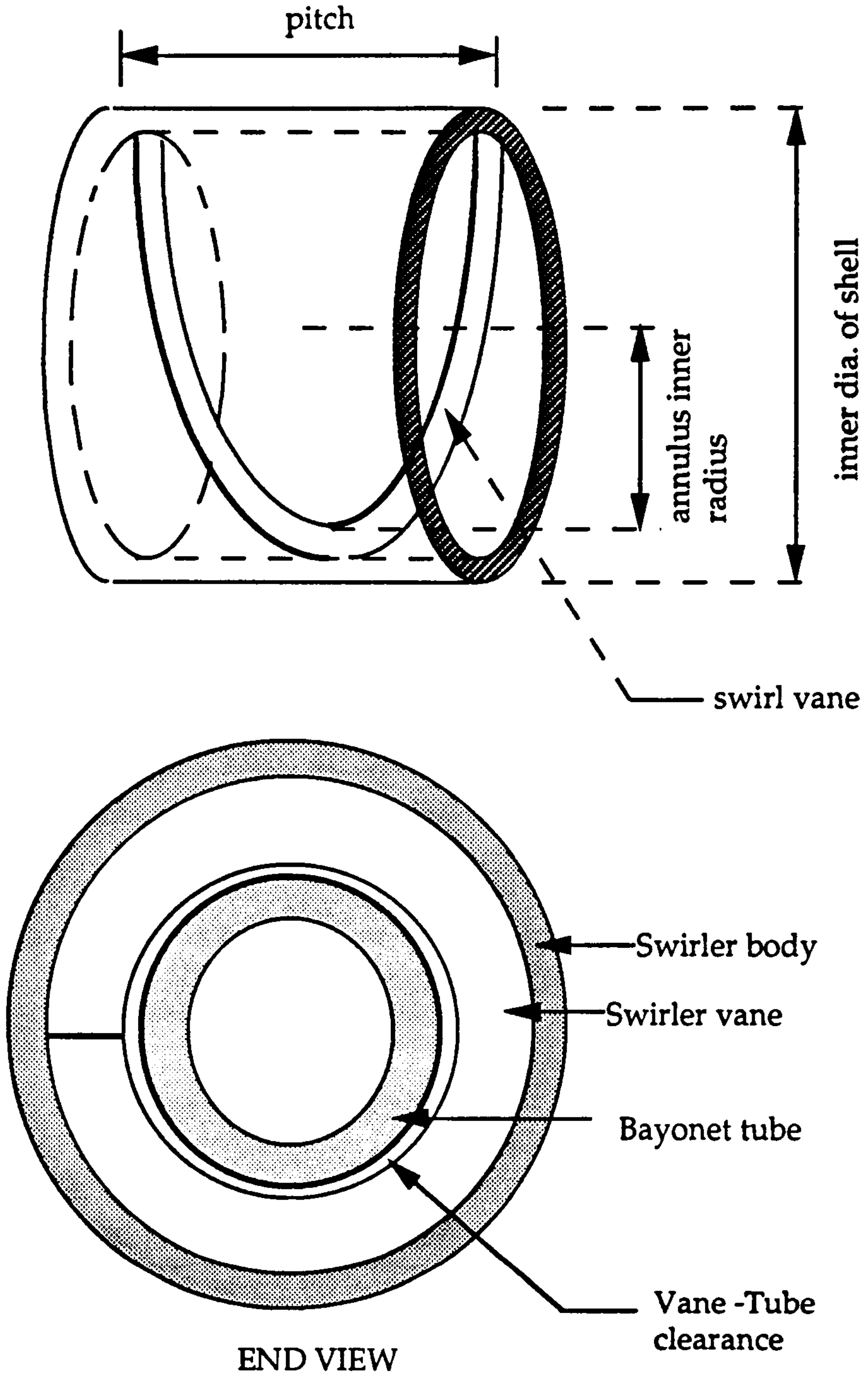

Figure A1.6 Single Vane Swirler

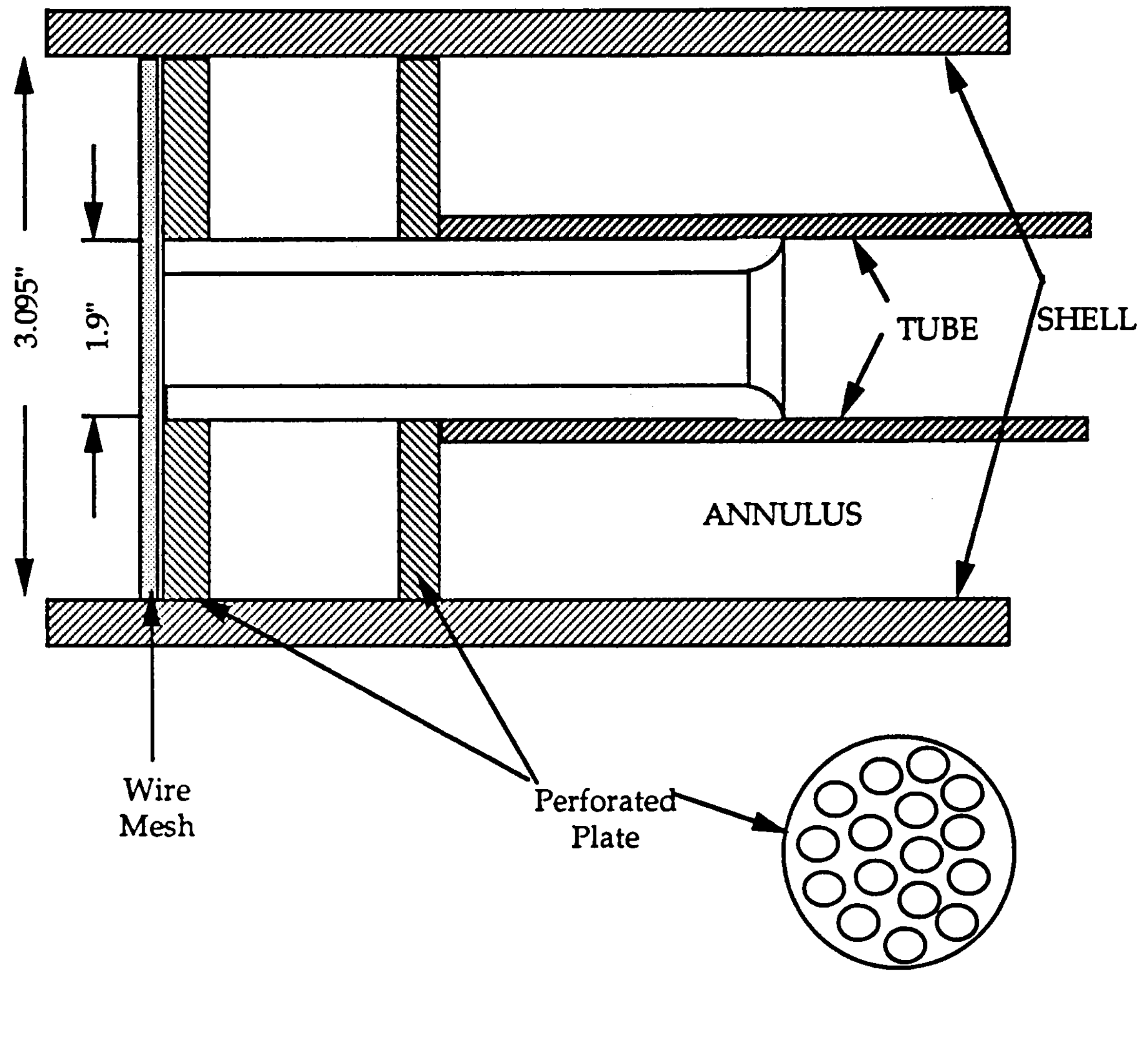

Figure A1.7 Flow Straightener for End Cap

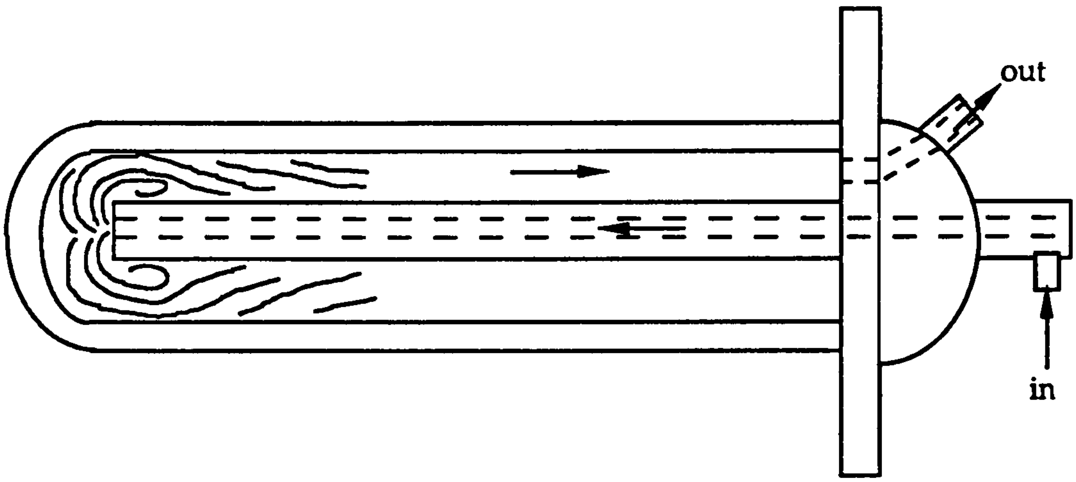

Postulated recirculation zones in the bayonet tube heat exchanger

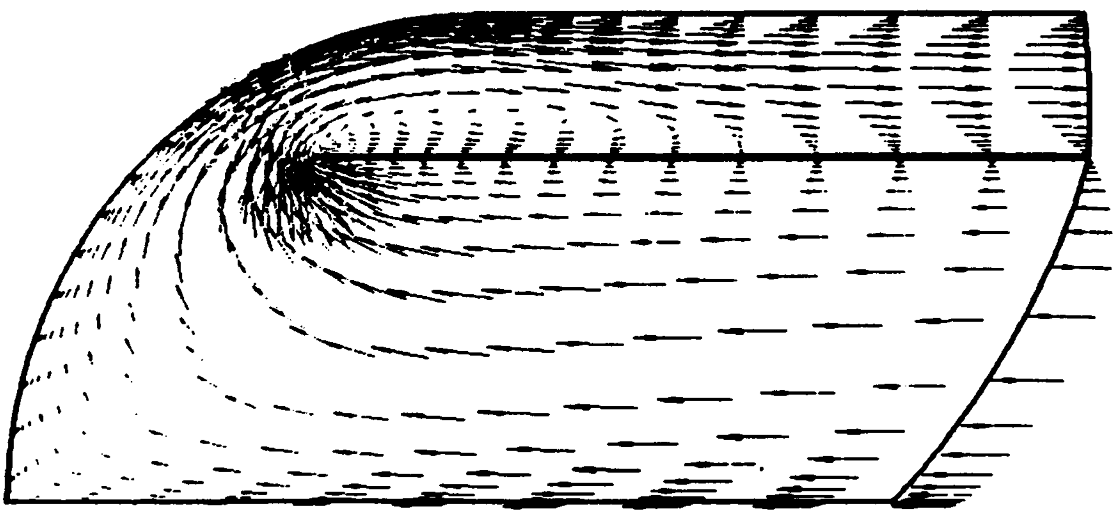

Velocity field near turning point (of a bayonet tube heat exchanger) for Re=500 Laminar flow condition.

Figure A1.8 Recirculation zones in a Bayonet Tube Heat Exchanger

(Source: Yang, S. L., and Hseih, C. K., "Fluid flow and heat transfer in a single pass return flow bayonet heat exchanger.", ASME Proceedings of 1988 Heat Transfer Conference.)

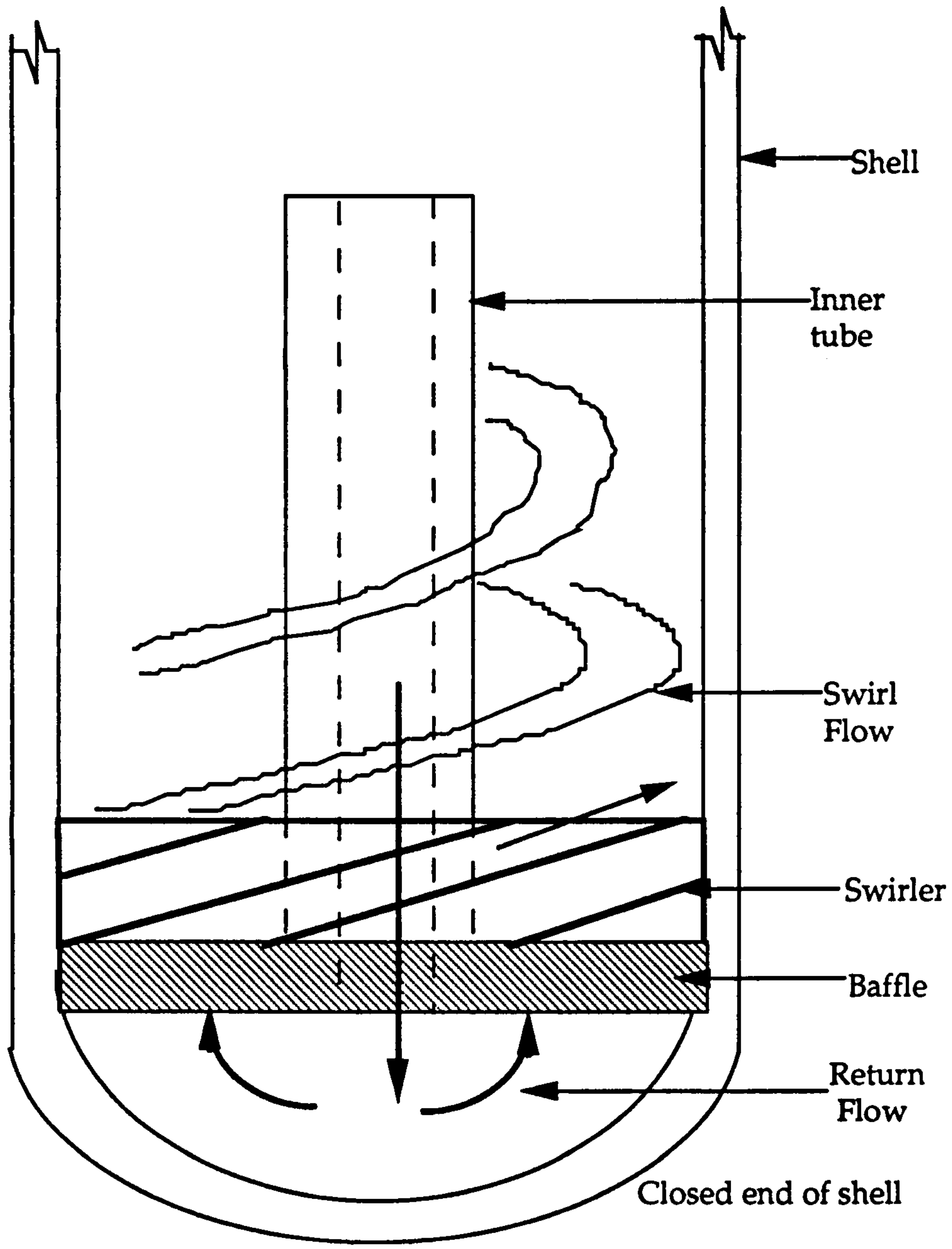

Figure A1.9 Swirl Flow inside a Bayonet Tube Heat Exchanger

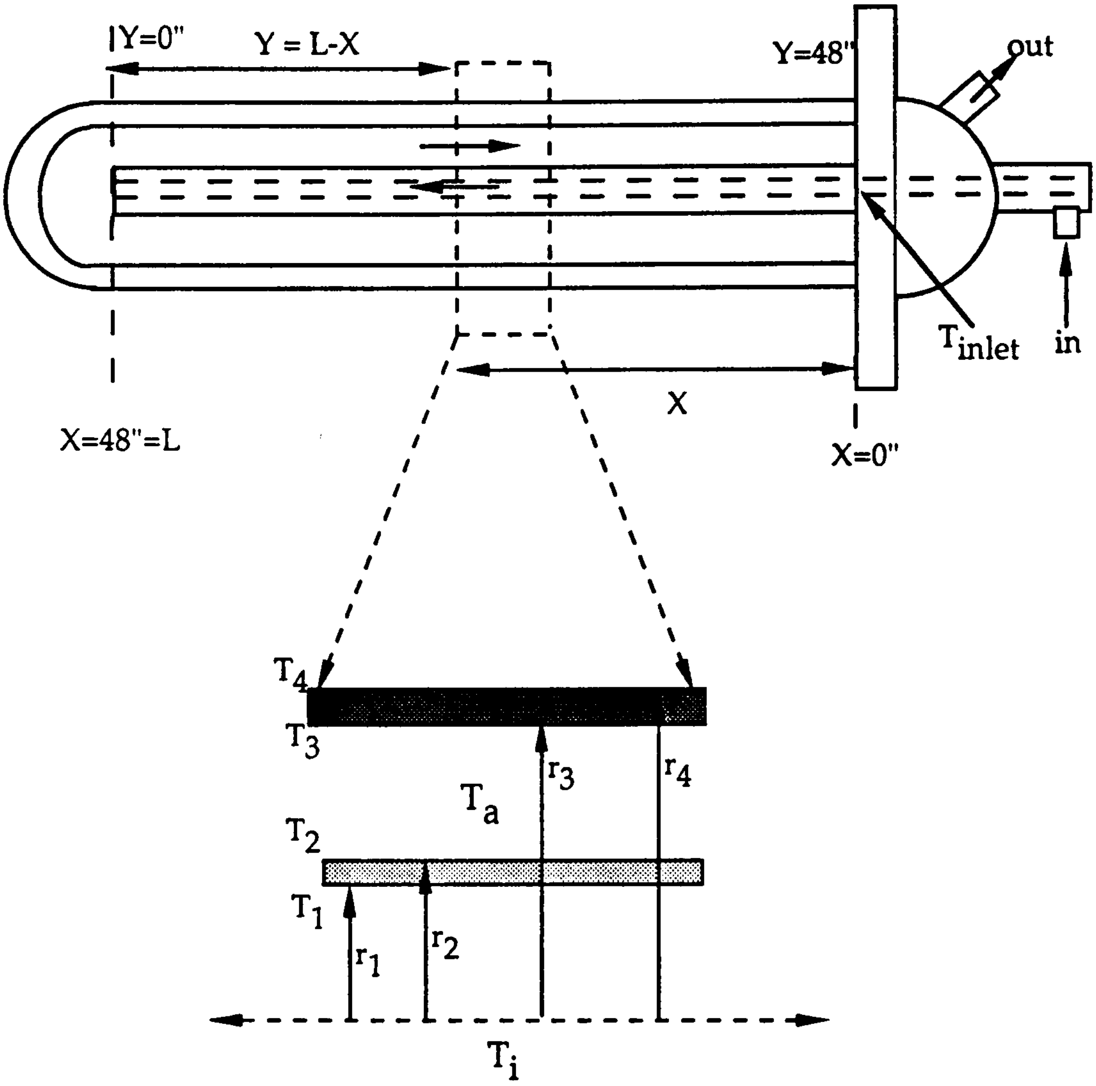

Figure A1.10 Nomenclature and Coordinate System

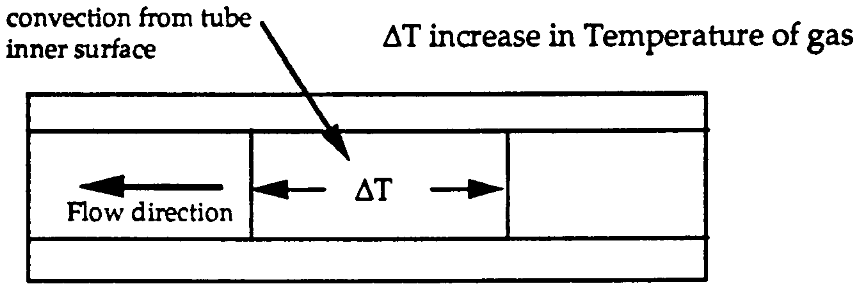

Heat Balance in a Gas Zone inside the Tube

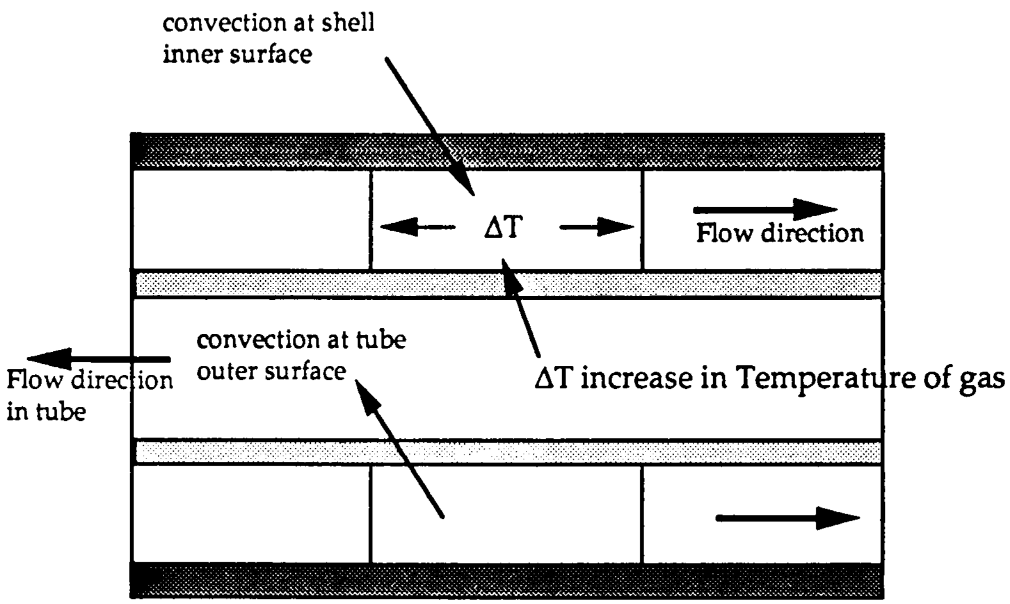

Heat Balance in a Gas Zone inside the Annulus

Figure A1.11 Control Volume for Heat Balance in Annular and Tube Gas Zones

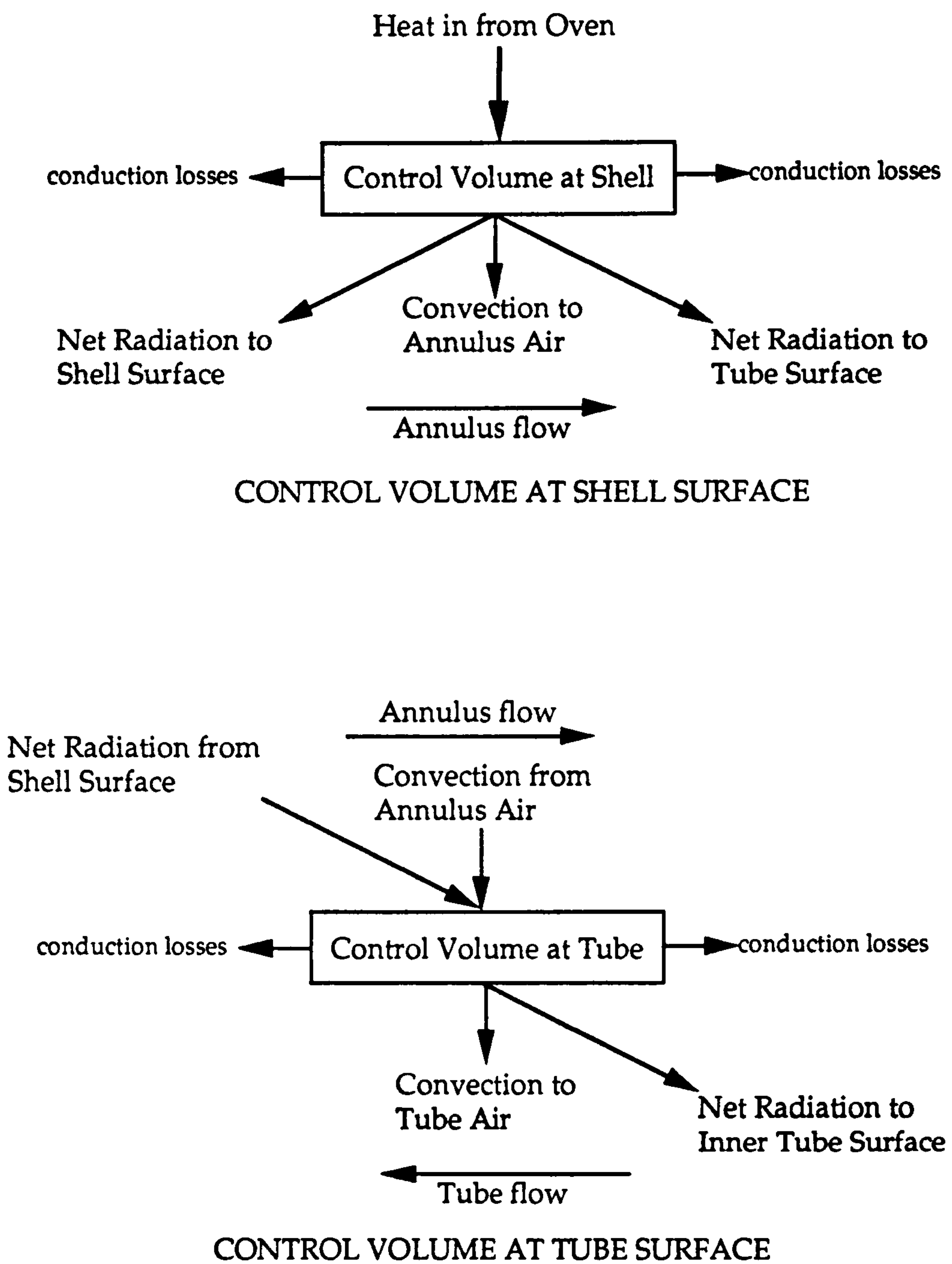

Figure A1.12 Control Volume for Heat Balance at Shell and Tube Surfaces

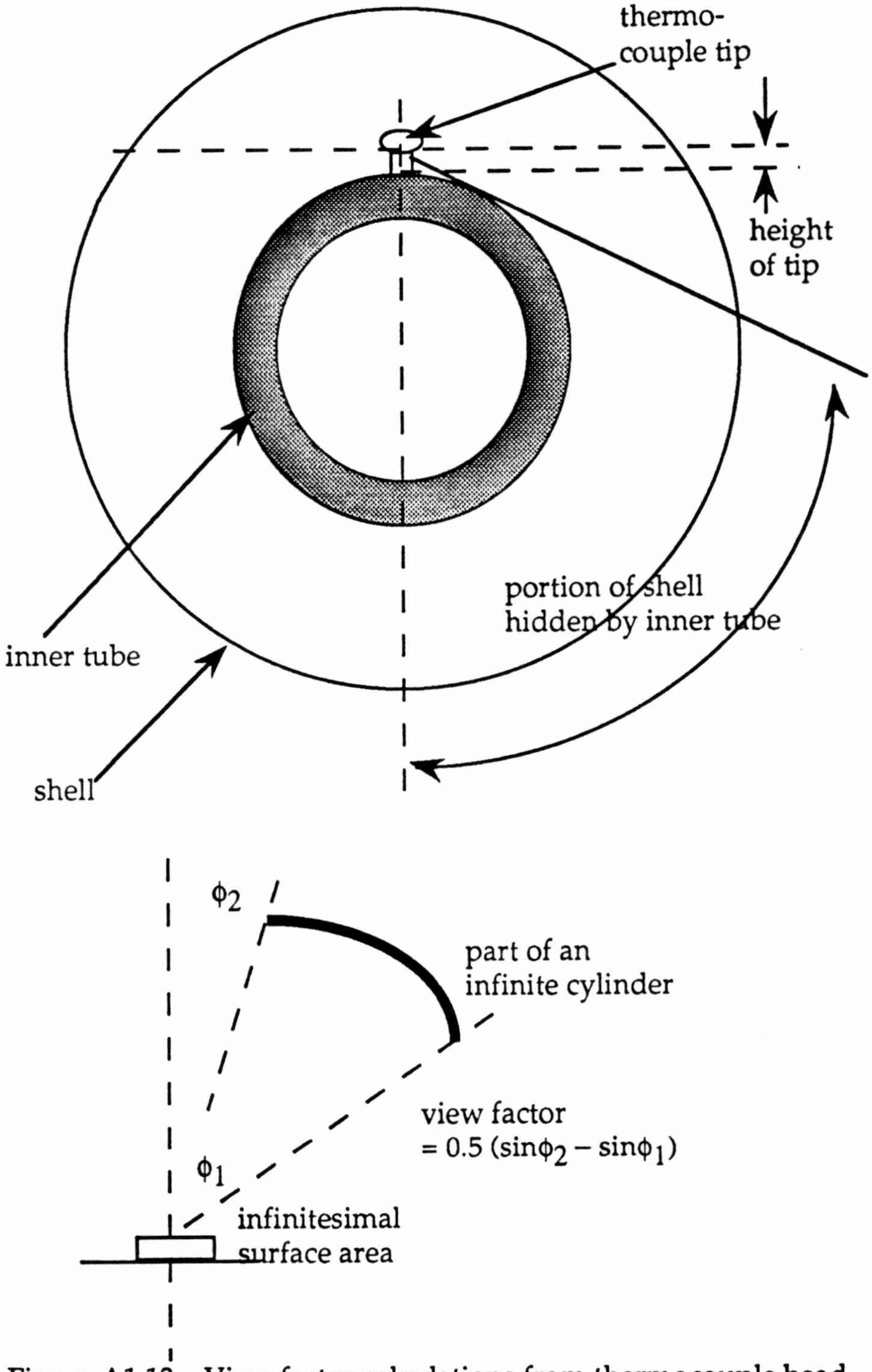

Figure A1.13 View factor calculations from thermocouple bead

APPENDIX A2

DATA FROM NON-SWIRL FLOW EXPERIMENTS

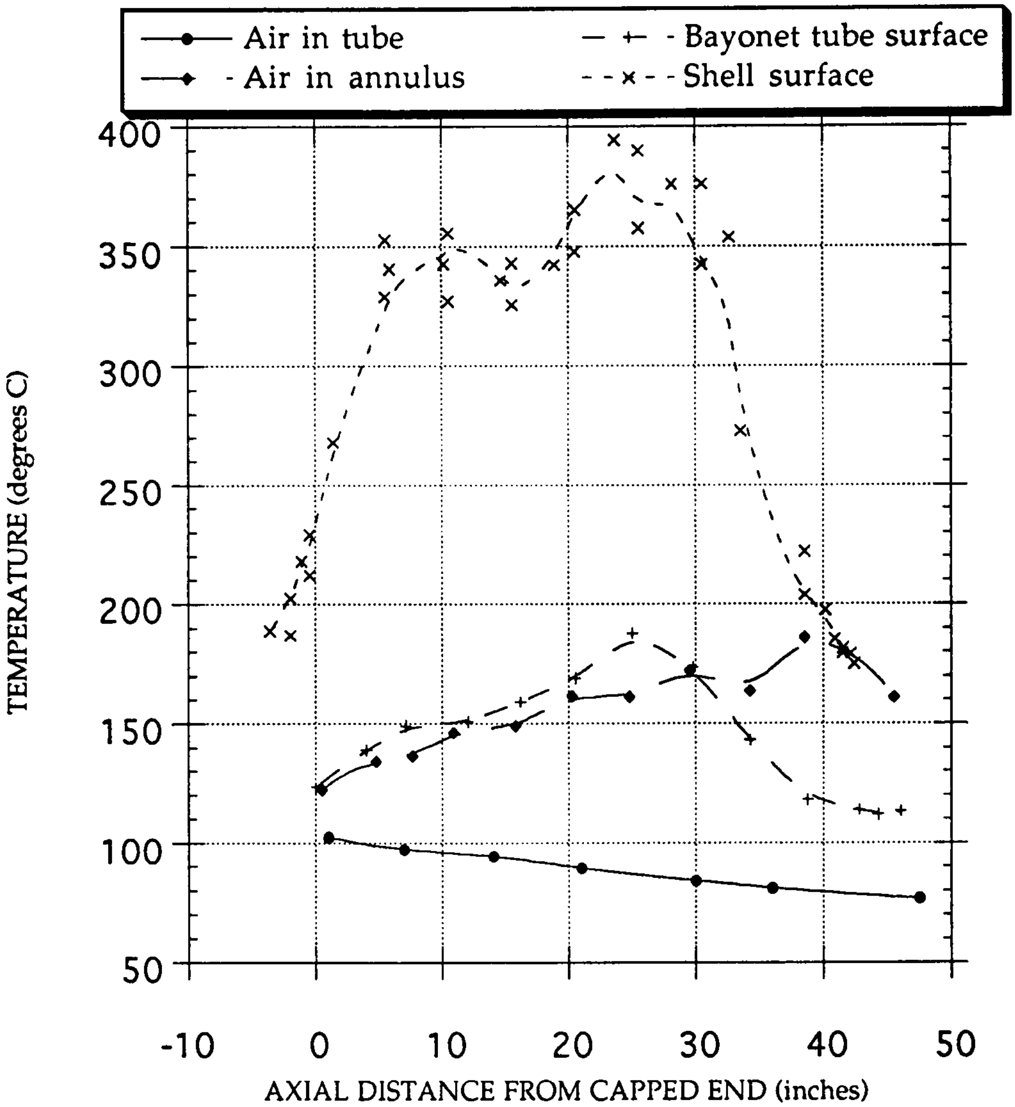

Figure A2.1 Temperature versus axial position distribution in bayonet tube assembly. Flow rate 40 scfm, oven temperature 800 °C.

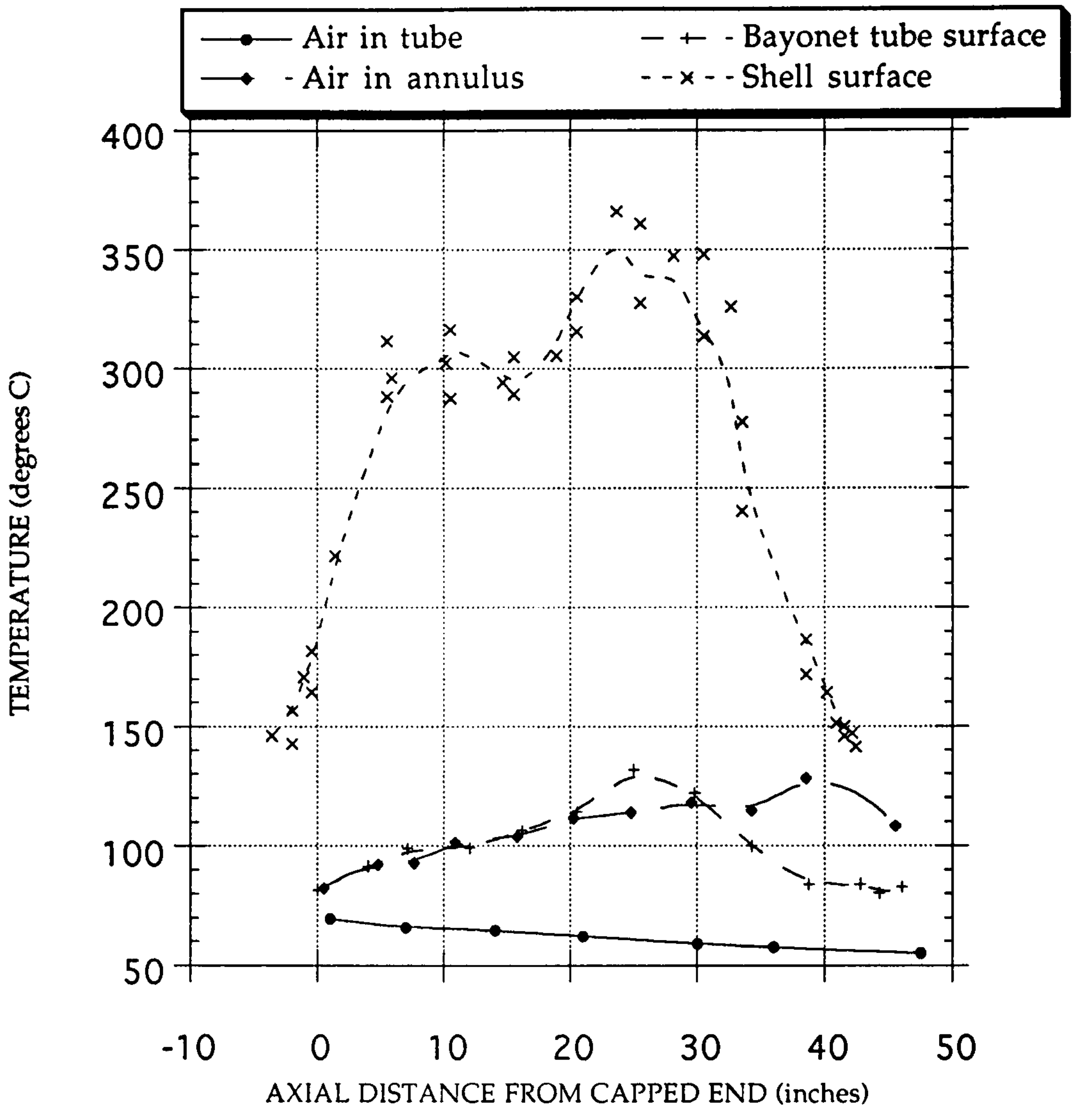

Figure A2.2 Temperature versus axial position distribution in bayonet tube assembly. Flow rate 60 scfm, oven temperature 800 °C.

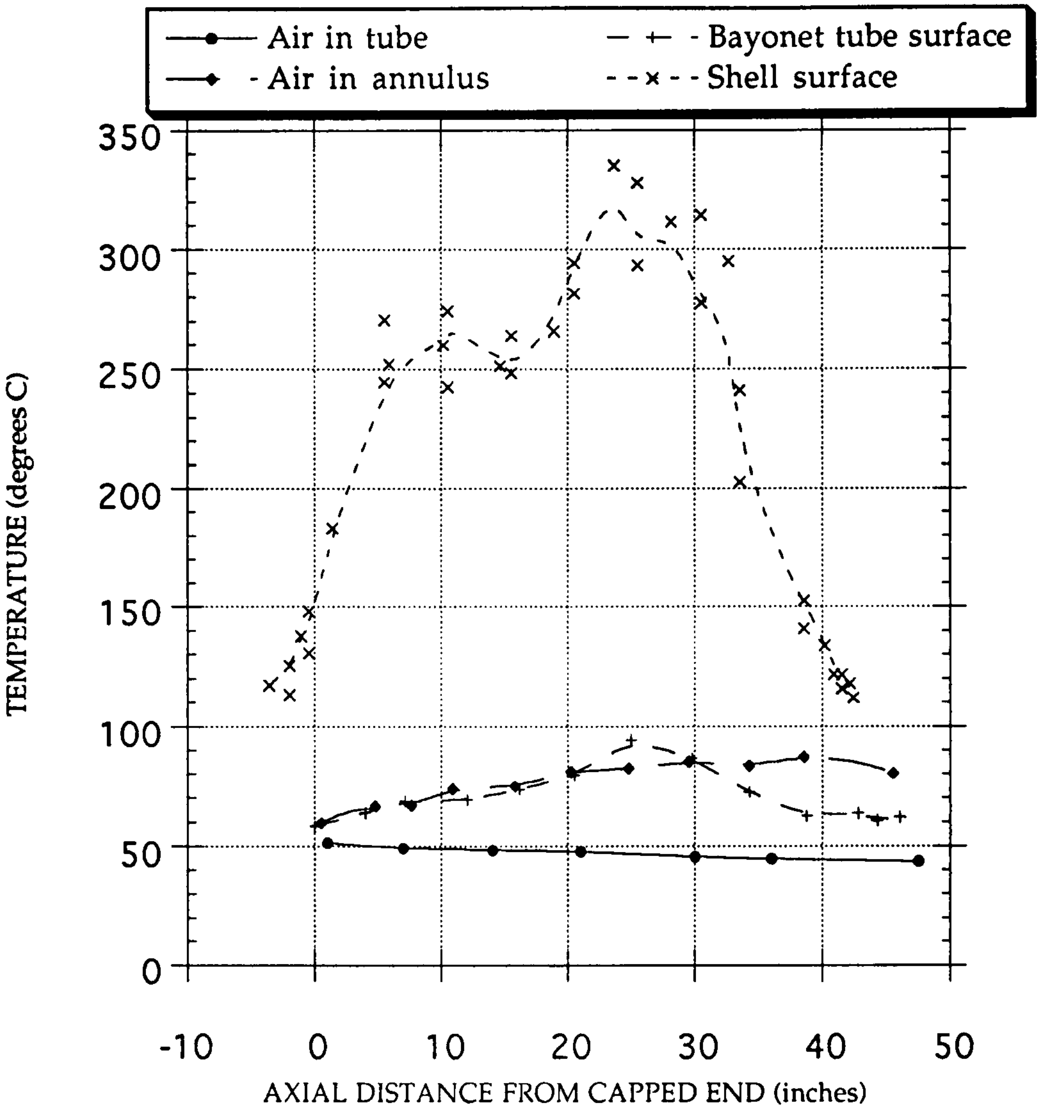

Figure A2.3 Temperature versus axial position distribution in bayonet tube assembly. Flow rate 80 scfm, oven temperature 800 °C.

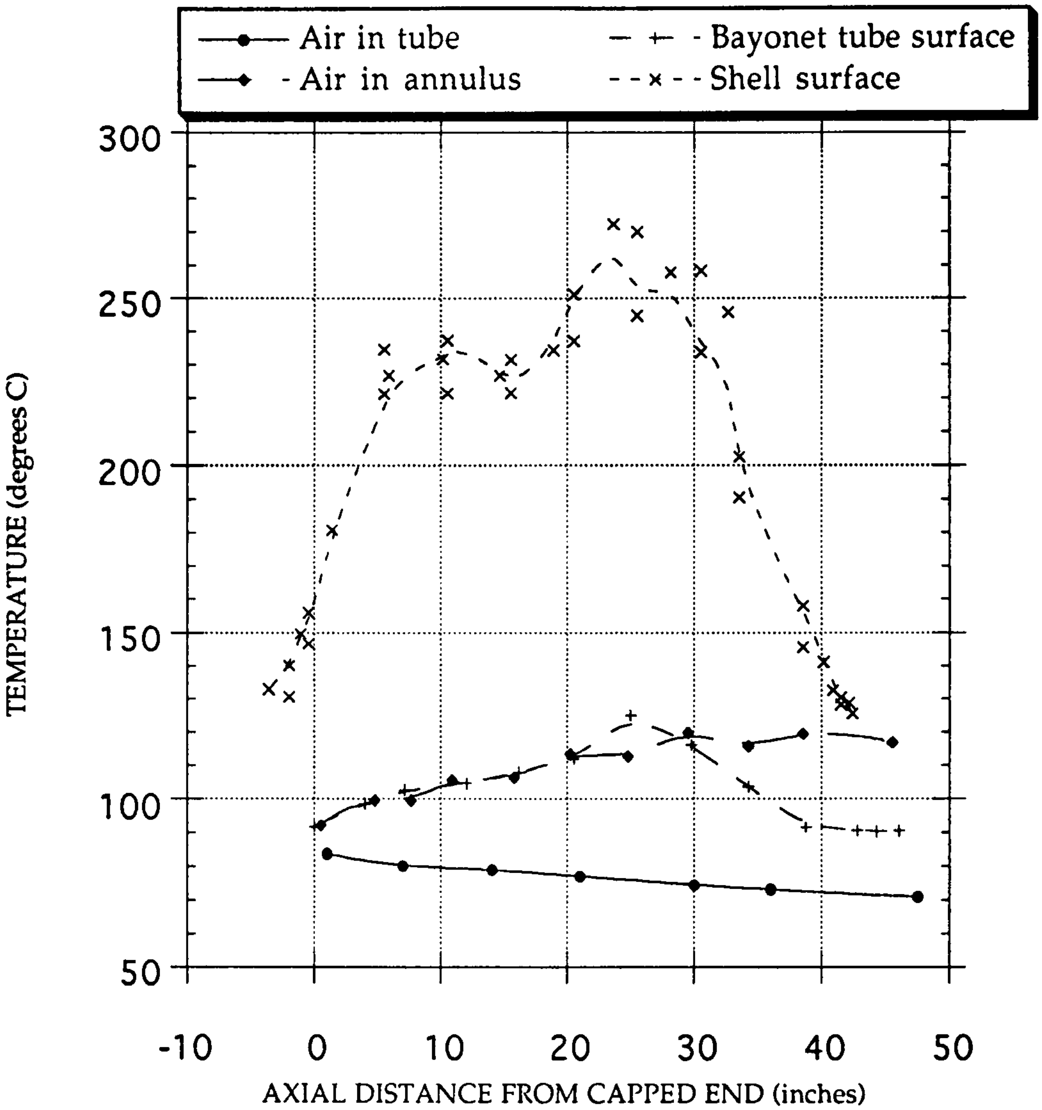

Figure A2.4 Temperature versus axial position distribution in bayonet tube assembly. Flow rate 40 scfm, oven temperature 600 °C.

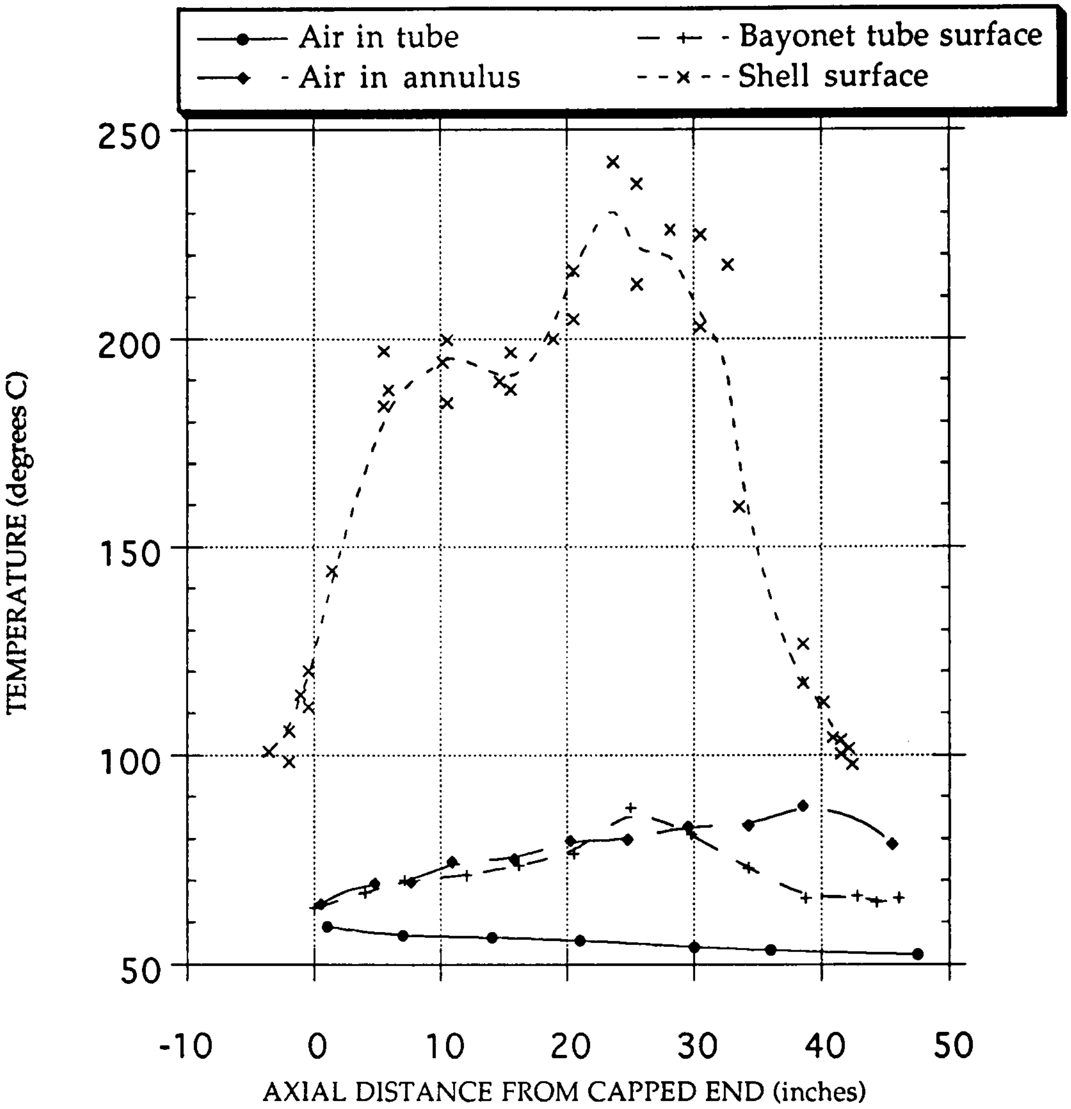

Figure A2.5 Temperature versus axial position distribution in bayonet tube assembly. Flow rate 60 scfm, oven temperature 600 °C.

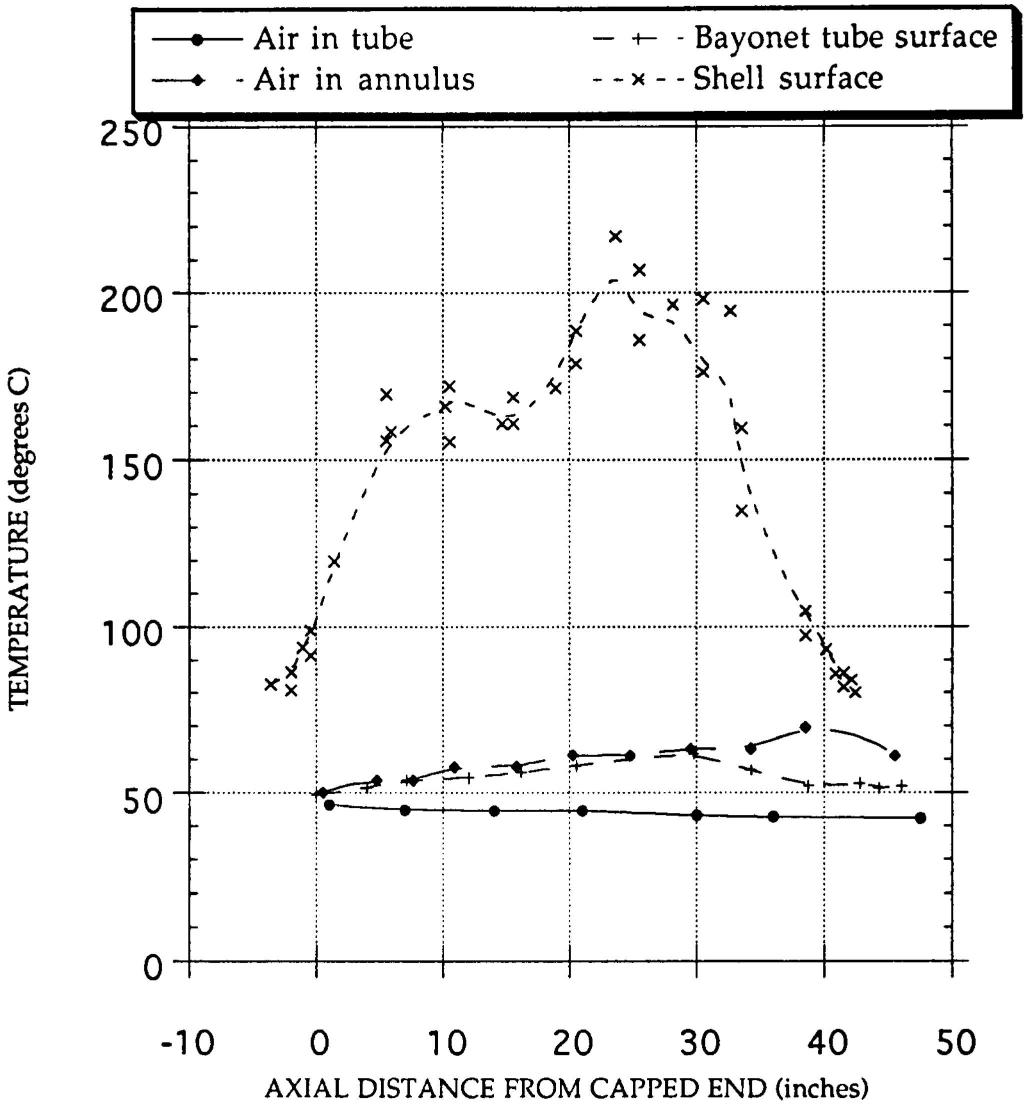

Figure A2.6 Temperature versus axial position distribution in bayonet tube assembly. Flow rate 80 scfm, oven temperature 600 °C.

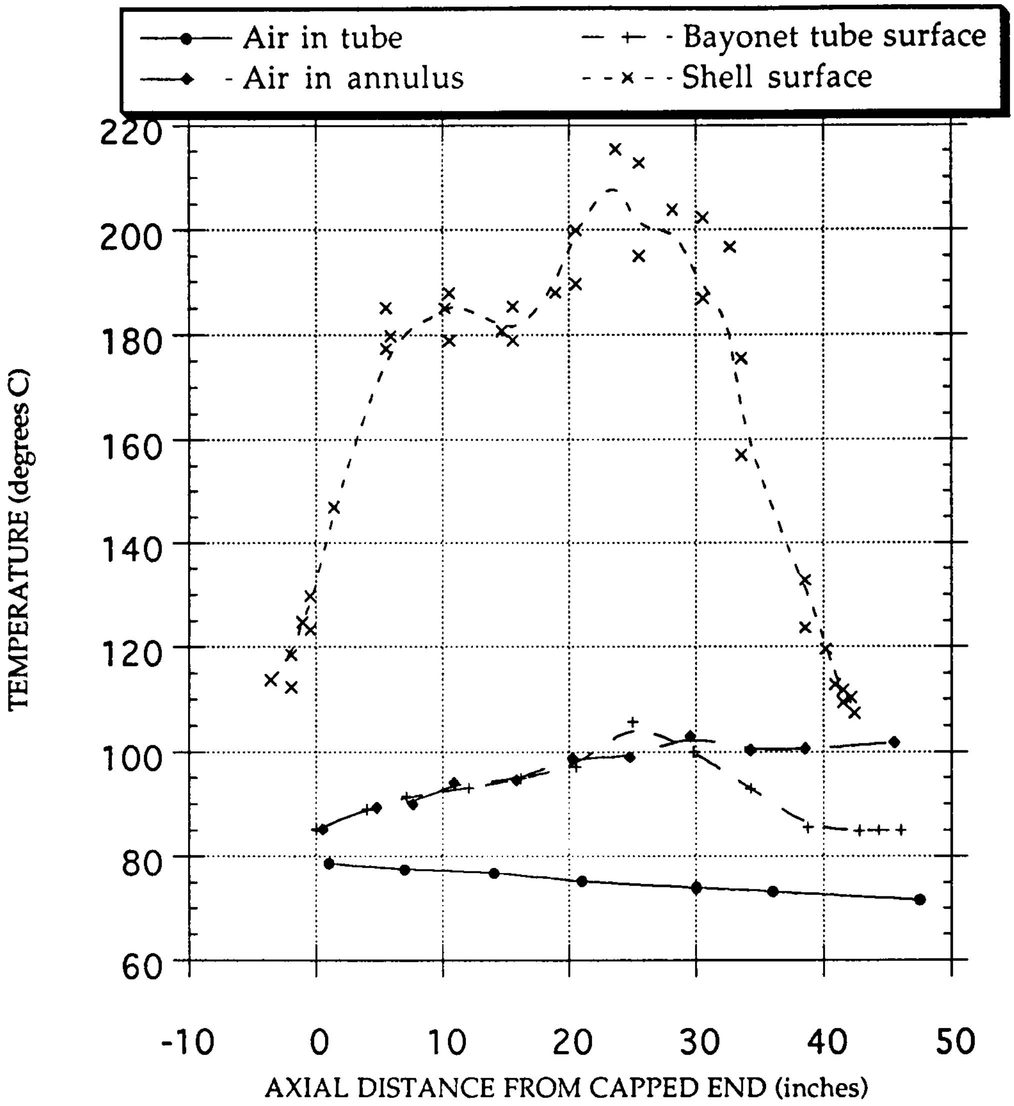

Figure A2.7 Temperature versus axial position distribution in bayonet tube assembly. Flow rate 40 scfm, oven temperature 500 °C.

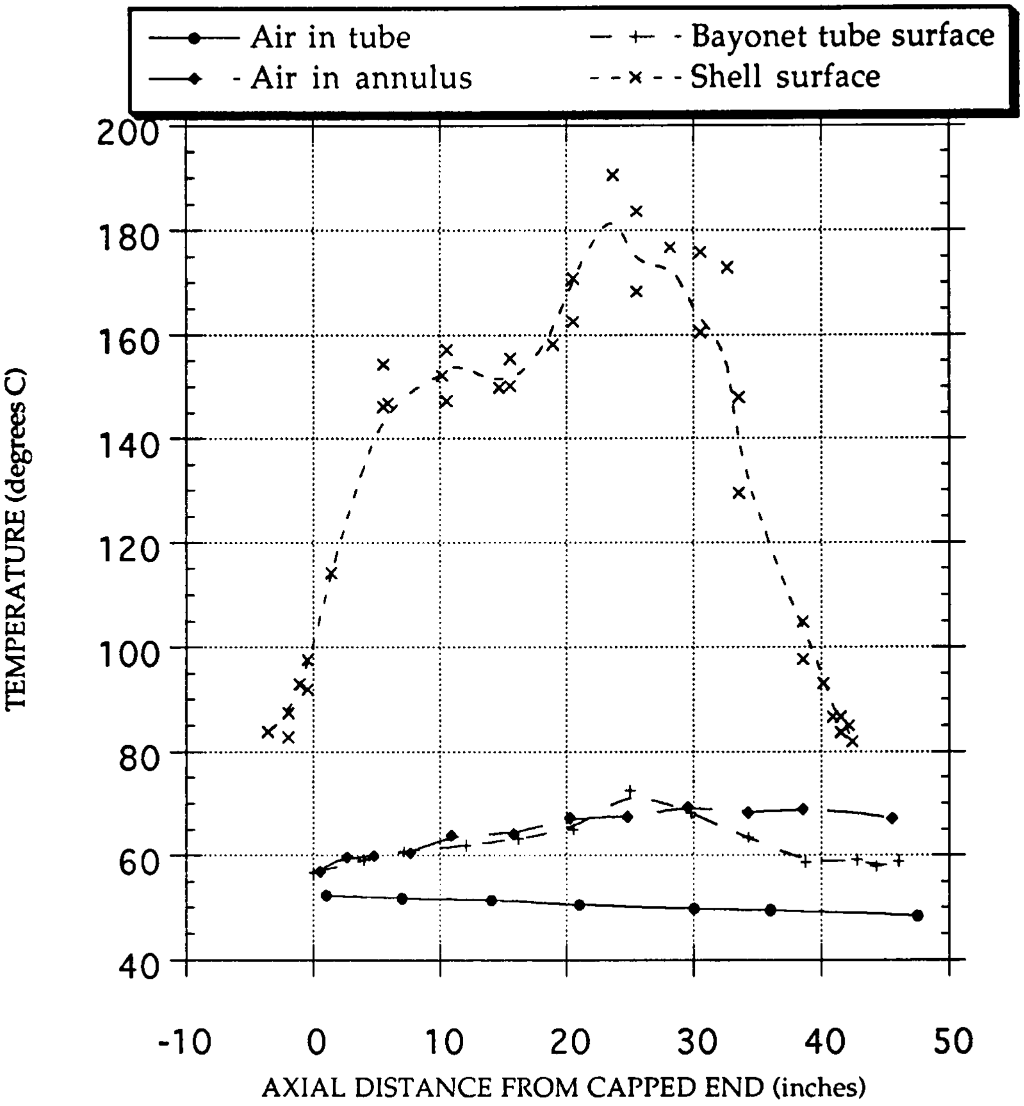

Figure A2.8 Temperature versus axial position distribution in bayonet tube assembly. Flow rate 60 scfm, oven temperature 500 °C.

APPENDIX A3

DATA FROM SWIRL FLOW EXPERIMENTS

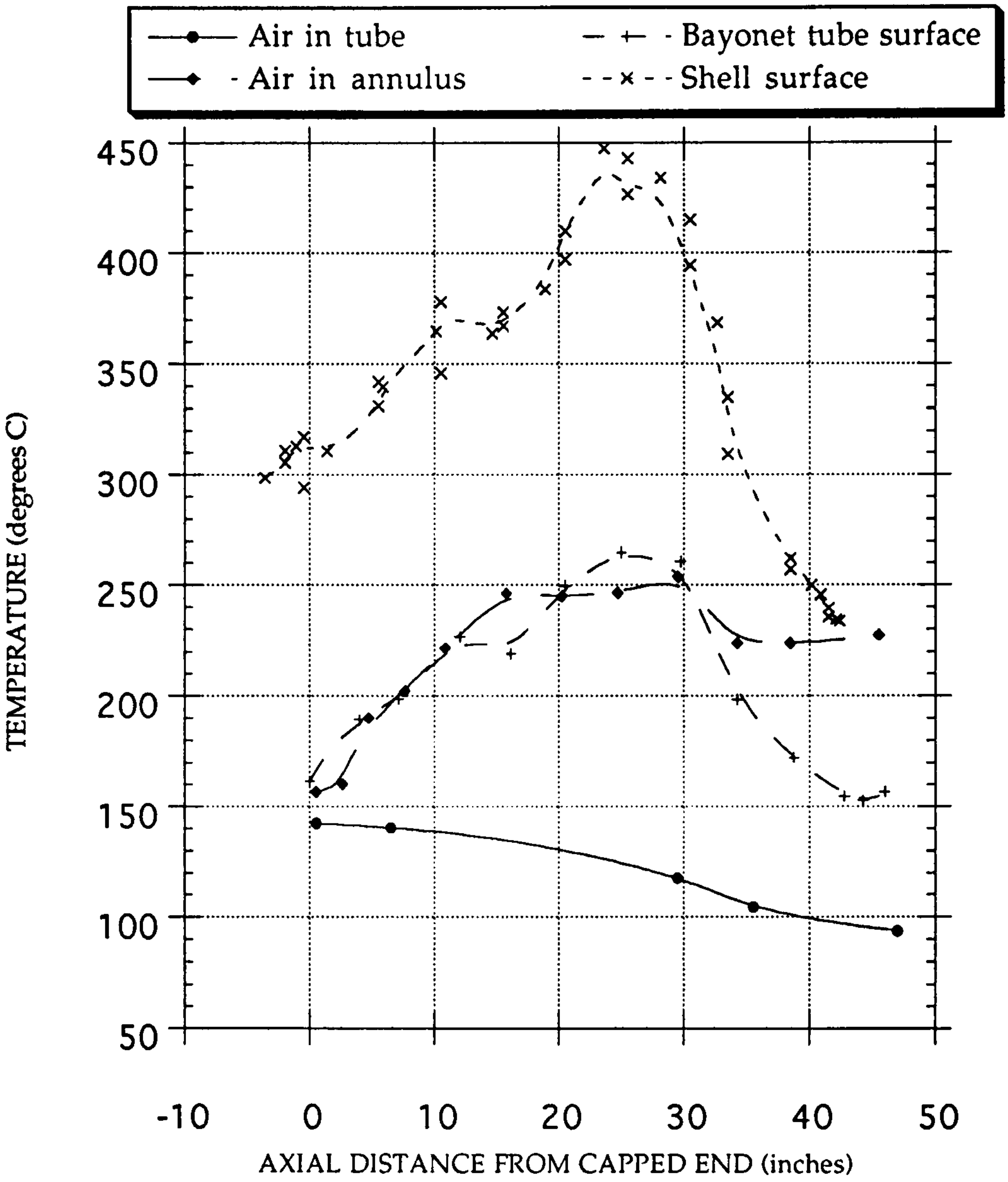

Figure A3.1 Temperature versus axial position distribution in bayonet tube assembly. Flow rate 30 scfm, oven temperature 900 °C

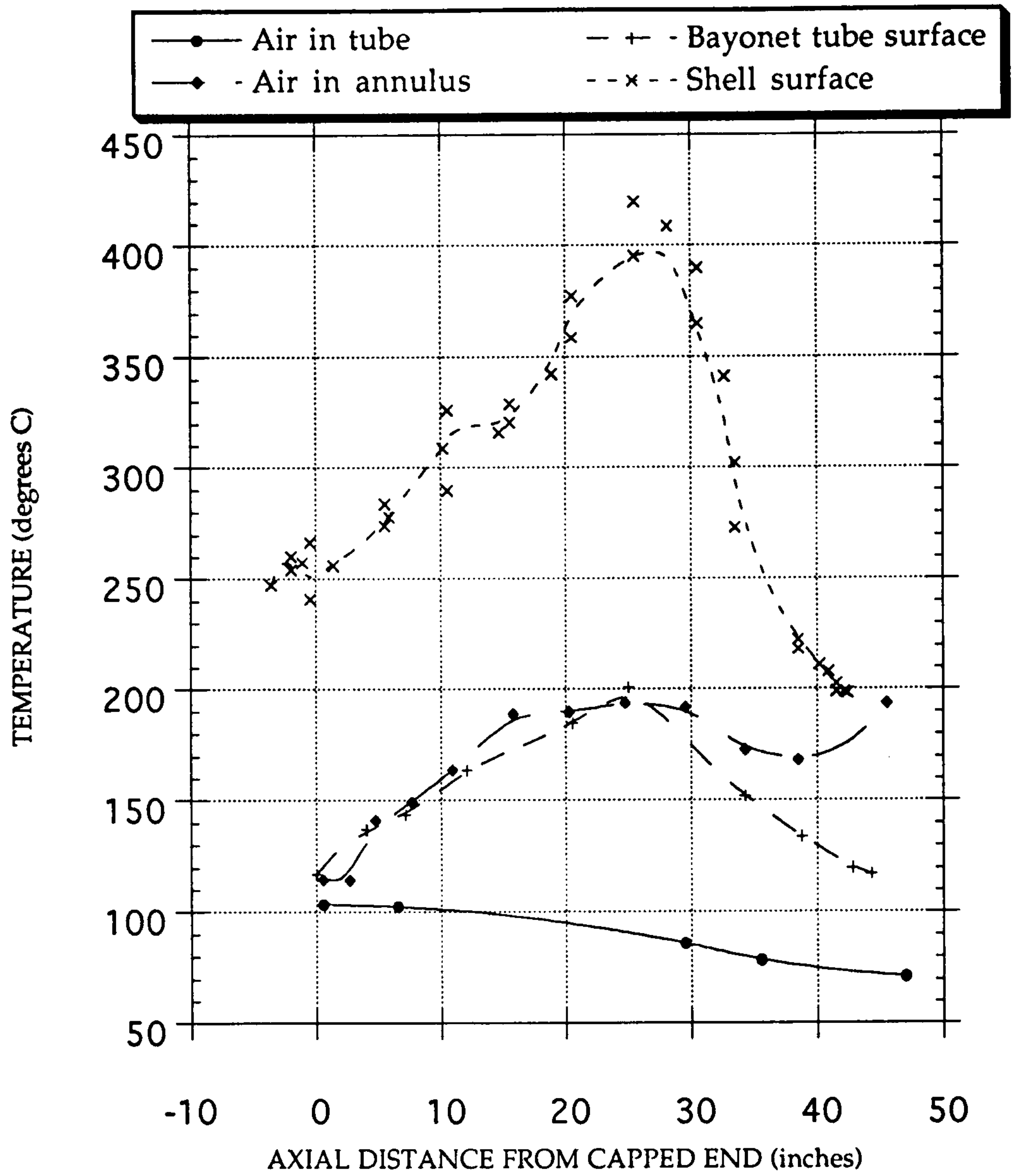

Figure A3.2 Temperature versus axial position distribution in bayonet tube assembly. Flow rate 40 scfm, oven temperature 900 °C

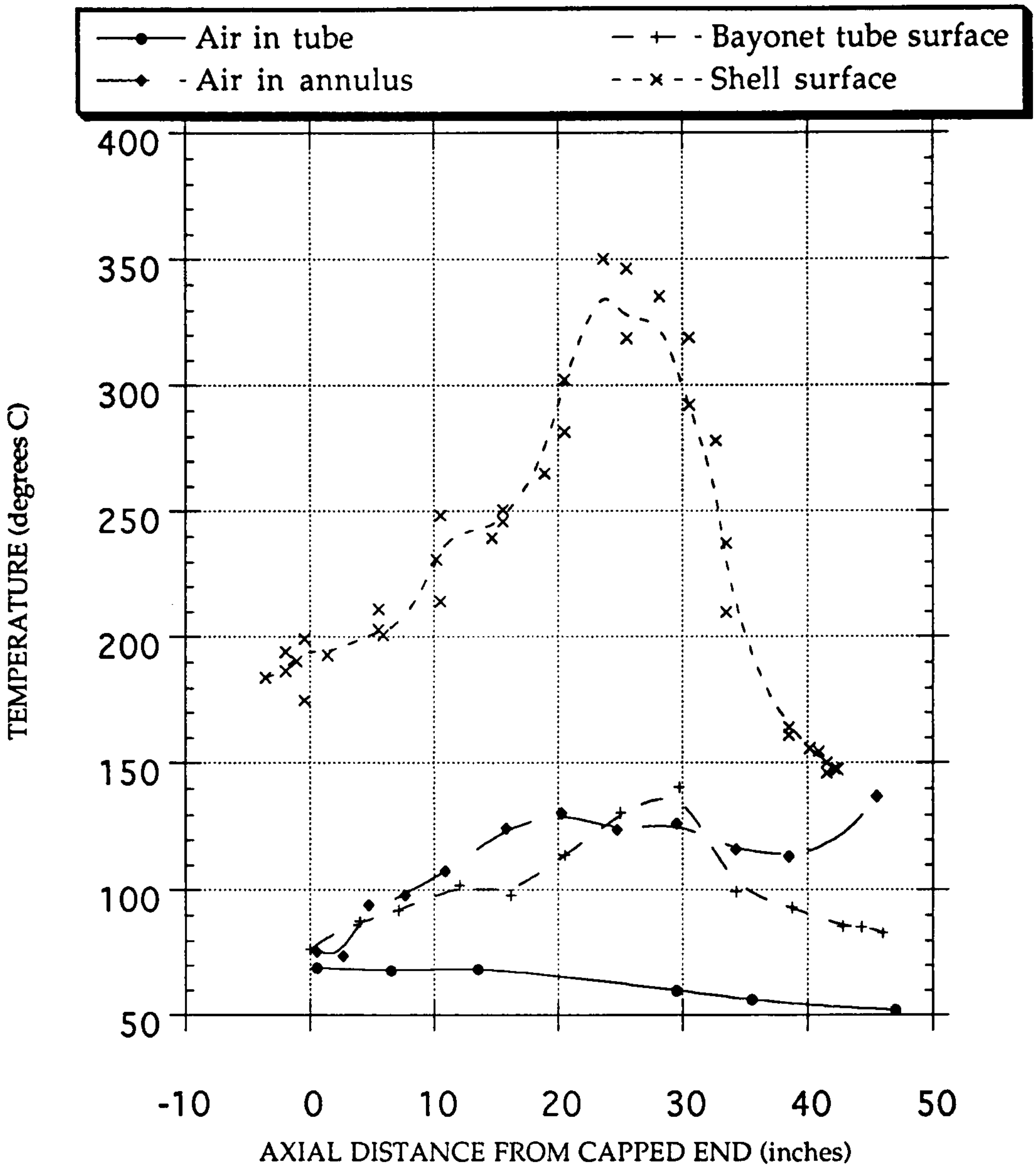

Figure A3.3 Temperature versus axial position distribution in bayonet tube assembly. Flow rate 60 scfm, oven temperature 900 °C

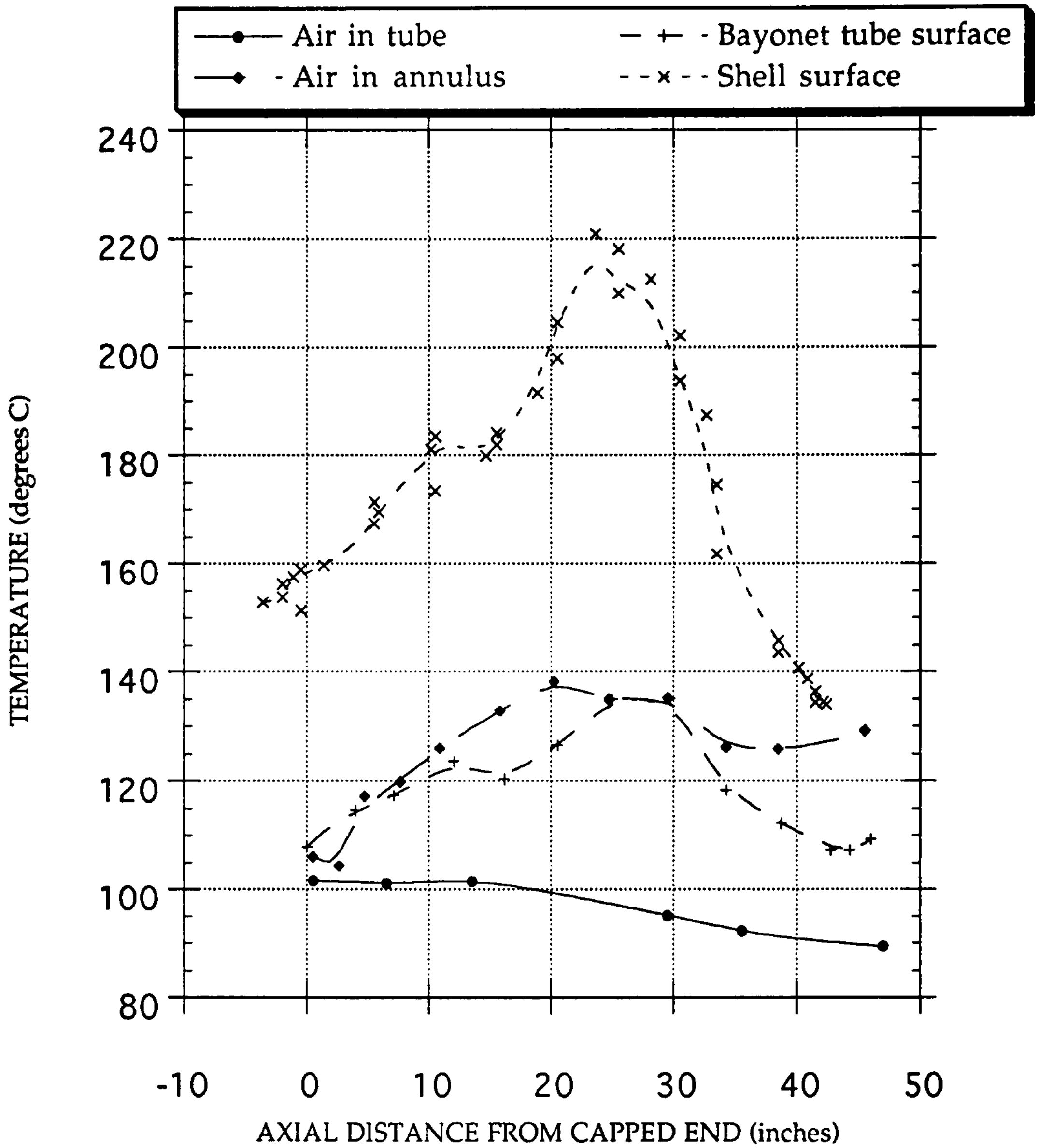

Figure A3.4 Temperature versus axial position distribution in bayonet tube assembly. Flow rate 30 scfm, oven temperature 500 °C

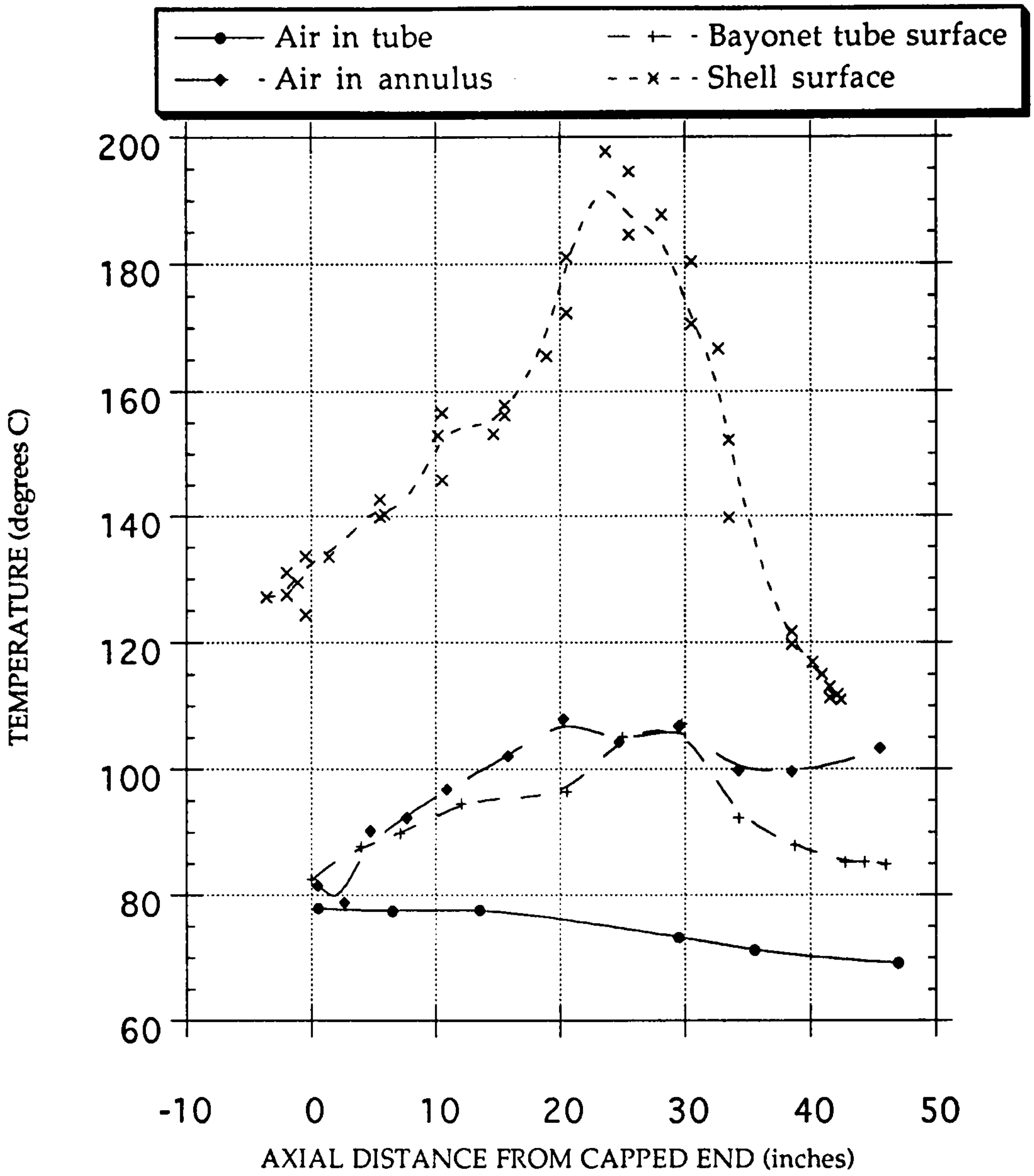

Figure A3.5 Temperature versus axial position distribution in bayonet tube assembly. Flow rate 40 scfm, oven temperature 500 °C

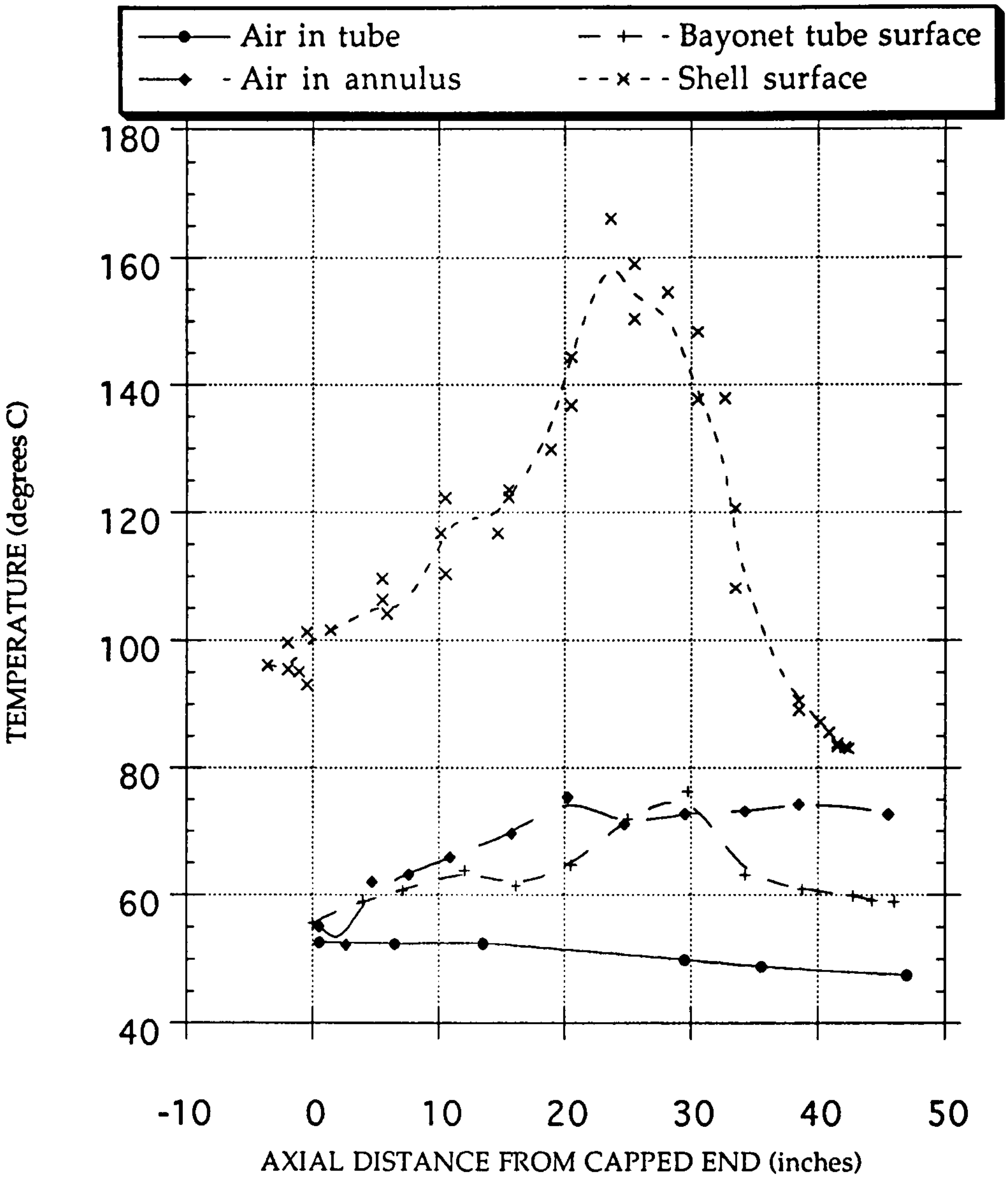

Figure A3.6 Temperature versus axial position distribution in bayonet tube assembly. Flow rate 60 scfm, oven temperature 500 °C

APPENDIX A4

EXPERIMENTAL VALUES OF HEAT TRANSFER COEFFICIENTS FOR NON-SWIRL AND SWIRL FLOW CONDITIONS

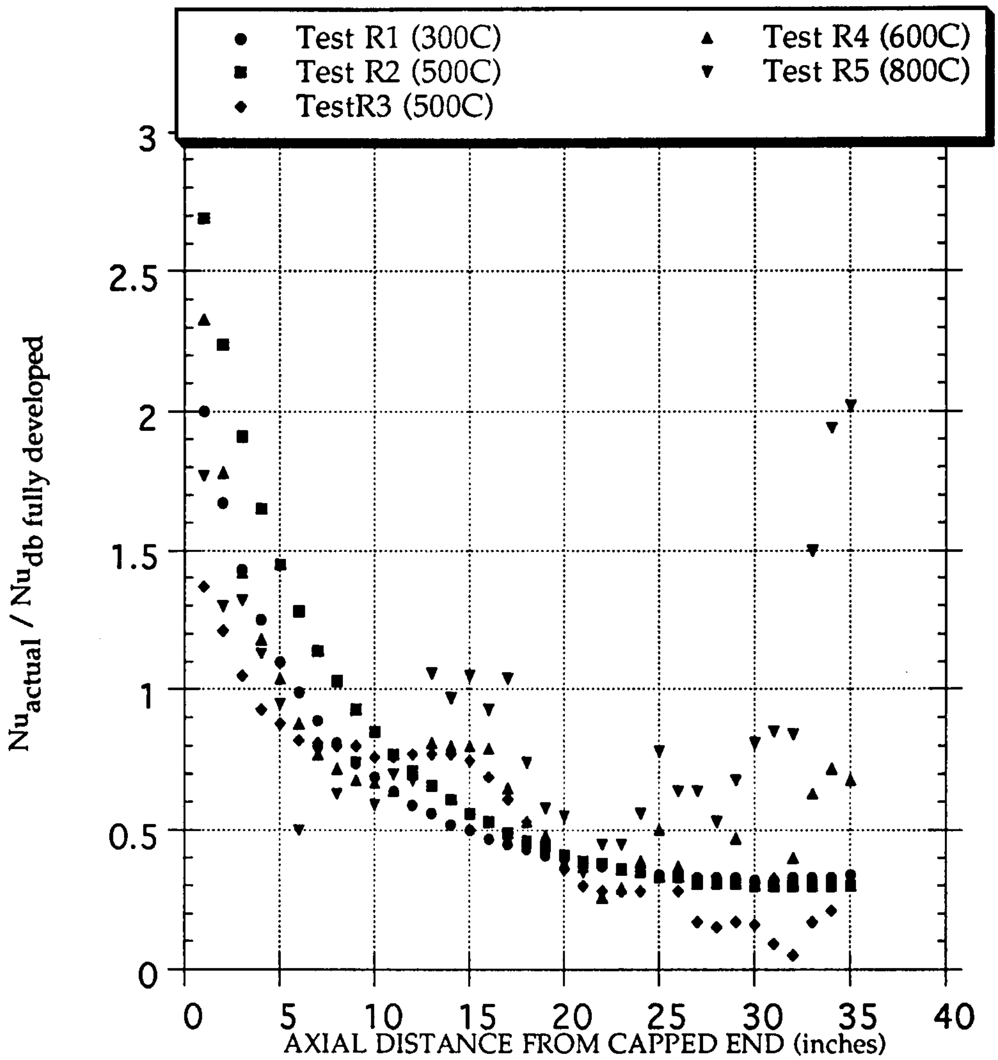

Figure A4.1 Shell-side annular (outer) heat transfer coefficients at 40 scfm flow rate.

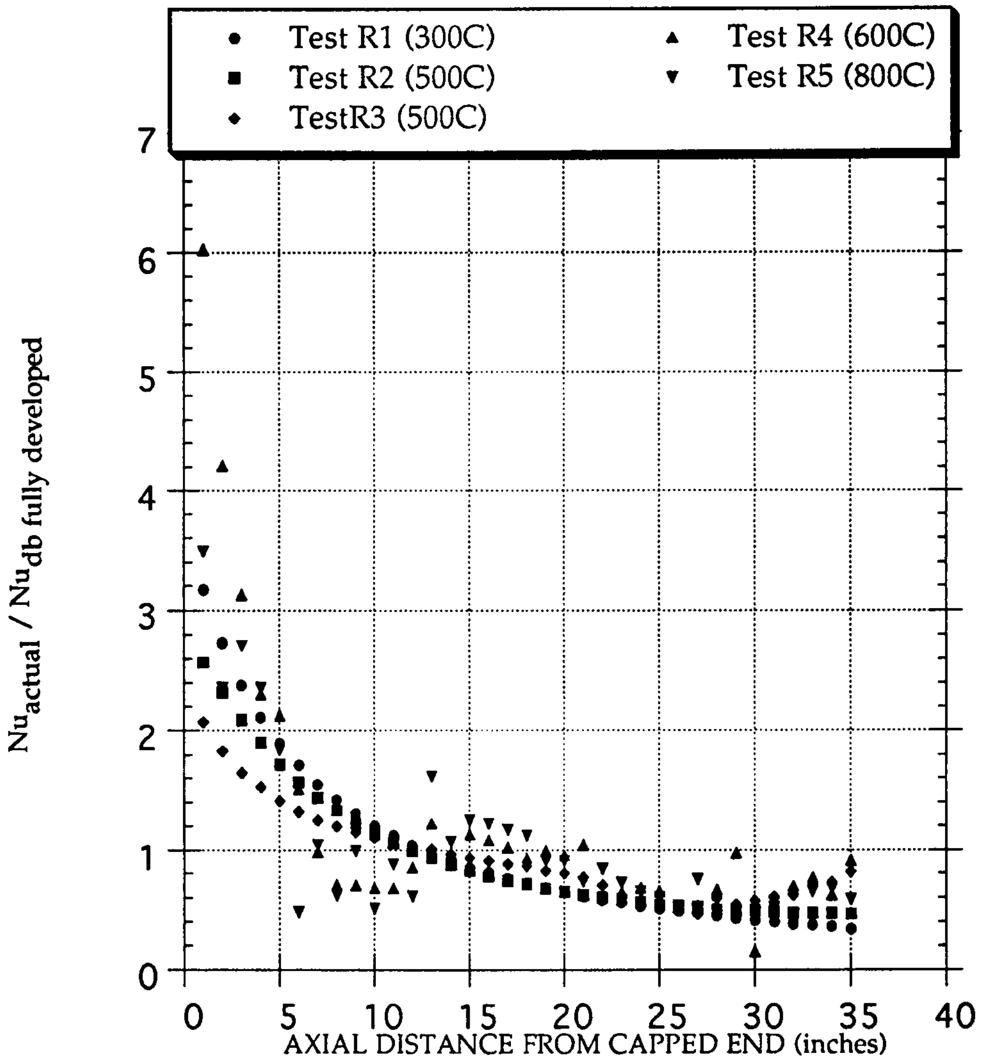

Figure A4.2 Heat transfer coefficients inside central tube at a flow rate of 40 scfm.

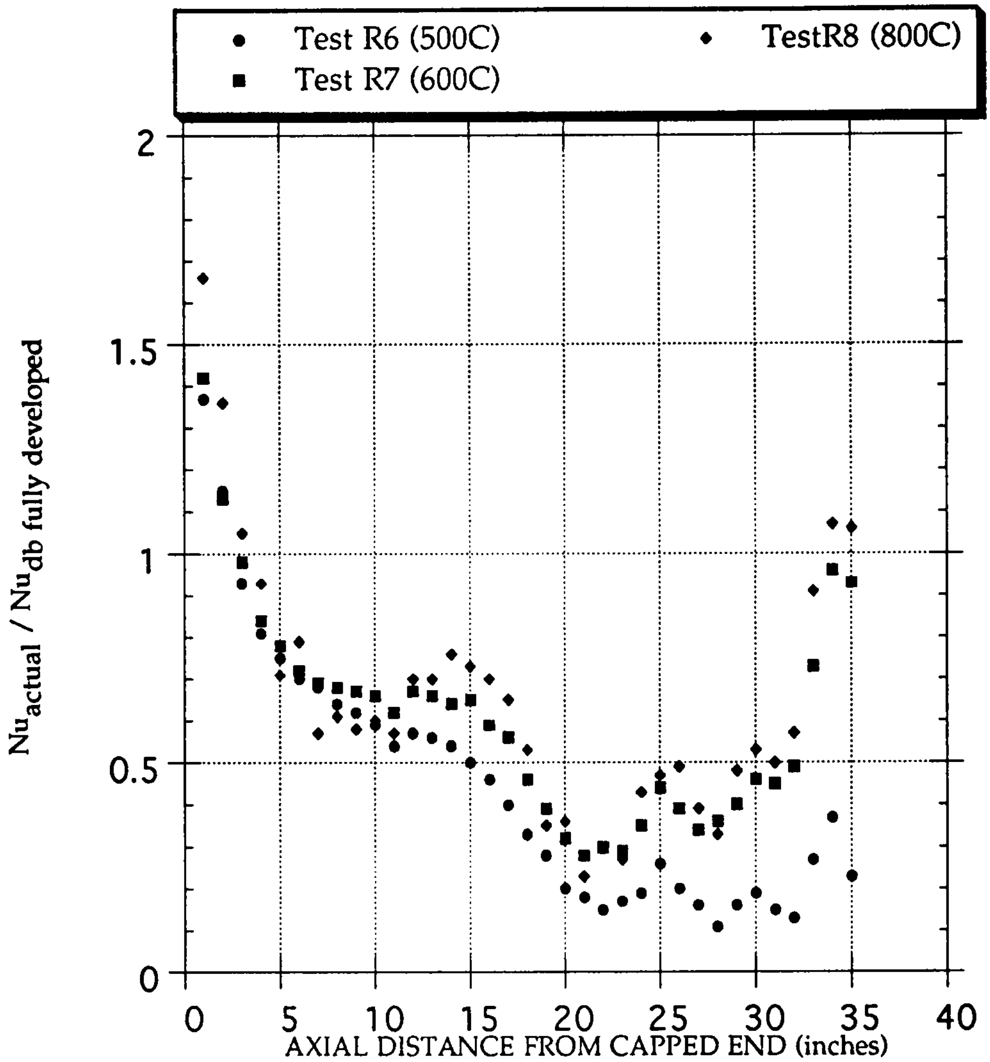

Figure A4.3 Shell-side annular (outer) heat transfer coefficients at 60 scfm flow rate.

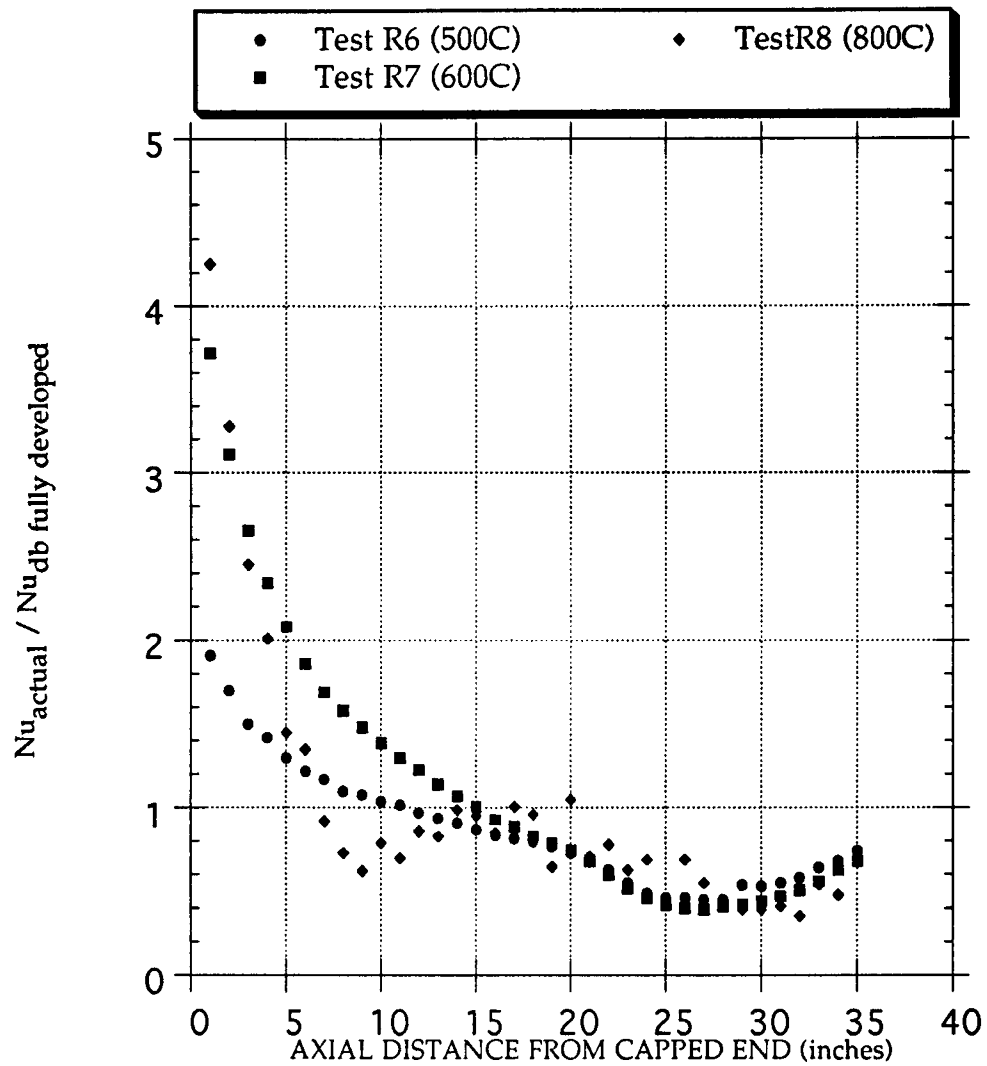

Figure A4.4 Heat transfer coefficients inside central tube at a flow rate of 60 scfm.

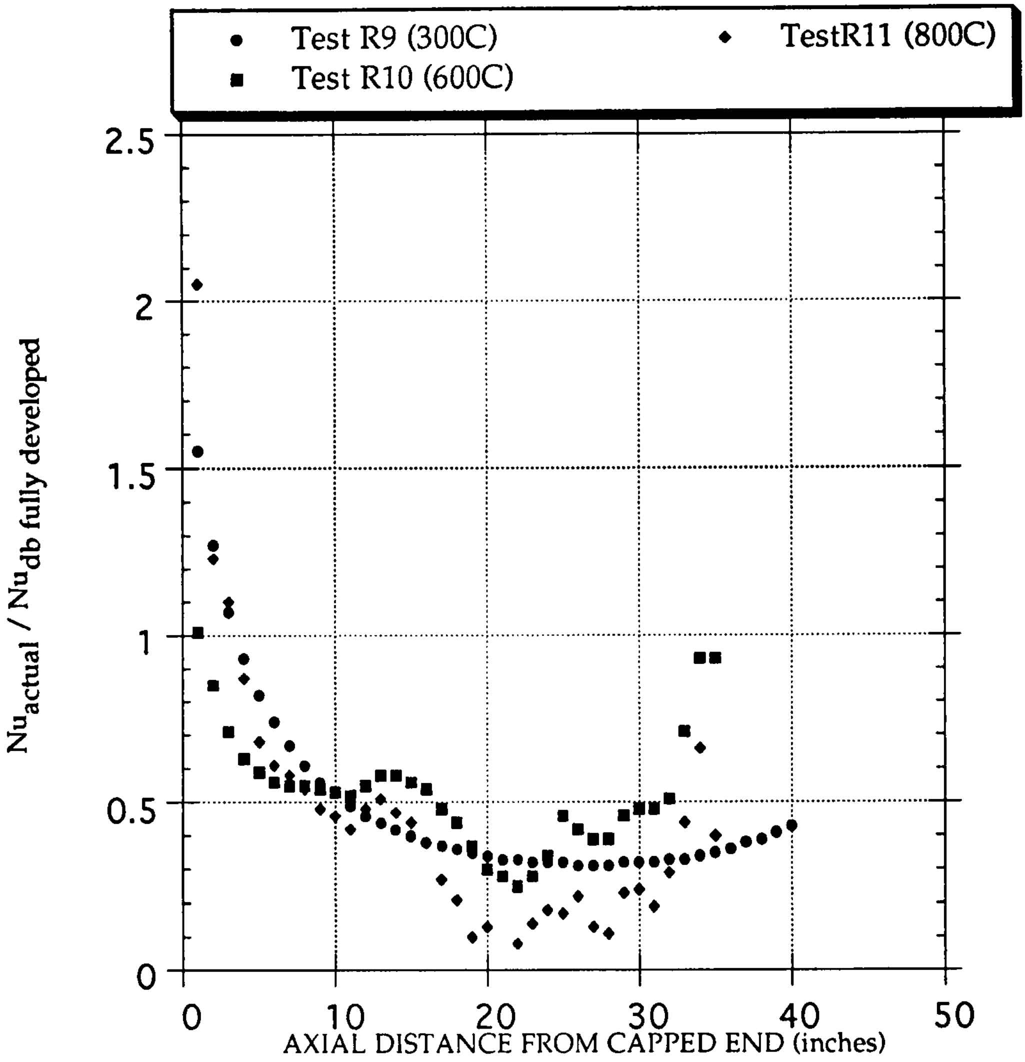

Figure A4.5 Shell-side annular (outer) heat transfer coefficients at 80 scfm flow rate.

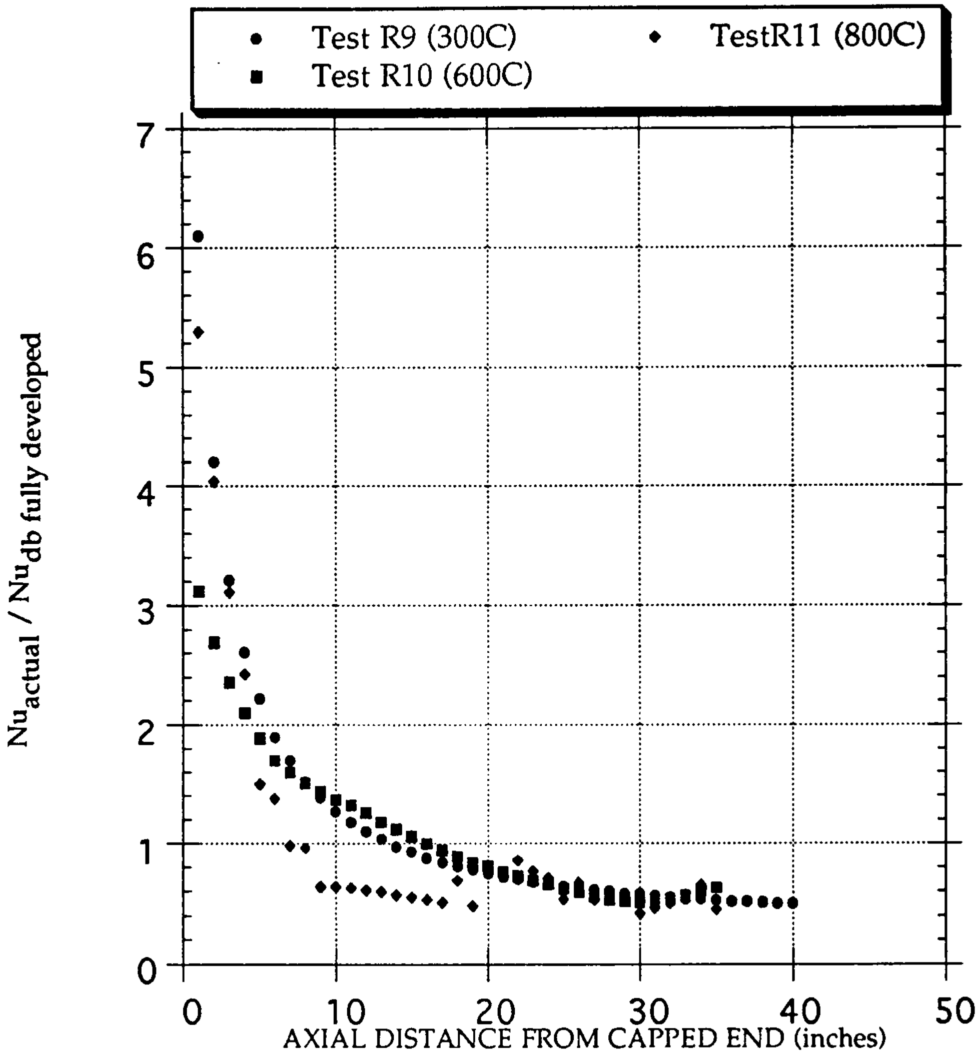

Figure A4.6 Heat transfer coefficients inside central tube at a flow rate of 80 scfm.

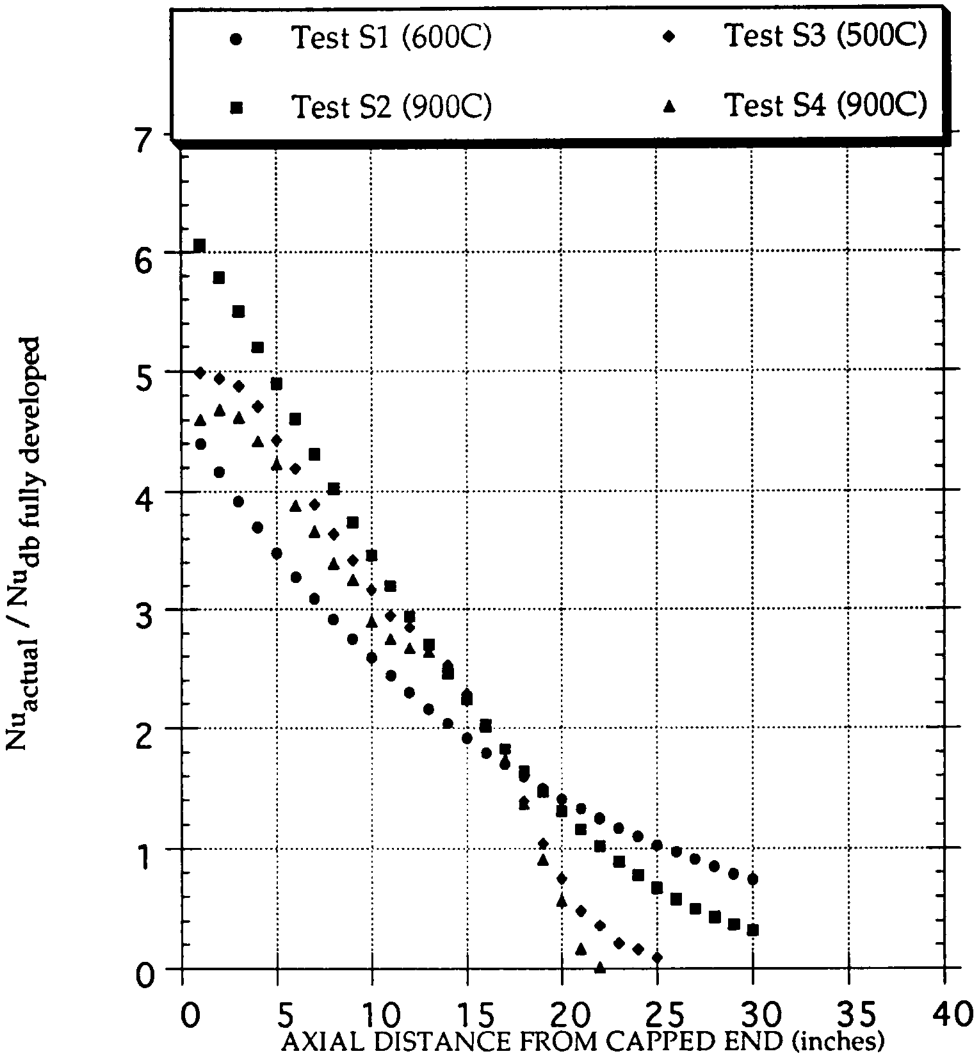

Figure A4.7 Swirl-enhanced shell-side annular (outer) heat transfer coefficients at 30 scfm flow rate.

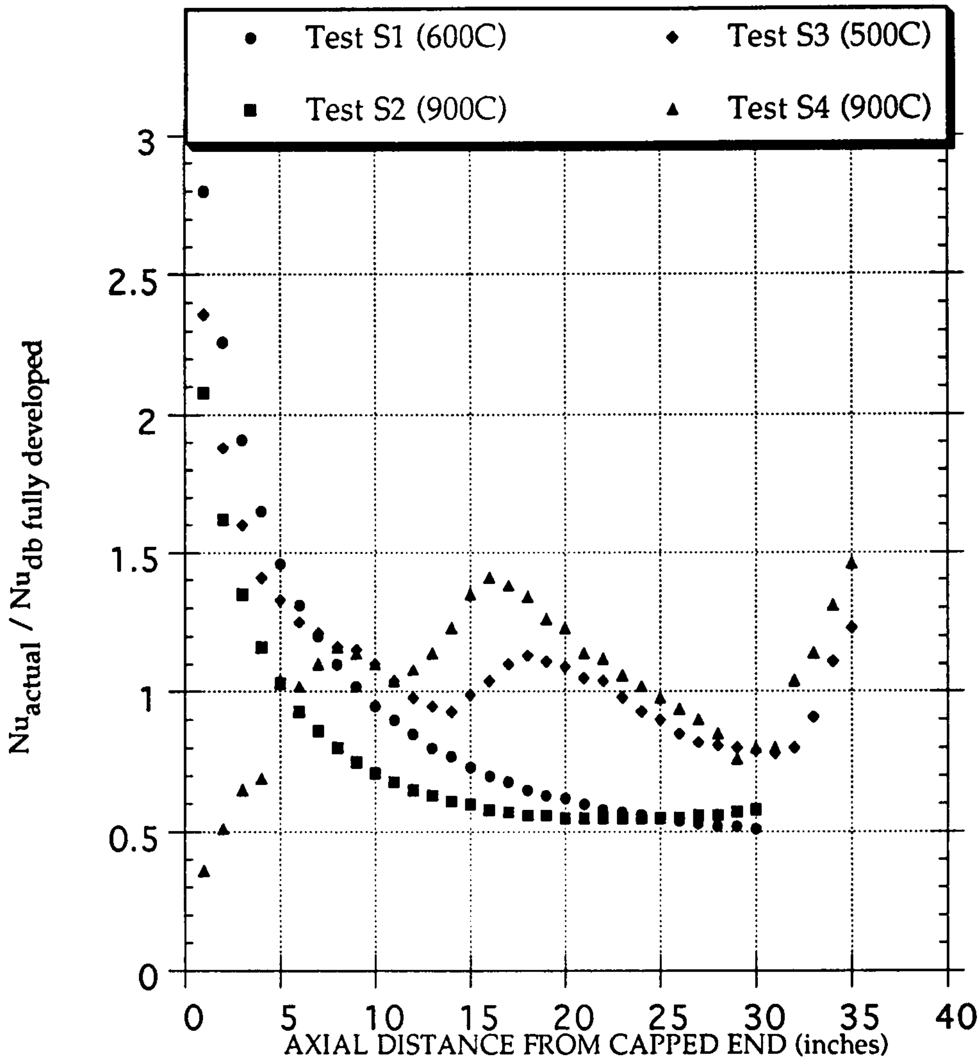

Figure A4.8 Heat transfer coefficients inside central tube at a flow rate of 30 scfm.

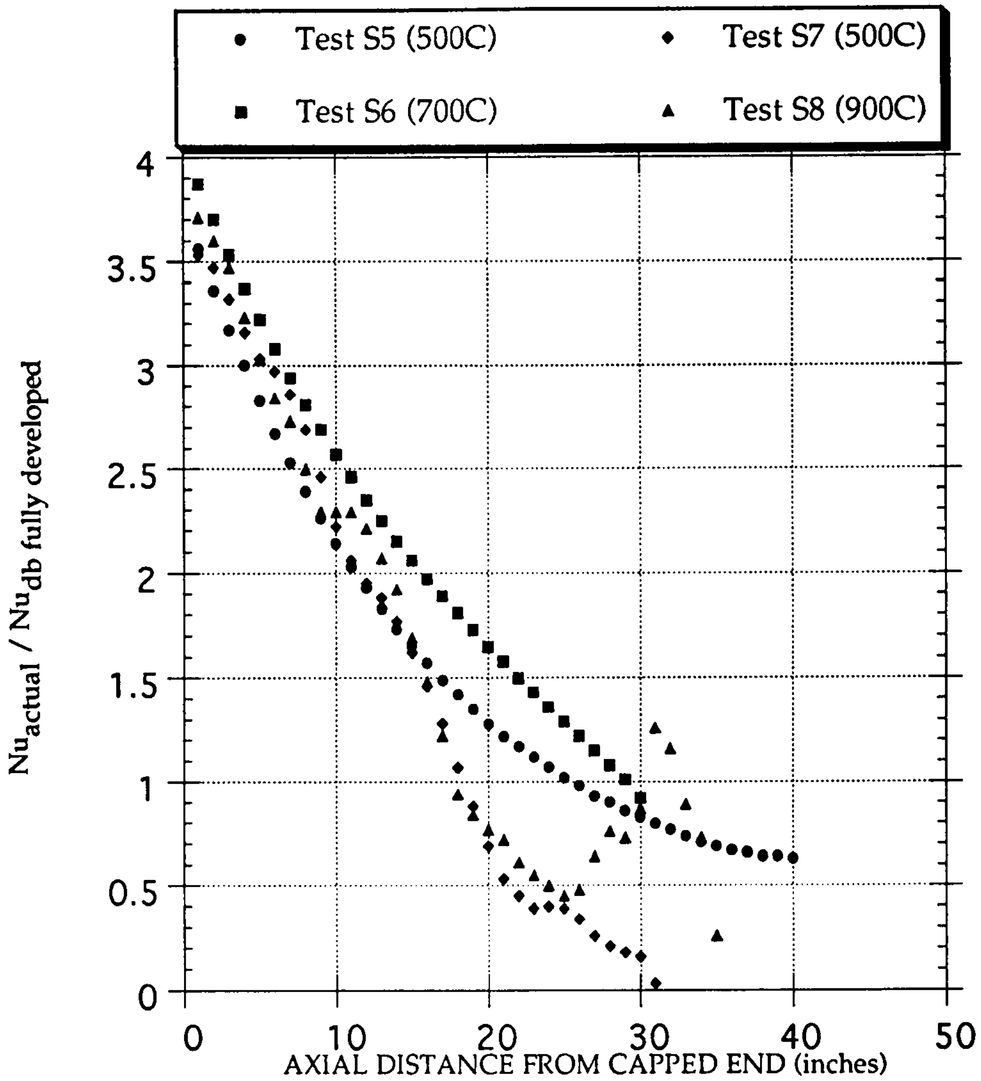

Figure A4.9 Swirl-enhanced shell-side annular (outer) heat transfer coefficients at 40 scfm flow rate.

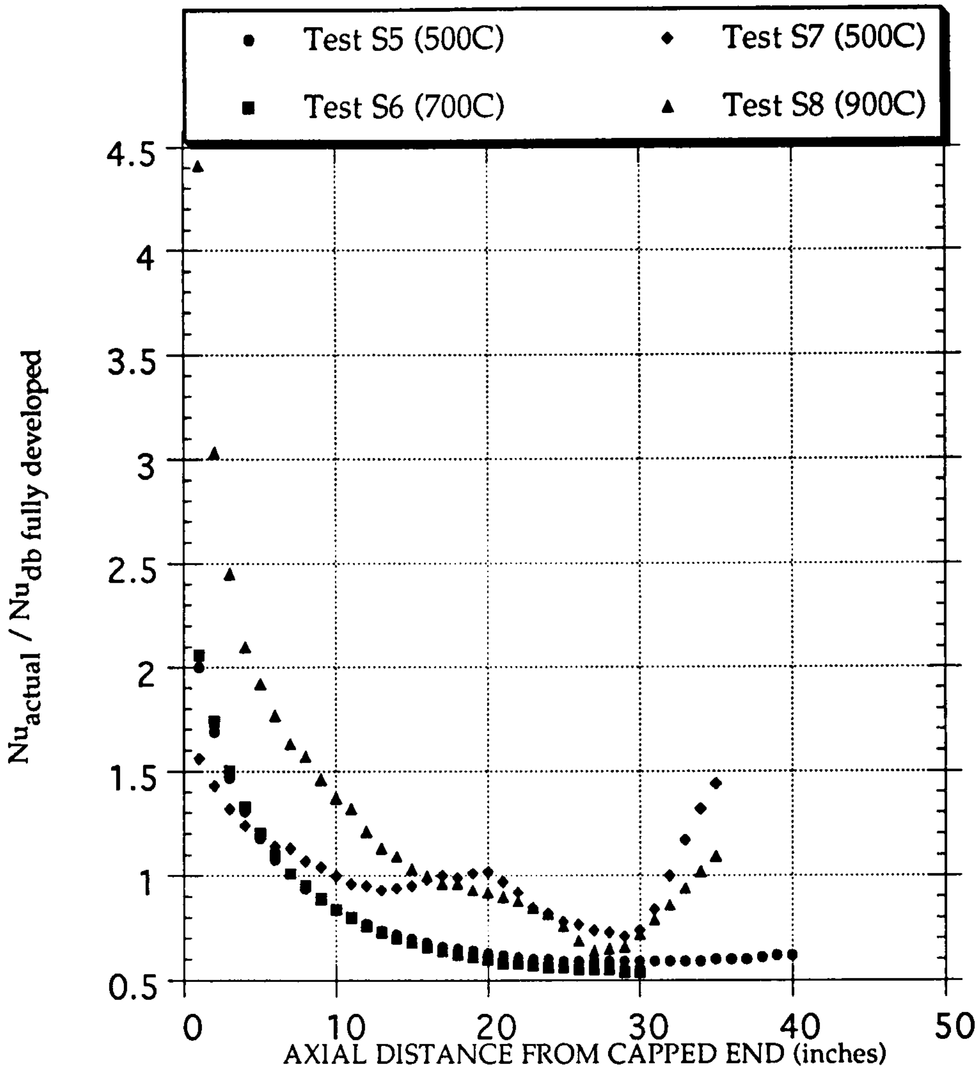

Figure A4.10 Heat transfer coefficients inside central tube at a flow rate of 40 scfm.

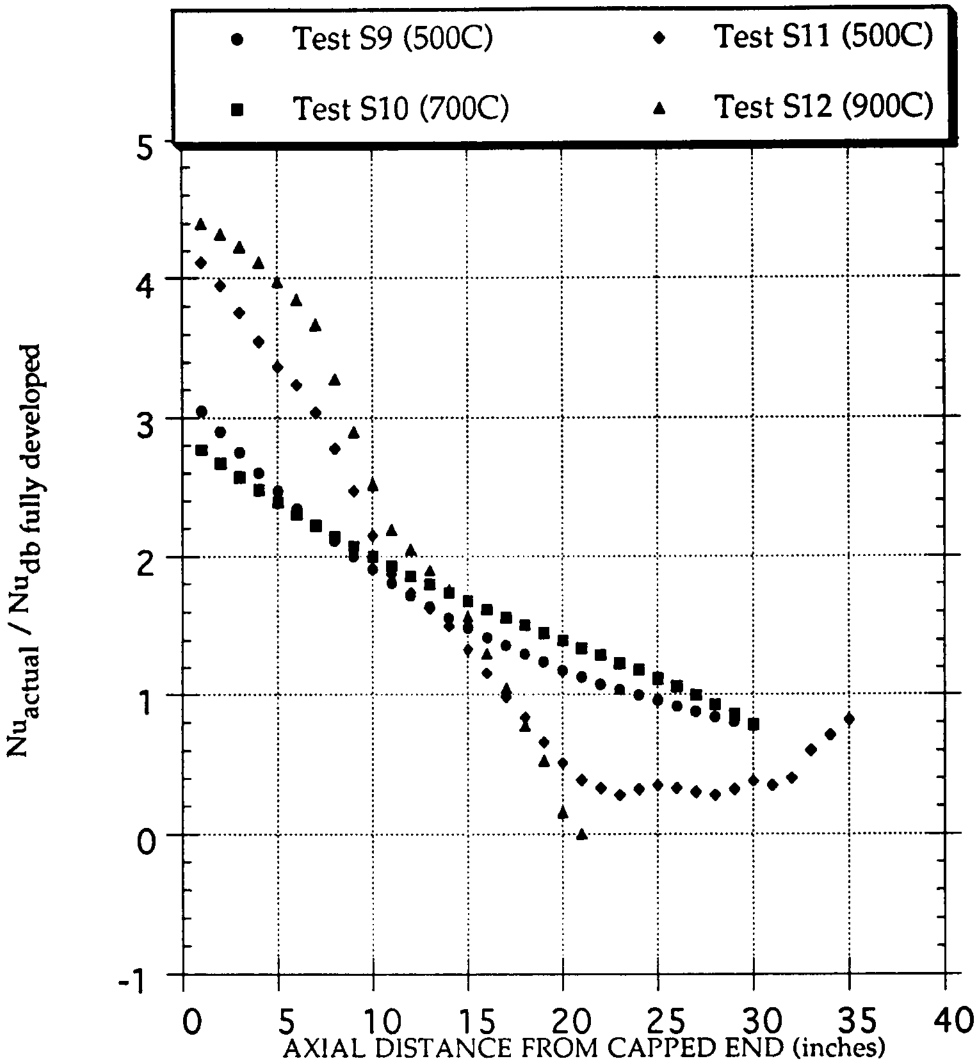

Figure A4.11 Swirl-enhanced shell-side annular (outer) heat transfer coefficients at 60 scfm flow rate.

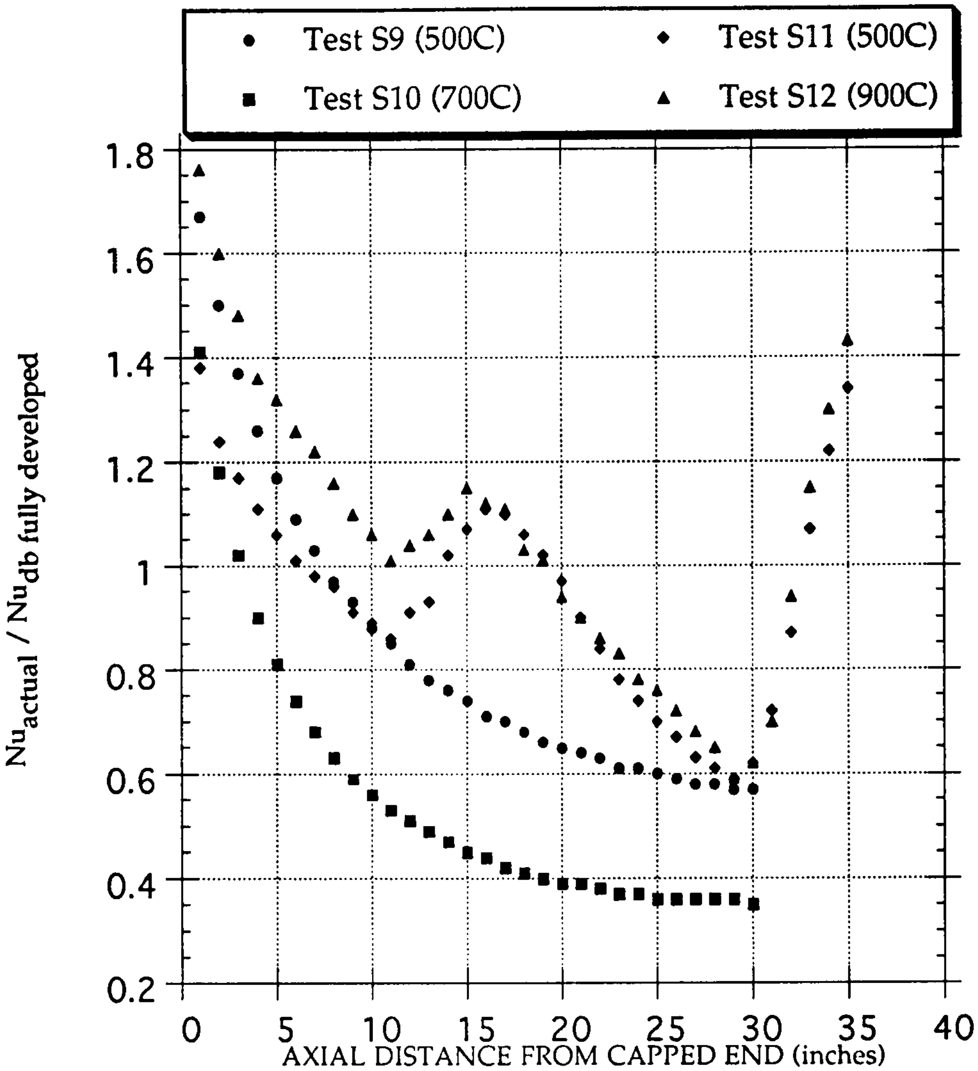

Figure A4.12 Heat transfer coefficients inside central tube at a flow rate of 60 scfm.

APPENDIX A5

COMPARISON OF PREDICTION TECHNIQUES WITH EXPERIMENTAL DATA

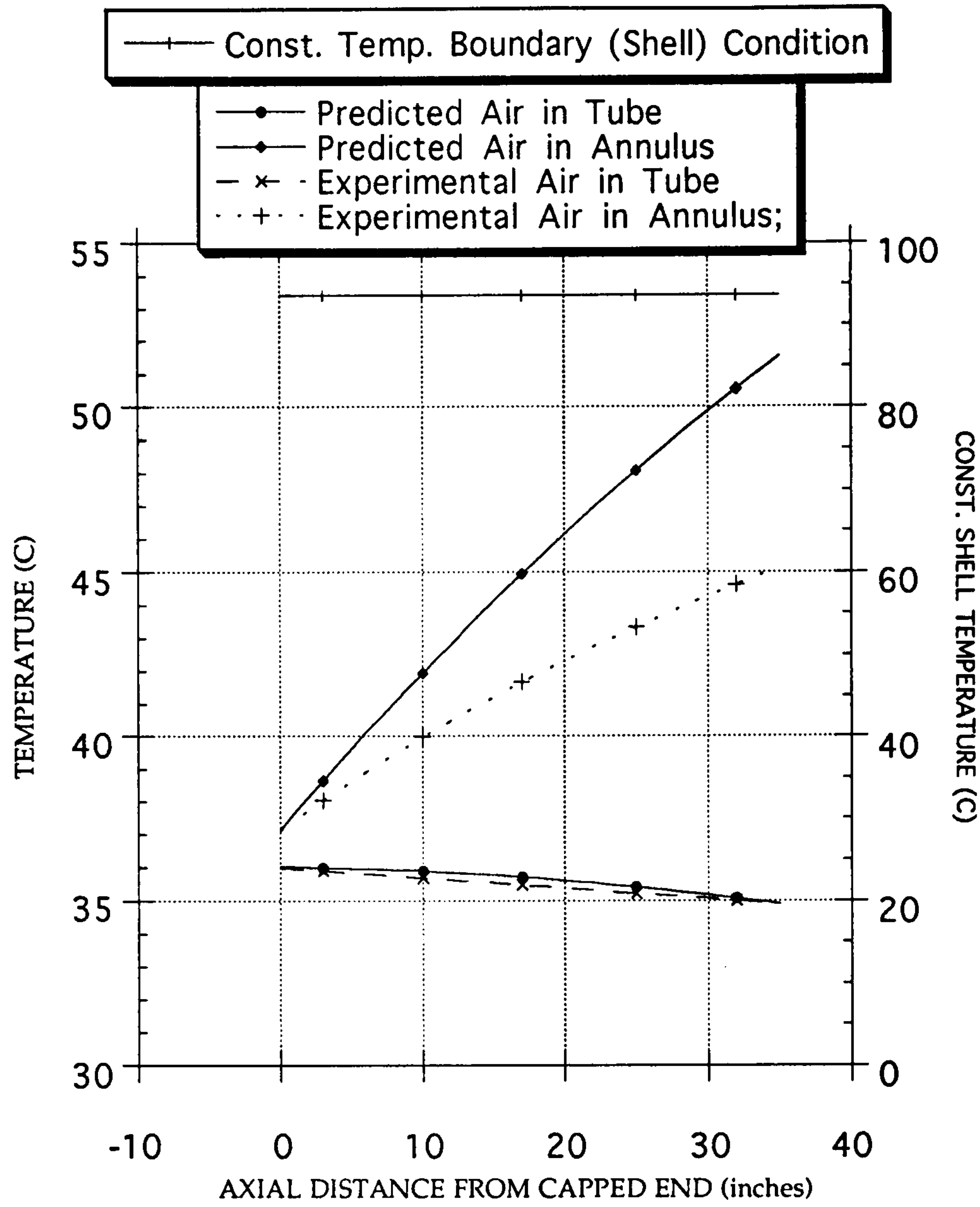

Figure A5.1 Comparison of experimental data with an analytical (convection-only) model for a bayonet tube heat exchanger (Test R1)

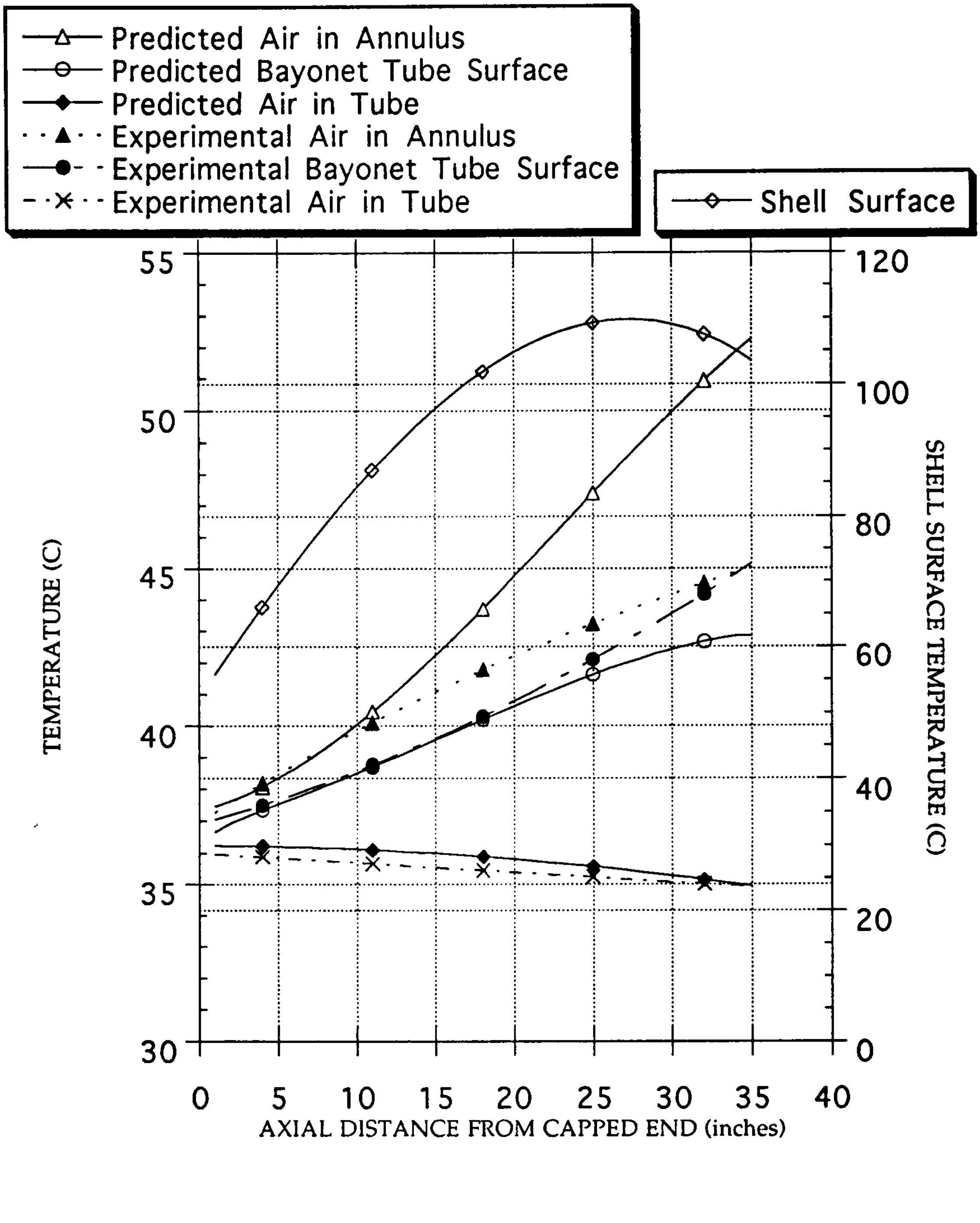

Figure A5.2 Comparison of experimental data with results from a numerical (UTSI) model (iterative) solution technique (Test R1)

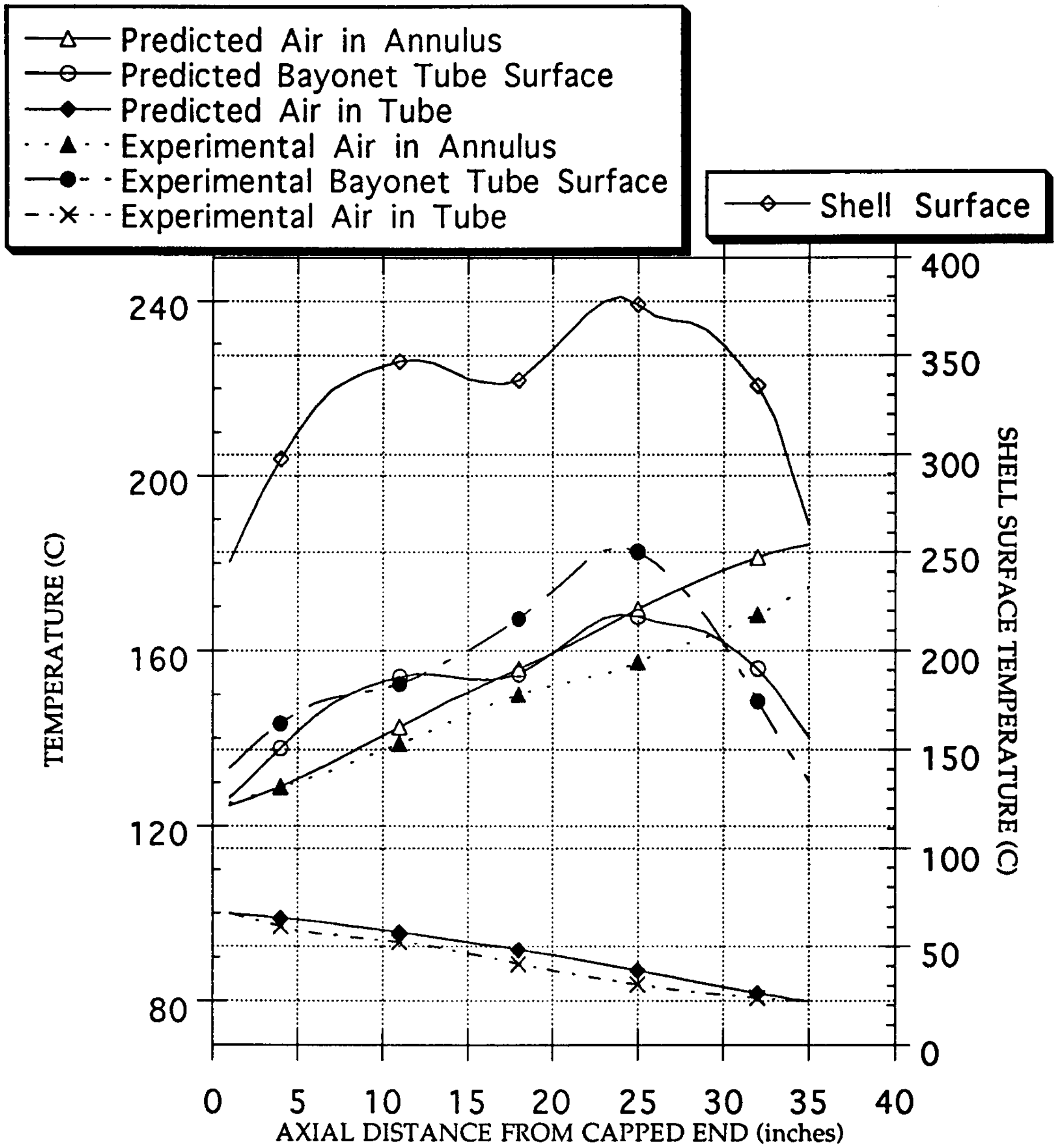

Figure A5.3 Comparison of experimental data with results from the numerical model, with constant convective coefficients. (Test R5, constant convective coefficients based on Dittus-Boelter correlation for fully developed flow)

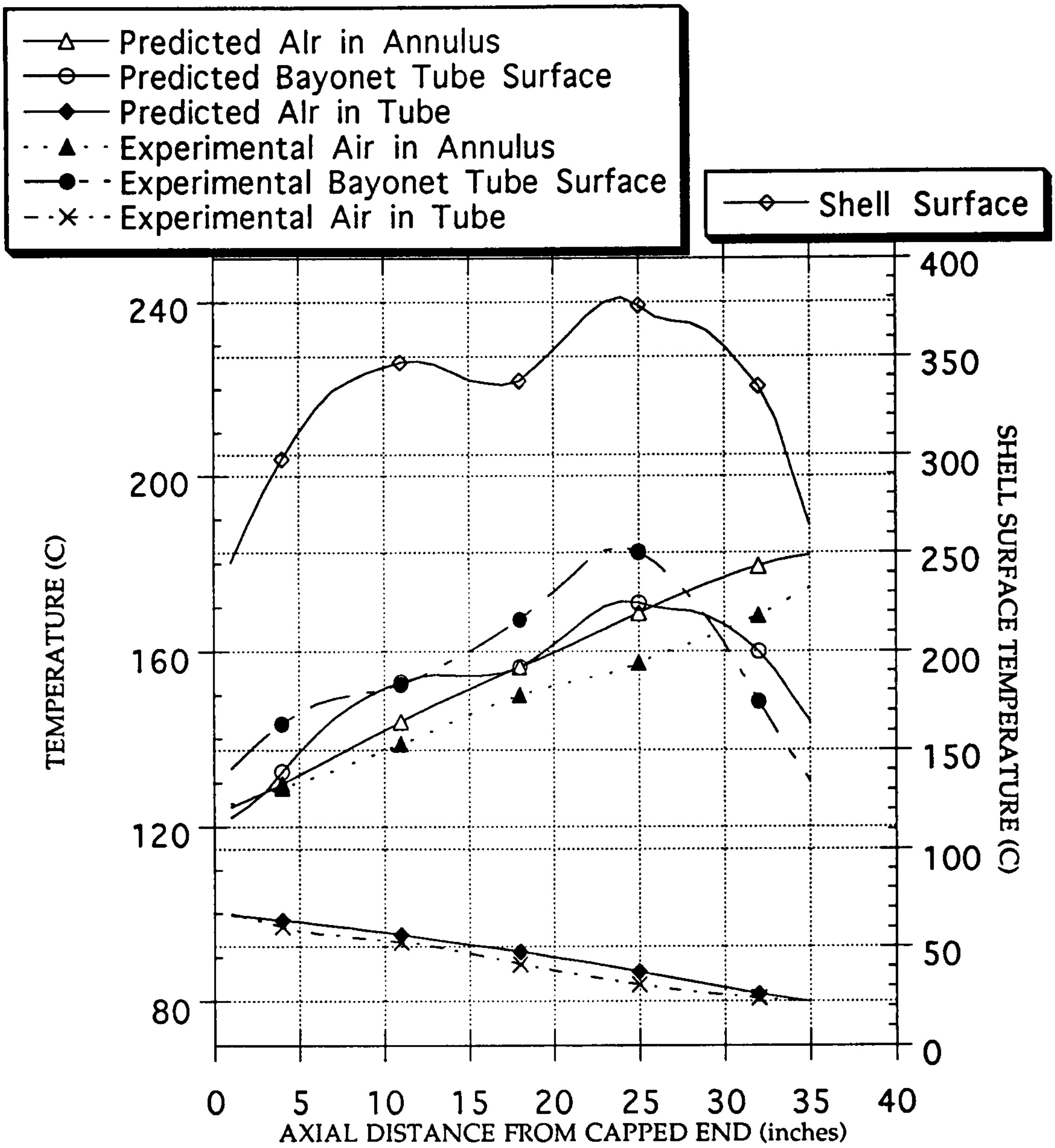

Figure A5.4 Experimental data versus numerical (UTSI) model predictions using modified convection coefficients and inlet (or exit) effects.

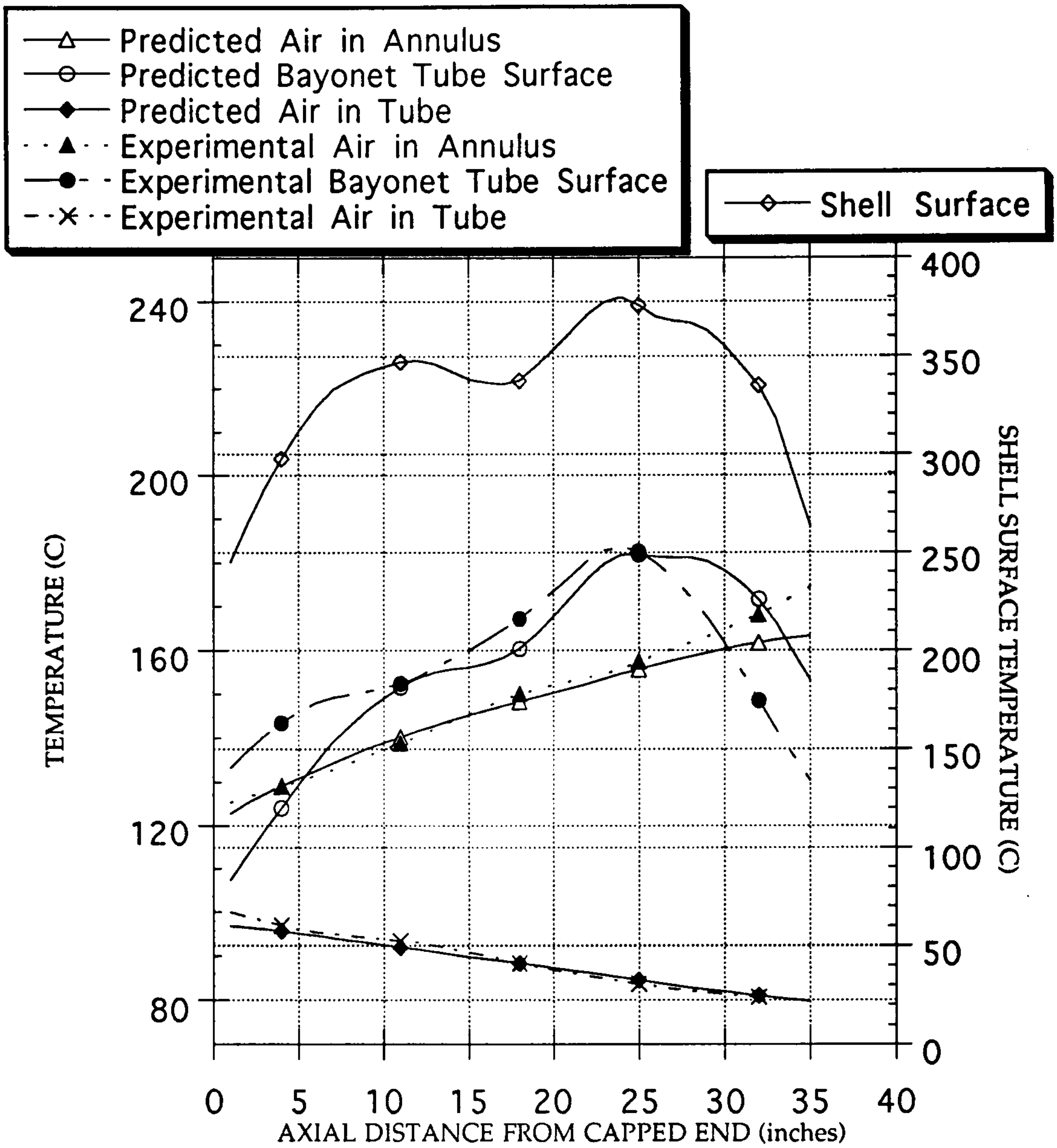

Figure A5.5 Experimental data versus numerical (UTSI) model predictions using experimental convection coefficients.

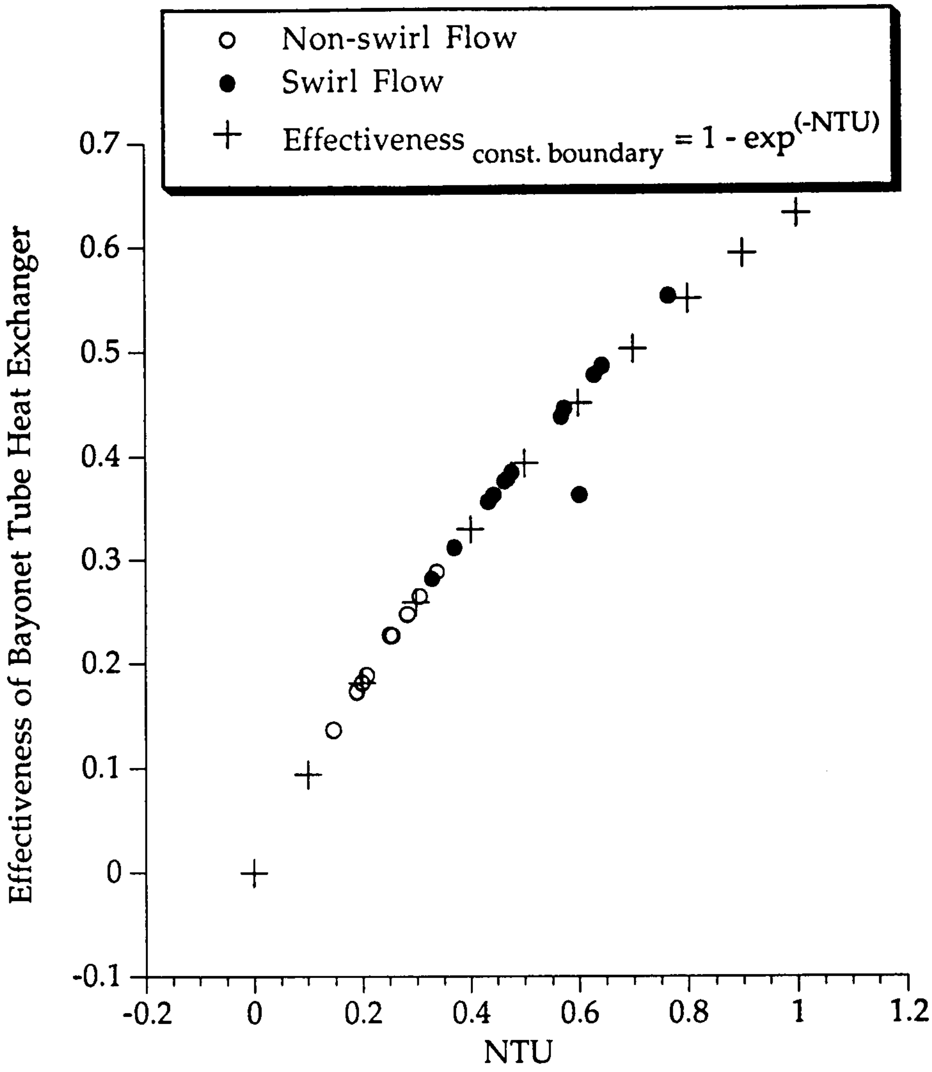

Figure A5.6 Comparison of experimental double-pipe bayonet tube heat exchanger effectiveness versus any heat exchanger effectiveness, as functions of NTU, for constant boundary temperature condition.

APPENDIX A6

TABLES

Table A6.1 Values of thermo-physical constants used in the analysis

Test Name	T_{shell} Avg.°C	T_{air} Avg. °C	C_p	μ_s (x10^{7})	K_{air} (x10^{3})	K_{tube}	K_{shell}	ε_{tube}	ε_{shell}
R1	93.62	40.02	1007.02	191.01	27.275	12.697	16.068	0.2	0.6
R2	151.28	47.89	1007.50	194.70	27.885	12.816	16.991	0.2	0.6
R3	182.17	86.25	1010.40	212.21	30.797	13.391	17.485	0.7	0.6
R4	227.57	94.64	1011.17	215.95	31.423	13.517	18.212	0.7	0.6
R5	333.14	127.23	1014.58	230.13	33.806	14.006	19.901	0.7	0.6
R6	153.06	58.41	1008.20	199.57	28.693	12.973	17.019	0.7	0.6
R7	192.69	68.89	1008.97	204.37	29.491	13.131	17.653	0.7	0.6
R8	296.72	88.53	1010.61	213.23	30.968	13.425	19.318	0.7	0.6
R9	73.30	39.36	1006.98	190.70	27.225	12.688	15.743	0.2	0.6
R10	166.4	54.32	1007.92	197.68	28.379	12.912	17.232	0.7	0.6
R11	258.14	63.64	1008.58	201.97	29.092	13.052	18.701	0.7	0.6
S1	191.93	69.40	1009.01	204.61	29.53	13.138	17.641	0.2	0.6
S2	348.34	127.94	1014.66	230.43	33.857	14.016	20.144	0.2	0.6
S3	185.54	110.57	1012.75	222.94	32.596	13.756	17.539	0.7	0.6
S4	371.57	163.25	1019.15	245.19	36.361	14.546	20.516	0.7	0.6
S5	130.36	52.29	1007.78	196.74	28.224	12.882	16.656	0.2	0.6

Table A6.1 (Continued)

Test Name	T_{shell} Avg.°C	T_{air} Avg. °C	C_p	μ_s ($\times10^{-7}$)	K_{air} ($\times10^{3}$)	K_{tube}	K_{shell}	ε_{tube}	ε_{shell}
S6	208.75	68.86	1008.97	204.36	29.489	13.13	17.91	0.2	0.6
S7	160.45	87.26	1010.49	212.66	30.873	13.41	17.137	0.7	0.6
S8	325.76	134.13	1015.39	233.06	34.30	14.11	19.783	0.7	0.6
S9	106.72	38.42	1006.93	190.26	27.15	12.674	16.278	0.2	0.6
S10	175.52	52.43	1007.79	196.81	28.24	12.884	17.379	0.2	0.6
S11	125.88	60.99	1008.38	200.76	28.89	13.012	16.58	0.7	0.6
S12	256.40	84.48	1010.25	211.42	30.67	13.365	18.67	0.7	0.6

Table A6.2 Convective coefficients and closed-end temperature discontinuity used in analysis

Test Name	$h_{annulus\ db\ fd}$	$h_{tube\ db\ fd}$	$\Delta T_{capped\ end}$ °C ($T_{ann\ in}$-$T_{tube\ out}$)
R1	31.7456	60.2973	1.14
R2	31.9627	60.7095	2.01
R3	32.9506	62.5859	7.59
R4	33.1528	62.9701	10.68
R5	33.8981	64.3857	26.03
R6	44.5996	84.7120	5.58
R7	44.9763	85.4274	7.30
R8	45.6526	86.7120	16.02
R9	55.2403	104.9226	0.35
R10	55.9522	106.2749	5.35
R11	56.3797	107.0869	12.60
S1	25.8425	49.0848	11.05
S2	26.9417	51.1726	20.18
S3	26.6327	50.5858	0.44
S4	27.5319	52.2938	18.24

Table A6.2 (continued)

Test Name	$h_{annulus\ db\ fd}$	$h_{tube\ db\ fd}$	$\Delta T_{capped\ end}$ °C ($T_{ann\ in}$-$T_{tube\ out}$)
S5	32.0817	60.9356	6.64
S6	32.5162	61.7609	11.49
S7	32.9752	62.6326	4.78
S8	34.0484	64.6710	5.64
S9	43.8474	83.2832	4.27
S10	44.3794	84.2937	9.02
S11	44.6934	84.8901	1.06
S12	45.5161	86.4528	7.81

Table A6.3 Effectiveness and Nusselt number correlations for the bayonet tube heat exchanger

Test Name	Re_{ann}	T_{ai} (°C)	T_{ao} (°C)	T_b (°C)	Effectiv - eness (%)	k=Nu * $Re_{an}^{-.8}$ $Pr^{-.4}$	length (inch)
R1	11435.7	34.92	45.11	93.62	17.3595	0.013751	35
R2	11219.4	35.12	65.65	151.28	22.7563	0.018076	35
R3	10293.4	72.54	99.69	182.17	24.7658	0.019791	35
R4	10115.4	72.21	117.07	227.57	28.8693	0.02347	35
R5	9492.05	79.46	175	333.14	37.6616	0.031665	35
R6	16418	48.93	67.88	153.06	18.1984	0.01548	35
R7	16032.2	53.04	84.73	192.69	22.6925	0.01964	35
R8	15366.36	56.74	120.32	296.72	26.4936	0.02312	35
R9	22908.6	36.87	41.86	73.3	13.6975	0.010695	40
R10	22099.85	42.63	66.01	166.4	18.8899	0.0171364	35
R11	21630.18	44.21	83.07	258.14	18.16482	0.016299	35
S1	8006.99	29.96	108.84	191.93	48.70038	0.050149	35
S2	7109.67	43.61	212.26	348.33	55.34517	0.057498	35
S3	7348.44	92.64	127.76	185.54	37.8041	0.030464	40
S4	6681.54	101.87	220.2	371.57	43.8747	0.035958	40
S5	11102.75	28.81	75.77	130.36	36.3077	0.037699	40

Table A6.3 (Continued)

Test Name	Re_{ann}	T_{ai} (°C)	T_{ao} (°C)	T_b (°C)	Effectiv - eness (%)	k=Nu * $Re_{an}^{-.8}$ $Pr^{-.4}$	length (inch)
S6	10688.84	24.89	112.86	208.75	47.84619	0.0519084	35
S7	10271.55	71.02	103.49	160.45	36.3077	0.0309987	40
S8	9372.49	79.09	189.17	325.76	44.62697	0.0390618	40
S9	17221.38	23.6	53.23	106.72	35.64726	0.0397531	35
S10	16648.63	23.07	81.79	175.52	38.51755	0.0432272	35
S11	16320.91	48.97	73.01	125.88	31.2573	0.0285887	40
S12	15497.96	56.21	112.74	256.40	28.2382	0.024962	40

APPENDIX A7

COMPUTER PROGRAM

Appendix A7

COMPUTER PROGRAM

```
C    FORTRAN PROGRAM TO CALCULATE HEAT TRANSFER COEFFICIENTS IN A
C     BAYONET TUBE HEAT EXCHANGER AND MODEL ITS PERFORMANCE
C     PLATFORM DEVELOPED ON:  VAX/VMS 785

C     OI-OUTER CYLINDER TO INNER CYLINDER, OO-OUTER CYLINDER TO OUTER
C     CYLINDER, OA-OUTER CYLINDER TO ANNULAR END, IA-INNER CYLINDER TO
C     ANNULAR END, II-INNER CYLINDER TO INNER CYLINDER, IE-INNER
C     CYLINDER TO INSIDE END
      DIMENSION OI(48,48),OO(48,48),OA(48),A(0:97,0:97),
     &AINV(0:97,0:97),AI_COEFF(48),AO_COEFF(48),HI_CALC(48),
     &W(0:97,0:97),TOA(48),TIA(48),TOO(48,48),TOI(48,48),TII1(48,48),
     &TII2(48,48),TIE(48),TGT(0:48),TGA(0:48),TM(96),TIW(48),QOC(48),
     &QOR(48),HTI(48),HTAI(48),HTAO(48),HEAT(48),TGA_ML(0:48),
     &Q_RAD(0:97),BAYONET(0:97),SHELL(0:97),IDENTITY(0:97,0:97),
     &EXCITATION(0:97,0:97),RESPONSE(0:97,0:97),EPSILON(0:97),
     &Q_AT_I_NET(0:97),A_E_BY_R(0:97),TOT_EX_AT_I(0:97,0:97),
     &AREA(0:97),THETA_INNER(0:48),THETA_OUTER(0:48),
     &RHO(0:97),W_AT_I_FROM_J(0:97,0:97),TOW(48),TIW_LAST(48),
     &SS(0:97,0:97),Q_AT_I(0:97),TEST(0:97,0:97),AREA_INNER(0:49),
     &EPSILON_INNER(0:49),RHO_INNER(0:49),TEMP_INNER(0:49),
     &W_AT_I_FROM_J_INNER(0:49,0:49),SS_INNER(0:49,0:49),
     &Q_AT_I_INNER(0:49),CONDUCTION_SHELL(48),CONDUCTION_TUBE(48),
     &TEMP_AIR_TUBE(0:49),TEMP_AIR_ANNULUS(0:49),CONV_HT_AIR_TUBE(48),
     &CONV_HT_AIR_ANNULUS(48),HT_COEFF_TUBE(48),T_COEFF(48),
     &HT_COEFF_ANNULUS_INNER(48),HT_COEFF_ANNULUS_OUTER(48),
     &TEMP_AIR_TUBE1(0:49),BAYONET1(0:97),SHELL_C1(0:97),
     &SHELL_R1(0:97),SHELL_C(0:97),SHELL_R(0:97),
     &TEMP_AIR_ANNULUS1(0:49),SHELL_VAR(0:97,3)
      INTEGER M
      REAL IA(48),II(48,48),IE(48),MCP,TEMP(0:97),K_SHELL,K_TUBE,
     &POWER_IN,POWER_AT_EACH_ZONE,NET_HEAT_AT_TUBE_ZONE(48),
     &NET_HEAT_AT_SHELL(48),MU_S,MU_INF,PRANDTL,K_AIR,E_SPHERE,
     &SPHERE_DIA,H_SPHERE_ANNULUS,H_SPHERE_TUBE,R_NUM_TUBE,
     &R_NUM_ANNULUS,NTU,M3,M1,M2,K,K1,K2
      CHARACTER*20 TESTNAME
      CALL ASSIGN(2,'CCYL.OUT')
      OPEN (UNIT=5,FILE='RESULTS.DAT',STATUS='NEW')
      OPEN (UNIT=8,FILE='SETUP.DAT',STATUS='OLD',READONLY)
      READ(8,*)
      READ(8,*)M
      READ(8,*)POWER_IN
      READ(8,*)MCP
      READ(8,*)Z
      READ(8,*)EMA
      READ(8,*)EMO
      READ(8,*)EMI
      READ(8,*)EME
      READ(8,'(A20)')TESTNAME
      WRITE(6,*)'READ TESTNAME.  TESTNAME IS:',TESTNAME
      OPEN (UNIT=14,FILE='DSK3:[BOSS.DEV.PROGRAM]DEV_SETUP.DAT',
     &STATUS='OLD',READONLY)
      READ(14,*)SPHERE_DIA
      READ(14,*)E_SPHERE
      READ(14,*)PRANDTL
      READ(14,*)MU_S
      READ(14,*)MU_INF
      READ(14,*)K_AIR
      READ(14,*)RES_TC_WALL
      DO1 I=0,2*M+1
      DO1 J=0,2*M+1
```

```
    IDENTITY(I,J)=0.0
    IF (I.EQ.J) IDENTITY(I,I)=1.0
1   CONTINUE
   PI=3.1415926
   RO=3.095/2*2.54E-2
   RI=1.9/2*2.54E-2
   Z=Z*2.54E-2
   SIGMA=5.67E-8
   AO=2.*PI*RO*Z
   AI=2.*PI*RI*Z
   AA=PI*(RO**2-RI**2)
   AE=PI*(RI-0.16*2.54E-2)**2
   CS_AREA_SHELL=PI*((RO+.2025*2.54E-2)**2-RO**2)
   CS_AREA_TUBE=PI*( RI**2 - (RI-0.16*2.54E-2)**2 )
    WRITE(6,*)'CS AREA TUBE= ',CS_AREA_TUBE
   K_SHELL=14.9
   K_TUBE=11.7
   AI_TUBE=2*PI*Z*(RI-0.16*2.54E-2)
    WRITE(2,*)'AO =',AO,'  AI',AI,'     AA',AA
    WRITE(2,*)'AE=',AE,'   CS_AREA_SHELL',CS_AREA_SHELL
    WRITE(2,*)'CS_AREA_TUBE',CS_AREA_TUBE,'AI_TUBE=',AI_TUBE
   OI(1,1)=AO*FOI(RO,RI,Z)
   DO 10 N=2,M
   OI(N,N)=OI(1,1)
   OI(1,N)=N*AO*FOI(RO,RI,N*Z)-N*OI(1,1)
   DO 20 I=2,N-1
   OI(1,N)=OI(1,N)-2*(N+1-I)*OI(1,I)
20  CONTINUE
   OI(1,N)=OI(1,N)/2.
   K=0
15  OI(1+K,N+K)=OI(1,N)
   OI(N+K,1+K)=OI(1+K,N+K)
   K=K+1
   IF(N+K .LE. M)GO TO 15
10  CONTINUE
   OO(1,1)=AO*FOO(RO,RI,Z)
   DO 30 N=2,M
   OO(N,N)=OO(1,1)
   OO(1,N)=N*AO*FOO(RO,RI,N*Z)-N*OO(1,1)
   DO 40 I=2,N-1
   OO(1,N)=OO(1,N)-2*(N+1-I)*OO(1,I)
40  CONTINUE
   OO(1,N)=OO(1,N)/2.
   K=0
35  OO(1+K,N+K)=OO(1,N)
   OO(N+K,1+K)=OO(1+K,N+K)
   K=K+1
   IF(N+K .LE. M)GO TO 35
30  CONTINUE
   FOA=(1.-FOO(RO,RI,Z)-FOI(RO,RI,Z))/2.
   OA(1)=AO*FOA
   DO 50 N=2,M
   FOA=(1.-FOO(RO,RI,N*Z)-FOI(RO,RI,N*Z))/2.
   OA(N)=N*AO*FOA
   DO 60 I=1,N-1
   OA(N)=OA(N)-OA(I)
60  CONTINUE
50  CONTINUE
   FIO=(AO/AI)*FOI(RO,RI,Z)
   FIA=(1.-FIO)/2.
   IA(1)=AI*FIA
   DO 70 N=2,M
   FIO=(AO/AI)*FOI(RO,RI,N*Z)
   FIA=(1.-FIO)/2.
   IA(N)=N*AI*FIA
   DO 80 I=1,N-1
   IA(N)=IA(N)-IA(I)
80  CONTINUE
```

```
70 CONTINUE
  FIO=AO*FOI(RO,RI,M*Z)/AI
  FIA=(1.-FIO)/2.
  FAI=M*AI*FIA/AA
  FOA=(1.-FOI(RO,RI,M*Z)-FOO(RO,RI,M*Z))/2.
  FAO=M*AO*FOA/AA
  FAA=1.-FAI-FAO
  AAA=AA*FAA
  FEI=1.-FEE(RI,Z)
  FIE=AE*FEI/AI
  FII=1.-2.*FIE
  IE(1)=AI*FIE
  II(1,1)=AI*FII
  DO 110 N=2,M
  II(N,N)=II(1,1)
  FEI=1.-FEE(RI,N*Z)
  FIE=AE*FEI/(N*AI)
  FII=1.-2.*FIE
  II(1,N)=N*AI*FII-N*II(1,1)
  DO 120 I=2,N-1
  II(1,N)=II(1,N)-2*(N+1-I)*II(1,I)
120 CONTINUE
  II(1,N)=II(1,N)/2.
  K=0
125 II(1+K,N+K)=II(1,N)
  II(N+K,1+K)=II(1+K,N+K)
  K=K+1
  IF(N+K .LE. M)GO TO 125
  IE(N)=N*AI*FIE
  DO 130 I=1,N-1
  IE(N)=IE(N)-IE(I)
130 CONTINUE
110 CONTINUE
  EE=AE*FEE(RI,M*Z)
  RHOA=1.0-EMA
  RHOO=1.0-EMO
  RHOI=1.0-EMI
  RHOE=1.0-EME
  A(0,0)=-AA/RHOA
  DO 210 I=1,M
  A(0,I)=OA(I)
  A(0,M+I)=IA(I)
210 CONTINUE
  A(0,2*M+1)=AAA
  DO 220 I=1,M
  A(I,0)=OA(I)
  DO 230 J=1,M
  A(I,J)=OO(I,J)
  IF(I .EQ. J)A(I,J)=A(I,J)-AO/RHOO
  A(I,J+M)=OI(I,J)
230 CONTINUE
  A(I,2*M+1)=OA(M+1-I)
220 CONTINUE
  DO 240 I=1,M
  A(I+M,0)=IA(I)
  DO 250 J=1,M
  A(I+M,J)=OI(I,J)
  IF(I .EQ. J)A(I+M,J+M)=-AI/RHOI
250 CONTINUE
  A(I+M,2*M+1)=IA(M+1-I)
240 CONTINUE
  A(2*M+1,0)=AAA
  DO 260 I=1,M
  A(2*M+1,I)=OA(M+1-I)
  A(2*M+1,M+I)=IA(M+1-I)
260 CONTINUE
  A(2*M+1,2*M+1)=-AA/RHOA
```

```
      CALL INV(2*M,A,AINV)
      DO 300 I=0,2*M+1
      DO 310 J=0,2*M+1
      IF(I .EQ. 0 .OR. I .EQ. 2*M+1)W(I,J)=-(AA*EMA/RHOA)*AINV(I,J)
      IF(I .GT. 0 .AND. I .LE. M)W(I,J)=-(AO*EMO/RHOO)*AINV(I,J)
      IF(I .GT. M .AND. I .LE. 2*M)W(I,J)=-(AI*EMI/RHOI)*AINV(I,J)
310   CONTINUE
300   CONTINUE

C  ************************************************************
C        MODIFICATIONS TO THE CODE START HERE
C  ************************************************************
C   SHELL(I) GIVES TEMP OF SHELL, BAYONET GIVES TEMP OF INNER TUBE
C   TEMP_AIR_TUBE & TEMP_AIR_ANNULUS GIVE TEMP OF AIR IN THESE REGIONS
C   TO ACCOUNT FOR CIRCUMFERENTIAL VARIATION OF TEMPERATURE WE
C   USE SHELL_VAR(I,1-3) FOR POSITIONS AT 0, 90 AND 30 DEGREES
C   _C AND _R ARE USED FOR CONDUCTION AND RADIATION EFFECTS.
C  ************************************************************
      OPEN (UNIT=13,FILE='TEMPERATURE.DAT',STATUS='OLD',READONLY)
      READ(13,*)
      TEMP_B=0.0
      DO 2998 J=0,M
      READ(13,*)SHELL_VAR(J,1),SHELL_VAR(J,2),SHELL_VAR(J,3),
     &BAYONET1(J),TEMP_AIR_TUBE1(J),TEMP_AIR_ANNULUS1(J)
      TEMP_AIR_TUBE1(J)=TEMP_AIR_TUBE1(J)+273.15
      BAYONET1(J)=BAYONET1(J)+273.15
      TEMP_AIR_ANNULUS1(J)=TEMP_AIR_ANNULUS1(J)+273.15
      SHELL_C1(J)=SHELL_VAR(J,1)+SHELL_VAR(J,2)+SHELL_VAR(J,3)
      SHELL_C1(J)=SHELL_C1(J)/3+273.15
      TEMP_B=TEMP_B+SHELL_C1(J)
      SHELL_R1(J)=(SHELL_VAR(J,1)+273.15)**4+
     &(SHELL_VAR(J,2)+273.15)**4+(SHELL_VAR(J,3)+273.15)**4
      SHELL_R1(J)= (SHELL_R1(J)/3)**0.25
      IF (J .GT. 0) THEN
      WRITE(2,*)J,TEMP_AIR_TUBE1(J-1),
     &TEMP_AIR_TUBE1(J),
     &TEMP_AIR_TUBE1(J-1)-TEMP_AIR_TUBE1(J),CONV_HT_AIR_TUBE(J)/MCP,
     &  HT_COEFF_TUBE(J)
      END IF
2998  CONTINUE
      TEMP_B=TEMP_B/(M+1)
      OPEN(UNIT=24,FILE='FINAL.DAT',STATUS='NEW')
      WRITE(24,*)'INPUTTED TEMPERATURES FOR SHELL'
      WRITE(24,*)' ZONE     SHELL@0     SHELL@90     SHELL@30
     &SHELL_C  SHELL_R'
      DO 2997 I=1,M
      SHELL_C(I)=(SHELL_C1(I-1)+SHELL_C1(I))/2
      SHELL_R(I)=(SHELL_R1(I-1)+SHELL_R1(I))/2
      BAYONET(I)=(BAYONET1(I-1)+BAYONET1(I))/2
      WRITE(24,9910)I,SHELL_VAR(I,1),SHELL_VAR(I,2),SHELL_VAR(I,3),
     &SHELL_C1(I),SHELL_R1(I)
2997  CONTINUE
      WRITE(2,*)
9910  FORMAT(I3,5(2X,F8.2))
C   ********************************************************
C   RADIATIVE CORRECTION FOR AIR TEMPERATURES
C   ********************************************************
C   H_SPHERE_ANNULUS, H_SPHERE_TUBE ARE HEAT TRANSFER COEFFS AT THE
C   THERMOCOUPLE TIP SURFACE
C   REFER SECTION: 9-5 PAGE 487 "PRN OF H.T. - KREITH 3ED"

      R_NUM_ANNULUS=(MCP/1007/AA)*SPHERE_DIA/MU_S
      R_NUM_TUBE=(MCP/1007/(PI*(RI-0.16*2.54E-2)**2))*SPHERE_DIA/MU_S
      WRITE(24,*)'REYNOLDS  NUMBER-  ANNULUS=',R_NUM_ANNULUS
      WRITE(24,*)'REYNOLDS  NUMBER-  TUBE =',R_NUM_TUBE

      H_SPHERE_ANNULUS=K_AIR/SPHERE_DIA*(2+(0.4*R_NUM_ANNULUS**0.5
```

```
  & +0.006*R_NUM_ANNULUS**0.67)*PRANDTL**0.4*(MU_S/MU_INF)**0.25)

    H_SPHERE_TUBE=K_AIR/SPHERE_DIA*(2+(0.4*R_NUM_TUBE**0.5
  & +0.006*R_NUM_TUBE**0.67)*PRANDTL**0.4*(MU_S/MU_INF)**0.25)
    OPEN(UNIT=25,FILE='CORRECTIONS.DAT',STATUS='NEW')
    WRITE(25,*)'HT_COEFF_TC_TIP:  ANNULUS=',H_SPHERE_ANNULUS,'
  & TUBE=',H_SPHERE_TUBE
    WRITE(25,*)'EMISSIVITIES:  O,I,SPHERE',EMO,EMI,E_SPHERE
    WRITE(25,*)
    WRITE(25,*)'ANNULUS TEMP:  DEL2      CONDUC'
    DO 2999 I=0,M
    DEL2=1/H_SPHERE_ANNULUS*SIGMA*(0.6*EMO*SHELL_R1(I)**4
  & +0.4*EMI*BAYONET1(I)**4-E_SPHERE*TEMP_AIR_ANNULUS1(I)**4)
C   BECAUSE RADIATION IS A SURFACE PHENOMENON WE USE THE SAME
C   AREA FOR CONVECTION AND RAD.  SEE THE TOTAL CONFIG FACTORS
C   THEY TOGETHER ADD UP TO 1.
    DEL3=1/H_SPHERE_ANNULUS*( SIGMA*(0.6*EMO*SHELL_R1(I)**4
  & +0.4*EMI*BAYONET1(I)**4-E_SPHERE*TEMP_AIR_ANNULUS1(I)**4)
  & -(TEMP_AIR_ANNULUS1(I)-BAYONET1(I))/RES_TC_WALL/(PI*4*
  & (SPHERE_DIA/2)**2) )
    WRITE(25,*)TEMP_AIR_ANNULUS1(I),DEL2,DEL3
    TEMP_AIR_ANNULUS1(I)=TEMP_AIR_ANNULUS1(I)-DEL2
    TEMP_AIR_TUBE1(I)=TEMP_AIR_TUBE1(I)-
  & 1/H_SPHERE_TUBE*SIGMA*(
  & 1.0*EMI*BAYONET1(I)**4-E_SPHERE*TEMP_AIR_TUBE1(I)**4)
2999 CONTINUE
    DO 2996 I=1,M
    TEMP_AIR_ANNULUS(I)=(TEMP_AIR_ANNULUS1(I-1)+
  & TEMP_AIR_ANNULUS1(I))/2
    TEMP_AIR_TUBE(I)=(TEMP_AIR_TUBE1(I-1)+TEMP_AIR_TUBE1(I))/2
     WRITE(5,*)I,SHELL_C(I),SHELL_R(I)
 2996 CONTINUE
    WRITE(24,*)'TUBE_AIR   ANNULUS_AIR  BAYONET_TEMP'
    DO 3996 I=1,M
    WRITE(24,*)I,TEMP_AIR_TUBE(I),TEMP_AIR_ANNULUS(I),
  &BAYONET(I)
    WRITE(5,*)'MID  PT',TEMP_AIR_TUBE(I),TEMP_AIR_ANNULUS(I),
  &BAYONET(I)
 3996 CONTINUE
C*****************************************************************
C   2ND SET OF MODIFICATIONS.
C*****************************************************************
    DO 401 I=0,2*M+1
    IF (I.EQ.0) THEN
        TEMP(I)=SHELL_R1(0)
        AREA(I)=AA
        RHO(I)=RHOA
        EPSILON(I)=EMA
      ELSE
        IF (I.GE.1 .AND. I.LE.M) THEN
        TEMP(I)=SHELL_R(I)
        AREA(I)=AO
        RHO(I)=RHOO
        EPSILON(I)=EMO
         ELSE
          IF (I.GE.M+1 .AND. I.LE.2*M) THEN
          TEMP(I)=BAYONET(I-M)
          AREA(I)=AI
          RHO(I)=RHOI
          EPSILON(I)=EMI
          ELSE
            IF(I.EQ.2*M+1) THEN
            TEMP(I)=SHELL_C1(M)
            AREA(I)=AA
             RHO(I)=RHOA
            EPSILON(I)=EMA
            ENDIF
          ENDIF
```

```
      ENDIF
     ENDIF
401  CONTINUE
     DO 404 I=0,2*M+1
     DO 404 J=0,2*M+1
     W_AT_I_FROM_J(I,J)=-(AREA(J)*EPSILON(J)/RHO(J))*
    & AINV(I,J)*SIGMA*TEMP(J)**4
404  CONTINUE
     DO 4081 I=0,2*M+1
     SUM1=0.0
     DO 408 J=0,2*M+1
      SS(I,J)=AREA(I)*EPSILON(I)/RHO(I)*(W_AT_I_FROM_J(I,J)/
    & (SIGMA*TEMP(J)**4)-IDENTITY(I,J)*EPSILON(J))
     SUM1=SUM1+SS(I,J)
408  CONTINUE
4081 CONTINUE
     WRITE(2,*)'I,  Q_AT_I(I)'
     Q_FROM_SHELL=0.0
     Q_AT_BAYONET=0.0
     SUM=0.0
     DO 405 I=0,2*M+1
     Q_AT_I(I)=0.0
     DO 407 J=0,2*M+1
     Q_AT_I(I)=Q_AT_I(I) + SS(I,J)*SIGMA*
    &(TEMP(I)**4-TEMP(J)**4)
407  CONTINUE
     IF (I.LE.M)THEN
        Q_FROM_SHELL=Q_FROM_SHELL+Q_AT_I(I)
     ELSE
        Q_AT_BAYONET=Q_AT_BAYONET+Q_AT_I(I)
     ENDIF
     SUM=SUM+Q_AT_I(I)
405  CONTINUE
     WRITE(2,*)'SUM TOTAL OF HEAT TRANSFER=',SUM
     WRITE(2,*)'FROM SHELL =',Q_FROM_SHELL-Q_AT_I(0)
     WRITE(2,*)'TO BAYONET =',Q_AT_BAYONET-Q_AT_I(2*M+1)
     WRITE(2,*)'FROM ANNULUS ENDS =',Q_AT_I(M+1)+Q_AT_I(0)
C    ************************************************
C    ************************************************
     DO 304 I=0,2*M+1
     DO 304 J=0,2*M+1
     IF(I.EQ.0)A_E_BY_R(I)=AA*EMA/RHOA
     IF(I.GE.1 .OR. I.LE.M)A_E_BY_R(I)=AO*EMO/RHOO
     IF(I.GE.M+1 .OR. I.LE.2*M)A_E_BY_R(I)=AI*EMI/RHOI
     IF(I.EQ.2*M+1)A_E_BY_R(I)=AA*EMA/RHOA
304  CONTINUE
     TA1A1=(AA*EMA/RHOA)*(W(0,0)-EMA)
     DO 320 J=1,M
     TOA(J)=(AO*EMO/RHOO)*W(0,J)
     TIA(J)=(AI*EMI/RHOI)*W(0,J+M)
320  CONTINUE
     TA1A2=(AA*EMA/RHOA)*W(0,2*M+1)
     DO 330 I=1,M
      SUM2=0.0
      SUM3=0.0
     DO 340 J=1,M
     IF(I .EQ. J)TOO(I,I)=(AO*EMO/RHOO)*(W(I,I)-EMO)
     IF(I .NE. J)TOO(I,J)=(AO*EMO/RHOO)*W(I,J)
     TOI(I,J)=(AI*EMI/RHOI)*W(I,J+M)
     IF(I .EQ. J)TII1(I,I)=(AI*EMI/RHOI)*(W(I+M,I+M)-EMI)
     IF(I .NE. J)TII1(I,J)=(AI*EMI/RHOI)*W(I+M,J+M)
      SUM2=SUM2+TOO(I,J)
      SUM3=SUM3+TII1(I,J)
340  CONTINUE
330  CONTINUE
C    **********************************************************
C        INNER TUBE EXCHANGE FACTORS CALCULATED HERE
C    **********************************************************
```

```
      A(0,0)=-AE/RHOE
      DO 610 I=1,M
      A(0,I)=IE(I)
 610  CONTINUE
      A(0,M+1)=EE
      DO 620 I=1,M
      A(I,0)=IE(I)
      DO 630 J=1,M
      A(I,J)=II(I,J)
      IF(I .EQ. J)A(I,J)=A(I,J)-AI/RHOI
 630  CONTINUE
      A(I,M+1)=IE(M+1-I)
 620  CONTINUE
      A(M+1,0)=EE
      DO 660 I=1,M
      A(M+1,I)=IE(M+1-I)
 660  CONTINUE
      A(M+1,M+1)=-AE/RHOE
      CALL INV(M,A,AINV)
      DO 700 I=0,M+1
      DO 710 J=0,M+1
      IF(I .EQ. 0 .OR. I .EQ. M+1)W(I,J)=-(AE*EME/RHOE)*AINV(I,J)
      IF(I .GT. 0 .AND. I .LE. M)W(I,J)=-(AI*EMI/RHOI)*AINV(I,J)
 710  CONTINUE
 700  CONTINUE
      TE1E1=(AE*EME/RHOE)*(W(0,0)-EME)
      DO 720 J=1,M
      TIE(J)=(AI*EMI/RHOI)*W(0,J)
 720  CONTINUE
      TE1E2=(AE*EME/RHOE)*W(0,M+1)
      DO 730 I=1,M
      DO 740 J=1,M
      IF(I .EQ. J)TII2(I,I)=(AI*EMI/RHOI)*(W(I,I)-EMI)
      IF(I .NE. J)TII2(I,J)=(AI*EMI/RHOI)*W(I,J)
 740  CONTINUE
 730  CONTINUE
C     *********************************************************
C     CALCS FOR INNER EXCHANGE FACTORS AND RADIATION AMOUNTS
C     *********************************************************
C     SETTING UP THE _INNER(I) MATRICES WITH KNOWN VALUES
       DO 4042 I=1,M
       AREA_INNER(I)=AI_TUBE
       EPSILON_INNER(I)=EPSILON(I+M)
       RHO_INNER(I)=RHO(I+M)
       TEMP_INNER(I)=TEMP(I+M)
 4042  CONTINUE
       AREA_INNER(0)=AE
       EPSILON_INNER(0)=EME
       RHO_INNER(0)=RHOE
       TEMP_INNER(0)=TEMP(0)
       AREA_INNER(M+1)=AE
       EPSILON_INNER(M+1)=EME
       RHO_INNER(M+1)=RHOE
       TEMP_INNER(M+1)=BAYONET1(M)
       DO 4041 I=0,M+1
       DO 4041 J=0,M+1
       W_AT_I_FROM_J_INNER(I,J)=-(AREA_INNER(J)*EPSILON_INNER(J)/
      & RHO_INNER(J))*
      & AINV(I,J)*SIGMA*TEMP_INNER(J)**4
 4041  CONTINUE
       DO 4083 I=0,M+1
       SUM1=0.0
       DO 4082 J=0,M+1
       SS_INNER(I,J)=AREA_INNER(I)*EPSILON_INNER(I)/RHO_INNER(I)*
      & (W_AT_I_FROM_J_INNER(I,J)/
      & (SIGMA*TEMP_INNER(J)**4)-IDENTITY(I,J)*EPSILON_INNER(J))
       SUM1=SUM1+SS_INNER(I,J)
 4082  CONTINUE
```

```
4083 CONTINUE
     SUM=0.0
     DO 4051 I=0,M+1
     Q_AT_I_INNER(I)=0.0
     DO 4071 J=0,M+1
     Q_AT_I_INNER(I)=Q_AT_I_INNER(I) + SS_INNER(I,J)*SIGMA*
    & (TEMP_INNER(I)**4-TEMP_INNER(J)**4)
4071 CONTINUE
     SUM=SUM+Q_AT_I_INNER(I)
4051 CONTINUE
     WRITE(2,*)'SUM TOTAL OF HEAT TRANSFER IN TUBE=',SUM
C    ***********************************************************
C    TO CALCULATE THE HEAT CONDUCTED AND CONVECTED FROM VARIOUS
C    SURFACES, AND LEAD TO ACCUMULATION OF HEAT IN CELL.
C    ***********************************************************
C    CONDUCTION INTO EACH CELL IN THE BAYONET TUBE
     DO 4052 I=1,M
     DIST1=Z
     DIST2=Z
     IF (I.EQ.1) THEN
     DIST1=Z/2  !HALF THE DISTANCE BETWEEN CENTER OF ZONE
     CONDUCTION_TUBE(I)=CS_AREA_TUBE*K_TUBE*(
    & (BAYONET(I)-BAYONET1(I-1))/DIST1 +
    & (BAYONET(I)-BAYONET(I+1))/DIST2)
     CONDUCTION_SHELL(I)=CS_AREA_SHELL*K_SHELL*(
    & (SHELL_C(I)-SHELL_C1(I-1))/DIST1
    &+ (SHELL_C(I)-SHELL_C(I+1))/DIST2)
     ELSE IF (I.EQ.M) THEN
     DIST2=Z/2
     CONDUCTION_TUBE(I)=CS_AREA_TUBE*K_TUBE*(
    & (BAYONET(I)-BAYONET(I-1))/DIST1 +
    & (BAYONET(I)-BAYONET1(I))/DIST2)
     CONDUCTION_SHELL(I)=CS_AREA_SHELL*K_SHELL*(
    & (SHELL_C(I)-SHELL_C(I-1))/DIST1
    & + (SHELL_C(I)-SHELL_C1(I))/DIST2)
     ELSE
     CONDUCTION_TUBE(I)=CS_AREA_TUBE*K_TUBE*(
    & (BAYONET(I)-BAYONET(I-1))/DIST1 +
    & (BAYONET(I)-BAYONET(I+1))/DIST2)
     CONDUCTION_SHELL(I)=CS_AREA_SHELL*K_SHELL*(
    & (SHELL_C(I)-SHELL_C(I-1))/DIST1
    & + (SHELL_C(I)-SHELL_C(I+1))/DIST2)
     ENDIF
     CONDUCTION_SUM_TUBE=CONDUCTION_SUM_TUBE+CONDUCTION_TUBE(I)
CONDUCTION_SUM_SHELL=CONDUCTION_SUM_SHELL+CONDUCTION_SHELL(I)
4052 CONTINUE
C    WRITE(6,*)'    CONDUCTION_SUM_TUBE=',CONDUCTION_SUM_TUBE
C    WRITE(6,*)'    CONDUCTION_SUM_SHELL=',CONDUCTION_SUM_SHELL
C    ***********************************************************
C    CONDUCTION INTO EACH ZONE OF THE SHELL
C    ***********************************************************
C    CONVECTION FROM THE INNER SURFACE OF THE TUBE
     WRITE(2,*)'ZONE T(I-1)  T(I)  DELTA[T(I-1)-T(I)]  CONV_HT
    &HT_COEFF_TUBE'
     DO 4053 I=1,M
     CONV_HT_AIR_TUBE(I)=MCP*(TEMP_AIR_TUBE1(I-1)-
    & TEMP_AIR_TUBE1(I))
     CONV_HT_AIR_ANNULUS(I)=MCP*(TEMP_AIR_ANNULUS1(I)-
    & TEMP_AIR_ANNULUS1(I-1))
C    HEAT TRANSFER COEFFICIENT INSIDE TUBE.
     TEMP_DIFF=BAYONET(I) - TEMP_AIR_TUBE(I)
     IF (ABS(TEMP_DIFF) .LE. 0.1) THEN
        HT_COEFF_TUBE(I)=0.0
     ELSE
        HT_COEFF_TUBE(I)=CONV_HT_AIR_TUBE(I)/
    &        (AI_TUBE*TEMP_DIFF)
     ENDIF
     WRITE(2,*)I,TEMP_AIR_TUBE1(I-1),TEMP_AIR_TUBE1(I),
```

```
 &TEMP_AIR_TUBE1(I-1)-TEMP_AIR_TUBE1(I),CONV_HT_AIR_TUBE(I)/MCP,
 &  HT_COEFF_TUBE(I)
C 4057  FORMAT(1X,3I,2(2X,F7.2)2X,F6.2,2X,F8.2,2X,F7.2)
 4053  CONTINUE
C   ************************************************************
C   NET AMOUNT OF HEAT IN EACH ZONE OF THE INNER TUBE AVAILABLE FOR
C   CONVECTION FROM THE OUTER SURFACE
C   ************************************************************
    DO 4054 I=1,M
    NET_HEAT_AT_TUBE_ZONE(I)=CONDUCTION_TUBE(I)+  CONV_HT_AIR_TUBE(I)
   &  +Q_AT_I_INNER(I)+Q_AT_I(M+I)
C   HT_COEFF_TUBE(I)*AI_TUBE*(BAYONET(I)-TEMP_AIR_TUBE(I))
C   WAS USED INSTEAD OF CONV_HT_AIR_TUBE(I)
C   ALWAYS HEAT OUT IS +VE., HEAT IN IS -VE.
C   ALL THE EXCESS HEAT THAT IS THERE AT EACH ZONE IS CONVECTED TO THE
C   ANNULAR AIR.  IF THE NET HEAT IS -VE IT MEANS HEAT HAS TO BE LOST,
C   IF THE NET HEAT IS +VE HEAT HAS TO BE ABSORBED FROM THE ANNULAR AIR.
    TEMP_DIFF=BAYONET(I)-TEMP_AIR_ANNULUS(I)
    IF (ABS(TEMP_DIFF) .LE. 0.1) THEN
       HT_COEFF_ANNULUS_INNER(I)=0.0
    ELSE
        HT_COEFF_ANNULUS_INNER(I)=-NET_HEAT_AT_TUBE_ZONE(I)
   &          /(AI*TEMP_DIFF)
    ENDIF
4054  CONTINUE
C   ************************************************************
C   HENCE HEAT TRANSFER COEFF FROM THE TUBE OUTER SURFACE.
C   HEAT GAINED BY AIR IN ANNULUS IS FROM (1) INNER SURFACE, (2) OUTER
C   SURFACE OF ANNULUS.  HEAT GAINED IS KNOWN, HEAT FROM INNER
C   SURFACE IS KNOWN  HENCE HEAT FROM OUTER SURFACE
C   ************************************************************
    DO 4055 I=1,M
    TEMP_DIFF= SHELL_C(I)-TEMP_AIR_ANNULUS(I)
    IF (ABS(TEMP_DIFF) .LE. 0.1) THEN
       HT_COEFF_ANNULUS_OUTER(I)=0.0
    ELSE
       HT_COEFF_ANNULUS_OUTER(I)=1/( AO* TEMP_DIFF )
   &  *(CONV_HT_AIR_ANNULUS(I)+(NET_HEAT_AT_TUBE_ZONE(I)))
    ENDIF
4055  CONTINUE
C   ************************************************************
C   HEAT INTO EACH ZONE OF THE SHELL FROM THE OUTSIDE OVEN COMPARED
C   TO WHAT IS LOST AT ITS INNER SURFACE
C   ************************************************************
    POWER_AT_EACH_ZONE=POWER_IN/(M+1)
    DO 4056 I=1,M
    NET_HEAT_AT_SHELL(I)=HT_COEFF_ANNULUS_OUTER(I)*AO*
   &  (SHELL_C(I)-TEMP_AIR_ANNULUS(I))+Q_AT_I(I)
 4056  CONTINUE
    OPEN(UNIT=23,FILE='CHECK_FOR_SIGN.DAT',STATUS='NEW')
    WRITE(23,9991)TESTNAME
    WRITE(24,9991)TESTNAME
    WRITE(23,*)'ZONE      NET_HEAT_AT_ZONE      DELTA_T   H_ANN_IN
   &CONV_HEAT_ANN     H_SHELL  COND_TUBE    CONV_TUBE     RAD_TUBE'
    WRITE(24,*)'ZONE      H_ANN_OUTER    H_ANNULUS_INNER
   &      H_TUBE'
    WRITE(5,*)
    WRITE(5,*)'     CONSOLIDATED RESULT TABLE     '
    WRITE(5,*)
    WRITE(5,*)
    DO 1114 I=1,M
    WRITE(5,1150)I,SHELL_C(I),BAYONET(I),TEMP_AIR_ANNULUS(I),
   &TEMP_AIR_TUBE(I),
   &CONV_HT_AIR_TUBE(I),CONV_HT_AIR_ANNULUS(I),
   &Q_AT_I(I),Q_AT_I(I+M),Q_AT_I_INNER(I),
   &CONDUCTION_SHELL(I),CONDUCTION_TUBE(I),
   &NET_HEAT_AT_TUBE_ZONE(I),
   &BAYONET(I)-TEMP_AIR_ANNULUS(I),
```

```
   &HT_COEFF_ANNULUS_INNER(I),
   &NET_HEAT_AT_SHELL(I),SHELL_C(I)-TEMP_AIR_ANNULUS(I),
   &HT_COEFF_ANNULUS_OUTER(I),BAYONET(I)-TEMP_AIR_TUBE(I),
   &HT_COEFF_TUBE(I)
    WRITE(23,1151)I,NET_HEAT_AT_TUBE_ZONE(I),BAYONET(I)
   &-TEMP_AIR_ANNULUS(I),
   &HT_COEFF_ANNULUS_INNER(I),CONV_HT_AIR_ANNULUS(I),
 &HT_COEFF_ANNULUS_OUTER(I),CONDUCTION_TUBE(I),CONV_HT_AIR_TUBE(I),
   &Q_AT_I(M+I)+Q_AT_I_INNER(I)
    WRITE(24,2222)I,HT_COEFF_ANNULUS_OUTER(I),HT_COEFF_ANNULUS_
   &INNER(I),HT_COEFF_TUBE(I)
1114  CONTINUE
2222  FORMAT(I3,3(2X,F9.2))
1150  FORMAT(I3,1X,F5.1,1X,F5.1,1X,F5.1,1X,F5.1,
   &1X,F5.2,1X,F6.2,1X,
   &F6.2,1X,F6.2,1X,F5.2,1X,
   &F5.2,1X,F5.2,1X,
   &F6.2,1X,F5.1,1X,
   &F9.2,1X
   &F8.2,1X,F5.1,1X,F8.2,1X,F6.1,1X,F5.1)
1151  FORMAT(I3,1X,F8.1,3X,F8.1,3X,F8.1,3X,F8.1,3X,F8.2,3X,
   &  F8.3,3X,F8.2,3X,F8.3,3X)
    WRITE(5,*)
    WRITE(5,9991)TESTNAME
9991 FORMAT(A80)
C    $$$$$$$$$$$$$$$$$$$$$$$$$$$
C    CALCULATIONS FOR DITTUS BOELTER HETA TRANSFER COEFFICIENTS
C    $$$$$$$$$$$$$$$$$$$$$$$$$$$$
    DITTUS_B_TUBE=K_AIR/(2*(RI-0.16*2.54E-2))*0.023*(MCP/1007/
   &  PI/(RI-0.16*2.54E-2)*2/MU_S)**0.8*PRANDTL**0.4
    DITTUS_B_ANNULUS=K_AIR/(2*(RO-RI))*0.023*(MCP/1007/AA*
   &  2*(RO-RI)/MU_S)**0.8*PRANDTL**0.4
C    ***************************************************
C    EVALUATION OF DIFFERENTIAL EQUATIONS TO OBTAIN TEMPERATURE
C    DISTRIBUTION IN ANNULUS
C    ***************************************************
C    WE DEFINE: THETA_T, THETA_A FOR DIMENSIONLESS TEMPERATURES IN
C    THE TUBE AND ANNULUS. NTU IS THE RATIO OF K*A/MCP FOR INNER TUBE
C    ETA IS THE NONDIMENSIONAL DISTANCE AND CHI IS THE RATIO OF
C    OVERALL HEAT TRANSFER COEFFICIENTS.
C    **************************************************************
C    OVERALL HEAT TRANSFER COEFFS
    U_OUT=DITTUS_B_ANNULUS
    AREA_OUT=2*PI*RO*M*Z
    AREA_IN=2*PI*RI*M*Z
    U_IN1=DITTUS_B_ANNULUS
    U_IN2=RI*LOG(RI/(RI-0.16*2.54E-2))/K_TUBE
    U_IN3=DITTUS_B_TUBE
    U_EQ_IN=1/(1/U_IN1+U_IN2+RI/(RI-0.16*2.54E-2)/U_IN3)
    NTU=U_EQ_IN*AREA_IN/MCP
    CHI=U_OUT*RO/(U_EQ_IN*RI)
    DELTA1=TEMP_AIR_ANNULUS1(0)-TEMP_AIR_TUBE1(0)
    DELTA=DELTA1/(TEMP_AIR_TUBE1(M)-TEMP_B)
    M1=(1+(1+4/CHI)**0.5)*CHI/2
    M2=(1-(1+4/CHI)**0.5)*CHI/2
    M3=M1*EXP(M1*NTU)-M2*EXP(M2*NTU)
    AA1 = ( DELTA-M2*EXP(M2*NTU) )/M3
    BB1 = (-DELTA+M1*EXP(M1*NTU) )/M3
    K=AA1*EXP(M1*NTU)+BB1*EXP(M2*NTU)+DELTA
    K1=(M1-M2)*EXP(M1*NTU)
    K2=(M2-M1)*EXP(M2*NTU)
    CC1=(DELTA+K*M1)/K1
    DD1=(DELTA+K*M2)/K2
    WRITE(24,*)
    WRITE(24,*)
    WRITE(24,*)'RESULTS FROM SOLN OF DIFFERENTIAL EQN WITH TB AS
   & BOUNDARY CONDITION'
    WRITE(5,*)
```

```
      WRITE(5,*)'     RESULTS OF SOL OF DIFF EQ'
      WRITE(5,*)
      WRITE(5,*)'TEMP_B= ',TEMP_B,' U_OUT= ',U_OUT,' U_EQ_IN= ',
     &U_EQ_IN
      WRITE(5,*)' NTU= ',NTU,' CHI = ',CHI, 'DELTA =',DELTA
      WRITE(5,*)'M1 ',M1,' M2 ',M2,' M3 ',M3
      WRITE(5,*)'A ',AA1, 'B ',BB1,'C ',CC1,' D ',DD1
      WRITE(5,*)' U_AT OUTER=',U_IN1
      WRITE(5,*)'RESISTANCE OF TUBE=',U_IN2/RI
      WRITE(5,*)'U_INNER SURFACE=',U_IN3
      OPEN(UNIT=9,FILE='DIFFEQ.DAT',STATUS='NEW')
     WRITE(9,*)'   I  DIST  T_INNER   T_OUTER   TEMP_AIR_TUBE1
     & TEMP_AIR_ANNULUS1'
      WRITE(24,*)'ZONE      T_INNER  T_OUTER    TEMP_B  TEMP_AIR_TUBE1
     & TEMP_AIR_ANNULUS1    BAYONET1    SHELL_C1'
      WRITE(5,*)'   THETA_INNER    THETA_OUTER'
     DO 9992 J=0,M
      I=M-J
      DIST=NTU*(I*2.54E-2)/(M*Z)
      THETA_INNER(I)=AA1*EXP(M1*DIST)+BB1*EXP(M2*DIST)
      THETA_OUTER(I)=CC1*EXP(M1*DIST)+DD1*EXP(M2*DIST)
      T_INNER=TEMP_B+(-TEMP_B+TEMP_AIR_TUBE1(M))*THETA_INNER(I)
      T_OUTER=TEMP_B+(-TEMP_B+TEMP_AIR_TUBE1(M))*THETA_OUTER(I)
      WRITE(24,2233)I,T_INNER,T_OUTER,TEMP_B,TEMP_AIR_TUBE1(M-I),
     &TEMP_AIR_ANNULUS1(M-I),BAYONET1(M-I),SHELL_C1(M-I)
2233 FORMAT(I3,7(1X,F9.2))
      WRITE(9,*)I,DIST,T_INNER,T_OUTER,TEMP_AIR_TUBE1(M-I),
     &TEMP_AIR_ANNULUS1(M-I)
      WRITE(5,*)THETA_INNER(I),THETA_OUTER(I)
9992  CONTINUE
      WRITE(24,*)
      WRITE(24,*)'BOUNDARY  CONDITION TB=',TEMP_B
      WRITE(5,*)'DITTUS BOELTER HEAT TRANSFER COEFFICIENTS'
      WRITE(5,*)'FOR ANNULUS =',DITTUS_B_ANNULUS,'  TUBE=',DITTUS_B_TUBE
      WRITE(5,*)'CONDUCTION SUMS: TUBE=',CONDUCTION_SUM_TUBE,'  SHELL=',
     & CONDUCTION_SUM_SHELL
      TOTAL_HEAT_FROM_SHELL=0.0
      DO 9990 I=1,M
      TOTAL_HEAT_FROM_SHELL=TOTAL_HEAT_FROM_SHELL+
     &NET_HEAT_AT_SHELL(I)
9990  CONTINUE
      WRITE(5,*)'HEAT IN FROM SHELL =',TOTAL_HEAT_FROM_SHELL
      WRITE(5,*)'HEAT INTO GAS =',MCP*( (TEMP_AIR_ANNULUS1(M)
     &-TEMP_AIR_ANNULUS1(0) )+(TEMP_AIR_TUBE1(0)-TEMP_AIR_TUBE1(M)) )
      WRITE(5,*)'CONDUCTION LOSS FROM TUBE=',CS_AREA_TUBE*K_TUBE*
     &  2/Z*((BAYONET(1)-BAYONET1(0))+(BAYONET(M)-BAYONET1(M)))
      WRITE(5,*)'    HEAT BALANCE'
      WRITE(5,*)' SHELL INPUT: ',TOTAL_HEAT_FROM_SHELL,' ?=? ',
     &MCP*( (TEMP_AIR_ANNULUS1(M)
     &-TEMP_AIR_ANNULUS1(0) )+(TEMP_AIR_TUBE1(0)-TEMP_AIR_TUBE1(M)) )
     &+CS_AREA_TUBE*K_TUBE*
     &  2/Z*((BAYONET(1)-BAYONET1(0))+(BAYONET(M)-BAYONET1(M))),
     &'  HEAT TO GAS +LOSSES'
      WRITE(5,*)'MCP= ',MCP,' TEMP_AIR_ANNULUS1(M)= ',
    &TEMP_AIR_ANNULUS1(M),'TEMP_AIR_ANNULUS1(0)=',TEMP_AIR_ANNULUS1(0),
     &' TEMP_AIR_TUBE1(0)=',TEMP_AIR_TUBE1(0),'  TEMP_AIR_TUBE1(M)=',
     &TEMP_AIR_TUBE1(M)
      WRITE(5,*)
      WRITE(5,*)'INPUT PARAMETERS  M, POWER IN, MCP,  Z'
      WRITE(5,*)M,POWER_IN,MCP,Z
      WRITE(5,*)'INPUT PARAMETERS EMA, EMO, EMI, EME '
      WRITE(5,*)EMA, EMO,EMI, EME
      WRITE(5,*)'AO =',AO,'  AI=',AI,'    AA=',AA
      WRITE(5,*)'AE=',AE,'   CS_AREA_SHELL',CS_AREA_SHELL
      WRITE(5,*)'CS_AREA_TUBE=',CS_AREA_TUBE,'   AI_TUBE=',AI_TUBE
      WRITE(5,*)
      WRITE(5,*)
      HEAT_CHK=0.0
```

```
      FINAL_HEAT_CHK=0.0
      WRITE(5,*)'I,SHELLH*A*DEL_T, CONV_HEATING TUBE  ANN  COND_TUBE  SUM'
      DO 4021 I=1,M
      HEAT_CHK=HT_COEFF_ANNULUS_OUTER(I)*AO*(SHELL_C(I)-
     & TEMP_AIR_ANNULUS(I))
      FINAL_CON_TUBE_CHK=FINAL_CON_TUBE_CHK+CONV_HT_AIR_TUBE(I)
      FINAL_CON_ANN_CHK=FINAL_CON_ANN_CHK+CONV_HT_AIR_ANNULUS(I)
      FINAL_HEAT_CHK=FINAL_HEAT_CHK+HEAT_CHK
      WRITE(5,1000)I,HEAT_CHK,CONV_HT_AIR_TUBE(I),
     & CONV_HT_AIR_ANNULUS(I),
     & CONDUCTION_TUBE(I),CONV_HT_AIR_TUBE(I)+CONV_HT_AIR_ANNULUS(I)+
     & CONDUCTION_TUBE(I)
4021  CONTINUE
1000  FORMAT(I3,2X,F8.3,2X,F8.3,2X,F8.3,2X,F8.4,2X,F8.3)
      WRITE(5,*)'FINAL HEAT CHECK CALC=    ',FINAL_HEAT_CHK
      WRITE(5,*)'FINAL TUBE CHECK CALC=    ',FINAL_CON_TUBE_CHK
      WRITE(5,*)'FINAL ANNU CHECK CALC=    ',FINAL_CON_ANN_CHK

C   <<<<<<<<<<RESULT TABLE>>>>>>>>>>>>>>>>>>>>>>>>>>>>
      RAD_CHK_SHELL=0.0
      RAD_CHK_BAYONET=0.0
      RAD_CHK_TUBE=0.0
      WRITE(5,*)'ZONE  RAD_FROM_SHELL   RAD_TO_TUBE  RAD_TO_INNER TUBE'
      DO 1110 I=1,M
      RAD_CHK_SHELL=RAD_CHK_SHELL+Q_AT_I(I)
      RAD_CHK_BAYONET=RAD_CHK_BAYONET+Q_AT_I(I+M)
      RAD_CHK_TUBE=RAD_CHK_TUBE+Q_AT_I_INNER(I)
1110  WRITE(5,*)I,Q_AT_I(I),Q_AT_I(M+I),Q_AT_I_INNER(I)
      WRITE(5,*)'SUM OF RADIATIONS:SHELL       BAYONET       TUBE'
      WRITE(5,*)RAD_CHK_SHELL,RAD_CHK_BAYONET,RAD_CHK_TUBE
      WRITE(5,*)'EXTRA RADIATION@ENDS: ANNULUS= ',Q_AT_I(0)
     &+Q_AT_I(2*M+1),'    TUBE=',Q_AT_I_INNER(0)+Q_AT_I_INNER(M+1)
      WRITE(5,*)
      WRITE(5,*)'CONVECTIVE HEATING EFFECTS - INSIDE TUBE   ANNULUS'
      DO 1111 I=1,M
1111  WRITE(5,*)I,CONV_HT_AIR_TUBE(I),CONV_HT_AIR_ANNULUS(I)
      WRITE(5,*)'I   CONDUCTION IN SHELL  CONDUCTION IN TUBE'
      DO 1112 I=1,M
      COND_CHK_SHELL=COND_CHK_SHELL+CONDUCTION_SHELL(I)
      COND_CHK_TUBE=COND_CHK_TUBE+CONDUCTION_TUBE(I)
1112  WRITE(5,*)I,CONDUCTION_SHELL(I),CONDUCTION_TUBE(I)
      WRITE(5,*)'   CONDUCTION CHECK TUBE,       SHELL'
      WRITE(5,*)COND_CHK_TUBE,COND_CHK_SHELL
      WRITE(5,*)'TUBE COND LOSS =',CS_AREA_TUBE*K_TUBE*
     & 2/Z*((BAYONET(1)-BAYONET1(0))+(BAYONET(M)-BAYONET1(M)))
      WRITE(5,*)'SHELL COND LOSS =',CS_AREA_SHELL*K_SHELL*
     & 2/Z*((SHELL_C(1)-SHELL_C1(0))+
     & (SHELL_C(M)-SHELL_C1(M)))
      WRITE(5,*)'<<<<<<<<<<HEAT TRANSFER COEFF>>>>>>>>>>>>>>>'
      WRITE(5,*)'TUBE    ANNULUS OUTER  ANNULUS INNER '
      OPEN (UNIT=7,FILE='PLOTDATA.DAT',STATUS='NEW')
      WRITE(7,*)' I  H_TUBE  H_ANN_OUTER     H_ANN_INNER'
      DO 1113 I=1,M
1113  WRITE(7,*)I,HT_COEFF_TUBE(I),HT_COEFF_ANNULUS_OUTER(I),
     & HT_COEFF_ANNULUS_INNER(I)
      WRITE(5,*)
C   ***********************************************************
C   ITERATION TECHNIQUE  STARTS HERE
C   ***********************************************************
      READ(8,*)AI_PERCENTAGE
      READ(8,*)AO_PERCENTAGE
      READ(8,*)T_PERCENTAGE
      OPEN(UNIT=27,FILE='DSK3:[BOSS.DEV.PROGRAM.DECEMBER]
     &INLET_COEFF.DAT',STATUS='OLD',READONLY)
      DO 1123 I=1,M
      READ(27,*)AI_COEFF(I),AO_COEFF(I),T_COEFF(I)
      AI_COEFF(I)=AI_COEFF(I)*AI_PERCENTAGE
      AO_COEFF(I)=AO_COEFF(I)*AO_PERCENTAGE
```

```
      T_COEFF(I)=T_COEFF(I)*T_PERCENTAGE
 1123  WRITE(6,*)AI_COEFF(I),AO_COEFF(I),T_COEFF(I)
C    AT 1113 WE HAVE SET THE VALUE OF HI_CALC(I) AND USE IT INSTEAD OF
C    HI BASED ON CORRELATIONS
     HAO=DITTUS_B_ANNULUS
     HAI=HAO
     HI=DITTUS_B_TUBE
     TI=TEMP_AIR_TUBE1(M)
     TGT(M)=TI
     TGT(0)=TI
     TGA(0)=TI
     DO 810 I=1,M
     TOW(I)=SHELL_R(I)
     TIW(I)=TI
     TGT(I)=TI
     TGA(I)=TI
 810 CONTINUE
      K=1
 880  TGAML=TGA(M)
C ++++SET THE NEW VALUES OF ANNULUS AND END PLATE TEMPS HERE
    TA0=SHELL_C1(0)  !TEMP OF ANN ON I=0 SIDE
     TAM=(SHELL_C1(M)+TIW(M))/2     !          I=M SIDE
     TE0=(SHELL_C1(0)+TIW(0))/2     !TEMP OF END ON I=0 SIDE
     TEM=TIW(M)     !          I=M SIDE
C ++++DONE--PROCEED
     DO 830 I=1,M
     BB=(TIA(I)+TIA(M+1-I)+TIE(I)+TIE(M+1-I))*SIGMA
     CC=AI_COEFF(I)*AI*HAI+AI_TUBE*T_COEFF(I)*HI
     DD=TIA(I)*SIGMA*TA0**4 + TIA(M+1-I)*SIGMA*TAM**4
    &+ TIE(I)*SIGMA*TE0**4 + TIE(M+1-I)*SIGMA*TEM**4
    &+ AI*HAI*AI_COEFF(I)*TM(I) + AI_TUBE*T_COEFF(I)*HI*TM(2*M+1-I)
     DO 840 J=1,M
     BB=BB+TOI(J,I)*SIGMA
     IF(I .NE. J)BB=BB+(TII1(J,I)+TII2(J,I))*SIGMA
     DD=DD+TOI(J,I)*SIGMA*TOW(J)**4
     IF(I .NE. J)DD=DD+(TII1(J,I)+TII2(J,I))*SIGMA*TIW(J)**4
 840 CONTINUE
 850 TL=TIW(I)
     TIW(I)=TL-(BB*TL**4+CC*TL-DD)/(4.*BB*TL**3+CC)
     IF(ABS(TIW(I)-TL) .GT. 0.1)GO TO 850
C    TYPE 1900,I,TIW(I)
      TIW_LAST(I)=TL
 1900 FORMAT(1X,'TIW(',I2,')=',F7.1)
 830 CONTINUE
C    WRITE(6,*)' NEWTON  RAPHSON COMPLETE'
    IF(ABS(TIW(M)-TIWML)  .GT. 0.1)GO TO 820
C    WRITE(6,*)' NEWTON  RAPHSON  SUCCESSFUL'
C+++++HEATING OF GAS IS DONE HERE+++++++++++
C-----INSIDE  TUBE--------C
     DO 870 I=1,M
     TM(M+I)=(2*MCP*TGT(M+1-I)+T_COEFF(M+1-I)*
    &HI*AI_TUBE*TIW(M+1-I))/
    &(2*MCP+T_COEFF(M+1-I)*HI*AI_TUBE)
     TGT(M-I)=TGT(M+1-I)+2*(TM(M+I)-TGT(M+1-I))
 870 CONTINUE
C-----INSIDE  ANNULUS-----C
     TGA(0)=TGT(0)+DELTA1     !DISCONTINUITY  IN GAS TEMP+++++
     DO 860 I=1,M
     TM(I)=(2.*MCP*TGA(I-1)+AO_COEFF(I)*HAO*AO*TOW(I)+
    &HAI*AI_COEFF(I)*AI*TIW(I))/(2.*MCP+HAO*AO*AO_COEFF(I)
    &+HAI*AI*AI_COEFF(I))
     TGA(I)=TGA(I-1)+2.*(TM(I)-TGA(I-1))
 1910 FORMAT(1X,'TGA(',I2,')=',F9.3)
 1911 FORMAT(1X,'TGT(',I2,')=',F9.3)
 860 CONTINUE
C    WRITE(6,*)' DONE WITH  ANNULUS TEMPS'
      WRITE(6,*)'ITERATION  NUM=',K,'IS  OVER STARTING NEXT'
      K=K+1
```

```
C    WRITE(6,*)'ITERATION #=',K,'  DIFFERENCE=',ABS(TGA(M)-TGAML)
C    ***************************************************************
C    DO 822 I=1,M
     IF(ABS(TGA(M)-TGAML) .GT. 0.1)GO TO 880
C    IF(ABS(TGA(M)-TGA_ML(I)) .GT. 0.1)GO TO 880
822  CONTINUE
      WRITE(24,*)'SOLUTION FOR TEMP BY DR. FOOTE METHOD - ACTUAL TEMP AS
     &BOUNDARY CONDITION'
      WRITE(2,*)' ZONE    DIST  SHELL  ANNULUS  TUBE AIR TUBE'
      WRITE(24,*)'ZONE     SHELL  ANNULUS     TUBE   TUBE_AIR'
     DO 950 I=1,M
     WRITE(2,*)'  ',I,(I-0.5)*Z,SHELL_R(I),TM(I),TIW(I),TM(2*M+1-I)
     WRITE(24,2223)I,SHELL_R(I),TM(I),TIW(I),TM(2*M+1-I),
     &TEMP_AIR_ANNULUS(I),BAYONET(I),TEMP_AIR_TUBE(I)
2223 FORMAT(I3,7(1X,F9.2))
950  CONTINUE
      WRITE(24,*)
      WRITE(24,*)'   HEAT TRANSFER COEFFICIENTS'
      WRITE(24,*)'ZONE  H_ANNULUS_OUTER  H_ANNULUS_INNER  H_TUBE'
     QA1=0.
     QA2=0.
     QE1=0.
     QE2=0.
     DO 900 I=1,M
     QA1=QA1+TIA(I)*SIGMA*(TA0**4-TIW(I)**4)
     QA2=QA2+TIA(M+1-I)*SIGMA*(TAM**4-TIW(I)**4)
     QE1=QE1+TIE(I)*SIGMA*(TE0**4-TIW(I)**4)
     QE2=QE2+TIE(M+1-I)*SIGMA*(TEM**4-TIW(I)**4)
900  CONTINUE
     SUMQW=QA1+QA2+QE1+QE2
     SUMQOC=0.
     SUMQOR=0.
     DO 910 I=1,M
     QOC(I)=HAO*AO*AO_COEFF(I)*(TOW(I)-TM(I))
     QOR(I)=0.
     DO 920 J=1,M
     QOR(I)=QOR(I)+TOI(I,J)*SIGMA*(TOW(I)**4-TIW(J)**4)
920  CONTINUE
     SUMQOC=SUMQOC+QOC(I)
     SUMQOR=SUMQOR+QOR(I)
     SUMQW=SUMQW+QOC(I)+QOR(I)
910  CONTINUE
     SUMQG=MCP*((TGT(0)-TGT(M))+(TGA(M)-TGA(0)))
     WRITE(2,1230)TGA(M),SUMQOC,SUMQOR,SUMQW,SUMQG
1230 FORMAT(/1X,'TGEX=',F6.1,'SUMQOC=',F8.1,' SUMQOR=',F8.1,' SUMQW=',
     &F8.1,' SUMQG=',F8.1)
C********CALCULATIONS  FOR HEAT TRANSFER COEFF BASED ON T-EX-AREA
C METHOD   ***********************************************************
      OPEN(UNIT=35,FILE='FOOTE_NEW1.DAT',STATUS='NEW')
      WRITE(35,*)' RAD   COND  MCP_T   C_F_ANN  T_A-BAY  MCP_A  H_AO
     &H_AI    H_T'
      TA0=TEMP(0)
      TAM=TEMP(2*M+1)
      TE0=TEMP(0)
      TEM=TEMP(2*M)  !BECAUSE THE INSIDE SEES ONLY THE TUBE
      TGA(0)=TEMP_AIR_ANNULUS1(0)
      TGT(0)=TEMP_AIR_TUBE1(0)
      TIW0=BAYONET1(0)
      TIWM=BAYONET1(M)
      DO 831 I=1,M
      TIW(I)=BAYONET(I)
      TGA(I)=TEMP_AIR_ANNULUS1(I)
      TGT(I)=TEMP_AIR_TUBE1(I)
      TM(I)=TEMP_AIR_ANNULUS(I)
      TM(I+M)=TEMP_AIR_TUBE(M+1-I)
831  CONTINUE
     HEATSUM=0.0
C    TOW(I) HAS BEEN CORRECTLY SET IN ABOVE ITERATIONS
```

```
      WRITE(24,*)'BASED ON TOTAL  EXCH AREA HEAT TRANSFER COEFFS ARE:'
      WRITE(24,*)'HAO=',HAO
      WRITE(24,*)'HAI=',HAI
      WRITE(24,*)'HI=',HI
      WRITE(24,*)'   I    HTAO/DITTUS    HTAI/DITTUS
     &HTI/DITTUS'
      DO 832 I=1,M
      BB=(TIA(I)+TIA(M+1-I)+TIE(I)+TIE(M+1-I))*SIGMA
      DD=TIA(I)*SIGMA*TA0**4 + TIA(M+1-I)*SIGMA*TAM**4
     &+ TIE(I)*SIGMA*TE0**4  + TIE(M+1-I)*SIGMA*TEM**4
      DO 841 J=1,M
      BB=BB+TOI(J,I)*SIGMA
      IF(I .NE. J)BB=BB+(TII1(J,I)+TII2(J,I))*SIGMA
      DD=DD+TOI(J,I)*SIGMA*TOW(J)**4
      IF(I .NE. J)DD=DD+(TII1(J,I)+TII2(J,I))*SIGMA*TIW(J)**4
 841  CONTINUE
      HEAT(I)=DD-BB*TIW(I)**4
       ONE=HEAT(I)
      HEATSUM=HEATSUM+HEAT(I)
C      WRITE(6,*)' I=',I,'  HEAT=',HEAT(I)
      IF(I.EQ.1)HEAT(I)=HEAT(I)-K_TUBE*CS_AREA_TUBE*
     &(2*(TIW(I)-TIW0)/Z+(TIW(I)-TIW(I+1))/Z)
      IF(I.GT.1 .AND. I.LT.M)HEAT(I)=HEAT(I)-K_TUBE*CS_AREA_TUBE*
     &(2*TIW(I)-TIW(I-1)-TIW(I+1))/Z
      IF(I.EQ.M)HEAT(I)=HEAT(I)-K_TUBE*CS_AREA_TUBE*
     &(2*(TIW(I)-TIWM)/Z+(TIW(I)-TIW(I-1))/Z)
       TWO=HEAT(I)
      DIFFT=TIW(I)-TM(2*M+1-I)
       THREE=MCP*(TGT(I-1)-TGT(I))
      IF (ABS(DIFFT).LT. .1) THEN
       HTI(I)=0
      ELSE
       HTI(I)=MCP*(TGT(I-1)-TGT(I))/(AI_TUBE*DIFFT)
      ENDIF
C     TAKING CONVENTION THAT HEAT FLUX INWARD IS +VE
      HEAT(I)=-(HEAT(I)-MCP*(TGT(I-1)-TGT(I)))
       FOUR=HEAT(I)
      DIFFI=-(TIW(I)-TM(I))
      IF (ABS(DIFFI).LT. .1) THEN
       HTAI(I)=0
      ELSE
       HTAI(I)=HEAT(I)/(AI*DIFFI)
      ENDIF
       FIVE=MCP*(TGA(I)-TGA(I-1))
      DIFFO=TOW(I)-TM(I)
      IF (ABS(DIFFO) .LT. .1) THEN
       HTAO(I)=0.0
      ELSE
       HTAO(I)=(MCP*(TGA(I)-TGA(I-1))+HEAT(I))/(AO*DIFFO)
      ENDIF
       WRITE(35,2225)ONE,TWO,THREE,FOUR,DIFFI,FIVE,HTAO(I)/HAO,
     &HTAI(I)/HAI,HTI(I)/HI
      WRITE(24,2224)I,HTAO(I)/HAO,HTAI(I)/HAI,HTI(I)/HI
 2224 FORMAT(I3,3(2X,F9.2))
 2225 FORMAT(5(2X,F6.2),2X,F7.2,3(2X,F6.2))
 832  WRITE(6,1834)I,DIFFO,HTAO(I),DIFFI,HTAI(I),DIFFT,HTI(I)
 1834 FORMAT(I3,6(1X,F8.1))
C     ++++++ CALCS FOR BALANCE ++++++++
      QA1=0.
      QA2=0.
      QE1=0.
      QE2=0.
      DO 901 I=1,M
      QA1=QA1+TIA(I)*SIGMA*(TA0**4-TIW(I)**4)
      QA2=QA2+TIA(M+1-I)*SIGMA*(TAM**4-TIW(I)**4)
      QE1=QE1+TIE(I)*SIGMA*(TE0**4-TIW(I)**4)
      QE2=QE2+TIE(M+1-I)*SIGMA*(TEM**4-TIW(I)**4)
 901  CONTINUE
```

```
      SUMQW=QA1+QA2+QE1+QE2
      SUMQOC=0.
      SUMQOR=0.
      SUMQG=MCP*((TGT(0)-TGT(M))+(TGA(M)-TGA(0)))
       WRITE(6,*)' SUMQOC  SUMQOR  SUMQW  SUMQG  HEATSUM'
      DO 911 I=1,M
      QOC(I)=HTAO(I)*AO*(TOW(I)-TM(I))
      QOR(I)=0.
      DO 921 J=1,M
      QOR(I)=QOR(I)+TOI(I,J)*SIGMA*(TOW(I)**4-TIW(J)**4)
  921 CONTINUE
      SUMQOC=SUMQOC+QOC(I)
      SUMQOR=SUMQOR+QOR(I)! NOT QOR BECAUSE NON UNIFORM BOUNDARY
C CONDITION AND HENCE HEAT TRANSFER VARIES -BUT THIS IS IMMATERIAL
      SUMQW=SUMQW+QOC(I)+QOR(I)
       WRITE(6,1233)SUMQOC,SUMQOR,SUMQW,SUMQG,HEATSUM
  911 CONTINUE
      WRITE(6,*)'SUMQOC,  SUMQOR,  SUMQW,  SUMQG,  HEATSUM'
      WRITE(6,1233)SUMQOC,SUMQOR,SUMQW,SUMQG,HEATSUM
 1233 FORMAT(1X,5(F8.2,1X))
C***********************************************************************
      STOP
      END

      FUNCTION FOO(RO,RI,Z)
      PI=3.1415926
      FOO=1.+Z/(4.*RO)-RI/RO+(2.*RI)/(PI*RO)*ATAN(2.*((RO/Z)**2
     &-(RI/Z)**2)**0.5)+Z/(2.*PI*RO)*ASIN(1.-2.*(RI/RO)**2)
     &-(4.+(Z/RO)**2)**0.5/(2.*PI)*(PI/2.+ASIN(1.-2.*(RI/RO)**2
     &/(4.*(RO/Z)**2-4.*(RI/Z)**2+1)))
      RETURN
      END

      FUNCTION FOI(RO,RI,Z)
      PI=3.1415926
      FOI=RI/RO-RI/(PI*RO)*ACOS(((Z/RO)**2+(RI/RO)**2-1.)/((Z/RO)**2
     &-(RI/RO)**2+1.))+1./(2.*PI)*((Z/RO+RO/Z+RI**2/(RO*Z))**2
     &-(2.*RI/Z)**2)**0.5*ACOS((RI/RO)*((Z/RO)**2+(RI/RO)**2-1.)
     &/((Z/RO)**2-(RI/RO)**2+1.))+1./(2.*PI)*(Z/RO-RO/Z+RI**2/(RO*Z))
     &*ASIN(RI/RO)-(Z/RO+RO/Z-RI**2/(RO*Z))/4.
      RETURN
      END

      FUNCTION FEE(R,Z)
      FEE=(2.*R**2+Z**2-((2.*R**2+Z**2)**2-4.*R**4)**0.5)/(2.*R**2)
      RETURN
      END

      SUBROUTINE INV(N,A,AI)
      DIMENSION A(0:97,0:97),AI(0:97,0:97),AA(98,196)
      DO 10 I=1,N+2
      DO 20 J=1,N+2
      AA(I,J)=A(I-1,J-1)
   20 CONTINUE
      DO 30 J=1,N+2
      AA(I,J+N+2)=0.
      IF(I .EQ. J)AA(I,J+N+2)=1.
   30 CONTINUE
   10 CONTINUE
      DO 40 I=1,N+2
      DO 50 K=I+1,N+2
      X=AA(K,I)/AA(I,I)
      DO 60 J=I,2*(N+2)
      AA(K,J)=AA(K,J)-X*AA(I,J)
   60 CONTINUE
   50 CONTINUE
   40 CONTINUE
      DO 70 I=N+2,1,-1
```

```
      DO 80 K=I-1,1,-1
      X=AA(K,I)/AA(I,I)
      DO 90 J=I,2*(N+2)
      AA(K,J)=AA(K,J)-X*AA(I,J)
90    CONTINUE
80    CONTINUE
70    CONTINUE
      DO 100 I=1,N+2
      DO 110 J=1,N+2
      AA(I,J+N+2)=AA(I,J+N+2)/AA(I,I)
      AI(I-1,J-1)=AA(I,J+N+2)
110   CONTINUE
100   CONTINUE
      RETURN
      END
```

VITA

Devdutt Dash was born at Cuttack, Orissa, India on the May 6, 1967. He attended schools in Orissa and in Bombay. He studied Mechanical Engineering at the University College of Engineering, Burla of the Sambalpur University, Orissa, India and graduated with a Bachelor of Science in Engineering degree with Honors in July 1989. In July 1990, he joined the Master of Management Studies (MMS) program of the Bombay University, at the Narsee Monjee Institute of Management Sciences, Bombay. He completed only the first year of the MMS program and in August 1991, he accepted admission to attend the University of Tennessee Space Institute (UTSI) at Tullahoma, Tennessee, U.S.A. He worked as a graduate research assistant with the Energy Conversion Programs at UTSI, and graduated with a Master of Science Degree in Mechanical Engineering in May, 1994.